NASA Contractor Report 181909, Volume I
DOT/FAA - CT - 89/36 - I

THE NASA DIGITAL VGH PROGRAM - EXPLORATION OF METHODS AND FINAL RESULTS

Volume I - Development of Methods

Norman L. Crabill

Eagle Engineering, Incorporated
Hampton Division
Hampton, Virginia 23666

Contract NASW 4430
December 1989

National Aeronautics and
Space Administration

Langley Research Center
Hampton, Virginia 23665

FOREWORD

This report was prepared by Eagle Engineering, Inc., Hampton Division, under contract NASW 4430, sponsored by NASA Langley Research Center and the Federal Aviation Administration Technical Center under the FAA-NASA Interagency Agreement No. DTFA03-890-A-00019 of 13 June 1989. This report fulfills the requirement of the Program Plan for the National Aging Aircraft Research Program, DOT/FAA/CT-88/32, August 1989, Paragraph 2.3.2.1, Flight Loads.

The Eagle Engineering, Inc. effort was performed by Norman L. Crabill and administered under the direction of Joseph W. Stickle (NASA Langley Research Center) and Thomas DeFiore (FAA Technical Center).

TABLE OF CONTENTS

VOLUME II - L 1011 Data 1978-1979: 1619 Hours
VOLUME III - B 727 Data 1978-1980: 1765 Hours
VOLUME IV - B 747 Data 1978-1980: 1689 Hours
VOLUME V - DC 10 Data 1981-1982: 129 Hours

THE NASA DIGITAL VGH PROGRAM-
EXPLORATION OF METHODS AND FINAL RESULTS
Volume I: Development of Methods

Normal L. Crabill

Eagle Engineering, Inc.

Hampton Division

SUMMARY

The results of a NASA effort to utilize data from existing Digital Flight Data Recorders on airline transport aircraft in routine airline service indicates that many statistical data types useful to aircraft designers and operators can be compiled from the limited measurement types selected. Techniques for solving the significant problem of data editing were developed, along with methods for separating maneuver and gust accelerations using 200 hours of data taken from L 1011 operations in 1973. Some results indicate that the acceleration derived exceedances at the 4 samples per second rate generally available from the Digital Flight Data Recorders may be only 1/2 to 1/3 those obtainable at 20 to 40 samples per second and, therefore, the present acceleration data must be used with caution. These techniques and methods are described and the results are given in Volume I. Similar analysis techniques were applied to about 5000 total hours for L 1011, B 727, B 747 and DC 10 aircraft operations of 1978 through 1982. These results are given in Volumes II, III, IV, and V, respectively.

INTRODUCTION

The NACA-NASA has long had an involvement in determining actual operating conditions of commercial aircraft to aid designers in developing satisfactory design criteria. Starting in 1933, the NACA VG Program, using the smoked glass and stylus technique (ref. 1), gave an analog representation of the operating VG diagram for direct comparison with the designer's load factor assumptions. A new "VGH" recorder was introduced in 1946 to give time histories of velocity, "G" load, and height, which had to be manually manipulated into suitable statistical forms to provide meaningful guidance to designers (refs. 1, 2). These programs involved many different types of aircraft, including general aviation and airline transport aircraft (refs. 3, 4). After 1971, however, the NASA VGH program was restricted to general aviation operations only (ref. 5). In 1977, with the cooperation of the manufacturers and airline operators, the NASA renewed the Data Recording Program to study airline operations and investigate the utilization of the Digital Flight Data Recorders (DFDRs) (ref. 6) required on all large turbine aircraft certificated since September 30, 1969. Limited early results of this effort are given in reference 7.

This report provides the final results of this exploratory Digital VGH (DVGH) program. Parameters utilized were a subset of those already available on the existing DFDRs without imposing any new requirements on data quality. No new recording system was used. The data quality problems that were encountered were handled with appropriate editing techniques.

The first volume of this report describes these data editing techniques, the analysis methods, and the many statistical data types developed in consultation with the airframe manufacturing industry using 200 hours of DFDR data taken from routine airline operations of a Lockheed L 1011-1 aircraft in 1973. Similar analysis techniques were subsequently applied to about 5000 total hours obtained from the L 1011, Boeing's B 727 and B 747, and the Douglas DC 10 aircraft in airline operations from 1978 through 1982. These results are given in Volumes II, III, IV, and V of the present paper.

Starting in 1982, NASA developed and flight-tested on contract, a brassboard version of a "Smart" Flight Recorder in which statistical data were computed in near real-time and stored on-board in the recorder (ref. 8). This approach eliminated the tedious manual labor required to edit-out the data errors introduced by the frequent off-nominal performance of the transcription process used in the DFDR system. This Smart Flight Recorder approach shows promise for obtaining large quantities of statistical data for this and similar applications. These techniques and the results obtained in 200 hours of operation on a Beechcraft King Air are not discussed further in this report since they are described in reference 8.

SYMBOLS

a_n	incremental component of normal acceleration near the aircraft cg; g units positive toward the top of the aircraft
a_n+1.0	total normal acceleration near the aircraft c.g.; g units; positive toward the top of the aircraft
a_{nG}	incremental normal acceleration, identified as due to gusts, g units; positive toward the top of the aircraft
a_{nM}	incremental normal acceleration, identified as due to maneuvers, g units; positive toward the top of the aircraft
a_y	lateral acceleration near the aircraft cg; g units; positive toward the right wing tip.
B	Boeing
c	aircraft mean wing chord, feet
CAS	calibrated airspeed, knots
cg	center of gravity
C_{L_α}	aircraft lift-curve slope, per radian as used in the equations
dB	decibels
DC	Douglas Commercial
deg	degree
DFDR	Digital Flight Data Recorder
DVGH	digital VGH
f	frequency, cycles per second
FAR	Federal Aviation Regulations
FLP	flap
ft	feet
g	acceleration of gravity
GW	gross weight, pounds

HP	pressure altitude, feet
Hz	frequency in cycles per second
kft	thousands of feet
K_g	$= \frac{0.88\ \mu_g}{5.3\ +\mu_g}$, gust alleviation factor from reference 13
klbs	thousands of pounds
kts	knots
L	Lockheed or Left; usage is obvious
LaRC	Langley Research Center
M	Mach number
NACA	National Advisory Committee for Aeronautics
NASA	National Aeronautics and Space Administration
R	right
S	aircraft reference wing area, square feet
SPL	spoiler
U_{de}	derived equivalent gust velocity, feet per second
VG	velocity and "G" load measurement system
VGH	velocity, "G" load, and height measurement system
US	United States
V_e	equivalent airspeed = True Air Speed x $\sqrt{\frac{\rho}{\rho_o}}$
ρ	air density, slugs per cubic feet
ρ_o	standard atmosphere sea level air density, slugs per cubic feet
μ_g	$\frac{2W}{C_{L_\alpha}\ \rho\ cgS}$, mass parameter from reference 13
$\lvert\ \rvert$	absolute value
>	greater than

AIRCRAFT AND INSTRUMENTATION

Aircraft

DFDR data were purchased from a U.S. airline operating a Lockheed L 1011-1 with three Rolls Royce RB-211-22 high-bypass-ratio turbofan engines of 42,000-pounds thrust each. A three-view drawing of the aircraft showing dimensions and control locations is given in figure 1. Weight and geometric characteristics are listed in Table I and the untrimmed flexible airplane lift-curve slope data used in the analysis are given in Table II.

Instrumentation

No new instrumentation was added to the aircraft. Instead, it was decided to access a small subset of the data already being obtained on the existing DFDR required by the FAR 121.343 and described in reference 6. Parameters finally selected by NASA, after discussions with the aircraft manufacturers, are given below with their range, sample rate, and accuracy taken from reference 6.

Parameter	Range and Units	Samples per Second	Accuracy
a_n+1.0	-3g to +6g	4	±.2 g's stabilized, ±10% transient (see page 6)
a_y	-1g to +1g	4	±.05 g's stabilized, ±10% transient (see page 6)
CAS	100 to 450 kts	4	±10kts
HP	-1000 to 50,000 ft	1	±100 to 700 ft
FLP	-5° to 60°	1	±3°
SPL 2R	-5° to 60°	1	unknown
SPL 5L	-5° to 60°	1	unknown

Accelerometer transient response is specified in reference 6 as:

> "8.4 Filtering (Output Frequency Response)
> The accelerometer should contain effective filtering means to screen out undesired high frequency vibration data. The output signal level should be 3 dB below the signal levels set for in Section 8.3.1 for vibration having a frequency of 4 Hz. At higher frequencies, the output signal levels should continue to decrease at the rate of 12 dB per octave."

The signal levels referred to in Section 8.3.1 of reference 6 are the null signal levels.

Appendix A shows that in one test, normal accelerations measured at 4 samples per second with a DFDR system, like that described in reference 6, correlated well with normal accelerations measured with a more accurate NASA data system. In this test, the standard deviation of the DFDR normal acceleration measurement with respect to that of the NASA system was 0.055 g's. Thus, the normal acceleration measurement from the DFDR can be expected to be well within the $\pm$0.2g quoted at 4 samples per second. Appendix A also shows, however, some unpublished results of a NASA B 57B flight test which indicate that for that test where the accelerometer cut-off was 10 Hz at 4 samples per second, the acceleration exceedances are 1/2 to 1/3 those obtained at 20 to 40 samples per second. Similar considerations may apply to the lateral acceleration exceedances. This possible limitation on the acceleration data presented herein, and in the companion Volumes II, III, IV, and V, must be considered in the application of the present results.

SCOPE OF DATA

The data were obtained from flight operations of one regularly scheduled airline operating over the route structure from February 1973 to May 1973, shown in figure 2. Some gaps in coverage did occur due to the characteristics of the DFDR "Crash Recorder" system which acts as a 25-hour loop tape erasing any data older than 25 hours. The aircraft flew 8 to 12 hours/day; thus, the airline company was asked to provide data from the recorder every 2 or 3 days to provide continuity of data on one aircraft. This was not always achieved, however, and gaps in continuity did appear. Furthermore, some whole tapes were rejected in the edit process, resulting in additional gaps in the coverage of the service record. This was not considered serious in the development of this prototype data system.

Eighty-three flights were utilized for a total of about 200 hours and 91,000 nautical miles. The data were obtained by the airline operator in 1973 and were purchased by NASA in 1977. Subsequent development of the reduction techniques, including editing and definition of the final statistical formats shown herein, involved several interactions with airliner manufacturers and operators.

DATA REDUCTION

Process

The basic data reduction process is shown in figures 3, 4, and 5. The airline company supplied transcription tapes of the requested parameters, takeoff and landing gross and fuel weights, strip charts, and listings of the first 300 seconds of all of the parameters. The transcription tapes were converted into NASA engineering units tapes from which time history plots were made for editing purposes.

Editing

Originally, the time histories were "raw" or unedited and the editing was done manually. Later, a computer algorithm was developed to assist, and after some experience was gained in its use, the edit program was used to produce the engineering units time history plots. Appendix B describes the development of the KEDIT program and its application. It is a two parameter local signature analysis program designed to "pluck" or remove wild points and replace them with reasonable values--it is not a smoother. Other edit functions manually performed include:

1. Identification of lift-off and touchdown times
2. Bias removal
3. Data overlap deletions
4. KEDIT performance
5. Acceptance or rejection of each flight

An example of the results of this process is given in figure 6.

Weight Calculation

The weight at any time is found by a linear interpolation between the gross weight at lift-off and touchdown. Calculations summarized in Appendix C using manufacturer's fuel-flow equations indicated that the discrepancy was, at most, 2 percent occurring at the top of the initial climb on long flights. The difference was considered small and not worth the effort to reduce it.

Counting Technique for Accelerations

It was decided to utilize the level-crossing counting technique for acceleration exceedance analysis, due to its ease of application on the computer and its preference for design criteria evolution as opposed to fatigue life tracking, as pointed out in reference 9. The previous analog VGH programs (refs. 1, 2, 3, 4), using manual and eyeball methods, of necessity employed a peak-between-means counting technique in which the exceedances are accumulated from the largest value to the smallest. The two methods are illustrated in figure 7. Appendix A, figure A-4, shows a comparison of the two counting methods on an acceleration time history obtained from a NASA B 57 test flight. These results indicate that the two techniques give the same values at the end points of the load factor range, and are within a factor of 2 in the midrange. This same behavior is also shown in the results on page 32 of reference 10.

Gust and Maneuver Acceleration Separation

Inspection of many power spectra of the cg normal acceration data indicated that usually the low-frequency maneuver accelerations were sufficiently far removed from the gust responses so that suitable low-pass and band-pass numerical filters could be used to separate them out. Examples of such power spectra are given in figure 8. In these spectra, it is believed that the peaks below about 0.1 Hz are due to pilot induced maneuvers; those between 0.2 and 0.5 Hz are the basic airframe response to atmospheric turbulence in the short period mode with autopilot off. The significant responses between 0.7 and 1.0 Hz were identified as the aircraft turbulence response with autopilot on in the later phase of the program (Vol. II) where autopilot status was monitored. The 1.5 Hz response peak is believed to be due to the wing first bending mode. Accordingly, the filters illustrated in figure 9 and described in Appendix D were developed based on the methods of reference 11 and utilized here to separate the pilot-induced accelerations from the aircraft gust response. The break frequency selected for this aircraft was 0.09 Hz; the top of the band-pass was set at 1.2 Hz to remove structural resonances, that is, wing first bending mode at 1.5 Hz (fig. 8). Results of the application of these filters to a typical time history are given in figure 10.

In the earlier analog VGH program, the gust peaks were identified by eye by their sharp rise times compared to the maneuver-induced g loads, and the increment of the gust

acceleration relative to the maneuver acceleration was measured directly from the time history trace (ref. 12). Due to the large amounts of manual labor involved, the minimum acceleration increment utilized was usually 0.2 g, and occasionally 0.4 g whereas in the present DVGH program, g increments of 0.05 g have been utilized at small absolute g levels.

Gust Velocities

Derived gust velocities U_{de} were computed using the method of reference 13, and the band-pass component of the normal acceleration at the cg, a_{nG}. Thus,

$$U_{de} = \frac{2W}{K_g \rho_o C_{L_\alpha} SV_e} a_{nG}$$

$$\text{where } K_g = \frac{0.88}{5.3 + \mu_g} \mu_g$$

$$\text{and } \mu_g = \frac{2W}{C_{L_\alpha} \rho cgS}$$

In the current program, the lift-curve slope C_{L_α} is the untrimmed flexible lift-curve slope for the entire airplane, and is a function of Mach number, altitude, and flap deflection and is given in Table II. Time histories of U_{de} were computed using the above equation; U_{de} exceedances were then determined using the level crossing technique on these U_{de} time histories.

Statistical Formats

Much of the data are given as a percentage of the total flight time that is spent in some particular condition, or combination of conditions. Thus, altitude is broken down into 9 bands (or bins

or intervals) 5000-feet thick, and the time spent therein is reported as a percentage of the total flight time (201 hours). (Some sorts were done using data base of 201.4 hours, some using a base of 201.13 hours.) The bands for the major parameters are:

Pressure altitude	5000 feet
Airspeed	10 knots
Mass	30,000 pounds
Duration	0.5 hours
Flap deflection	detent

In other instances, data are given as a percentage of total flights for a particular condition such as trip length, maximum altitude, and maximum normal acceleration.

RESULTS AND DISCUSSION

Organization

The detailed numerical results are presented in two sections:

1. Flight Profile Statistics
2. Acceleration Derived Statistics

Flight Profile Statistics are given on a Percent of Total Flight Time (201 hours) and Percent of Total Flights (83) basis. Some Flight Profile Statistics are given for the entire flight (flaps up or down), for flaps down only, and for spoilers deployed. The Acceleration Derived Statistics are given on a Counts/Hour and Percent of Flights basis. The groupings for both results are given in figure 11 together with their corresponding figures 12 through 24. The differences between the DVGH and VGH systems are summarized on figure 25, and figure 26 attempts to show the effects of several of these differences on the exceedance results.

In addition, some effects of autopilot operation on normal accelerations are discussed in the section "Autopilot Effects" and illustrated in figure 27.

Flight Profile Statistics

Many Flight Profile Statistics hitherto not generally available have been compiled using a subset of the data types available on the original DFDR. These statistics are discussed here for the three conditions shown in figure 11: (1) for the "Entire Flight" from takeoff to landing with flaps up or down, (2) for "Flaps Down Only," and (3) for "Spoiler Deflections."

Entire Flight.- After several iterations with airline aircraft designers, it was decided to provide the Flight Profile Statistics for entire flights in the following ways:

12(a)	-	Gross weight histograms for takeoff and landing
12(b)	-	Fuel weight at takeoff and landing versus trip duration: matrices
13(a),(b),(c)	-	Gross weight and altitude times for flight modes of climb, level, and descent: matrices and plots
14(a),(b),(c)	-	Airspeed and altitude times for flight modes of climb, level, and descent: matrices
15(a),(b),(c)	-	Maximum altitude per flight versus flight duration: matrix and plots

The plots do not include all data in the parent matrices; rather they represent summary trends of interest. The matrix formats themselves show all available data and are constructed

to permit rapid identification of areas of maximum activity by a visual scan without plotting.

Figure 12(a) shows that no flights took off weighing more than 430,000 pounds; over 40 percent weighed between 370,000 to 400,000 pounds. The smallest takeoff mass, 280,000 to 310,000 pounds was used for about 7 percent of the flights. In landing, none of the aircraft grossed less than 280,000 pounds, nor more than 370,000 pounds. The matrices of fuel weight at takeoff and landing versus trip duration, figure 12(b), show the most popular trip length (31.3 percent of the flights) was 2 to 2-1/2 hours carrying 70,000 to 100,000 pounds of fuel at takeoff; 22.9 percent of flights landed with between 10,000 to 40,000 pounds of fuel. For all trip lengths, 57.7 percent of the flights landed with between 40,000 to 70,000 pounds of fuel.

The joint distributions of total flight time spent in weight and altitude bands for climb, level, and descent flight modes are given in matrix form in figure 13(a) and plotted in summary form in figure 13(b). The matrix shows that in climb, 6.5 percent of the time is spent at 370,000 to 400,000 pounds with each 5,000 feet altitude band up to 34,500 feet showing roughly the same 1 percent usage. In level flight, the most frequent condition is between 340,000 to 370,000 pounds gross weight at 33 percent of the time. At these conditions, 17 percent of the total time is spent between 29,500 and 34,500 feet, with the next higher and lower altitude band carrying 9 percent and 5 percent, respectively. In descent, 7 percent of the time is at 310,000 to 340,000 pounds, with each

of the three altitude bands below 14,500 feet showing 1 to 1.7 percent of the total flight time. The summary column on the right, plotted in figure 13(a), shows that about 16 percent of the time is spent in climb at all weights and altitudes, 69 percent in level flight, and 15 percent spent in descent. The summary rows for time spent in each altitude band for climb, level, and descent flight modes are plotted in figure 13(c).

Joint distributions of the total flight time spent in 10-knot CAS intervals and 5000-feet altitude bands are given in matrix form in figures 14(a), 14(b), and 14(c) for climb, level, and descent flight modes, respectively. Figure 14(a) shows that in climb, CAS as high as 370 to 380 knots were used in the altitude range 9500 through 24,500 feet for 0.0093 percent of the total flight time (about 1 minute). And for 3.2 percent of the total flight times, climb airspeeds of 340 to 360 knots were used in traversing this altitude band as indicated by the dotted boxes. The lower CAS used above and below this altitude band can be readily identified as shown in the remaining dotted boxes in the figure. In level flight, the most prevalent conditions are CAS = 300 to 320 knots at 29,500 to 34,500 feet about 25 percent of the time, and 290 to 300 knots at 34,500 to 39,500 feet about 12.5 percent of the time. Descent shows a broader distribution; the single most popular condition is 140 to 150 knots in the lowest altitude layer in terminal cruise, approach, and landing conditions. These matrix-type plots readily lend themselves to hand-sketching-in of contours of constant percent time; an example of

this is given in figure 14(c), for descent, where a contour enclosing all points greater than 0.25 percent of time has been indicated by dashed lines to illustrate the broad distribution for this parameter.

Figure 15(a) gives the matrix of percent of flights to maximum altitude versus flight duration. Plots in figures 15(b) and 15(c) show that more than 75 percent of all flights went to a maximum altitude greater than 29,500 feet. Most of these had flight durations greater than 2 hours. About 23 percent of the flights went to a maximum altitude between 34,500 and 39,500 feet for trips 2 to 2-1/2 hours long. About 5 percent of the flights had maximum altitudes less than 9,500 feet and durations of one hour or less.

Flaps Down Only.- Flap detent position data for the trailing-edge flap surface are given in figure 16. Note that any flap deflection within the detent limits shown in figure 16 were categorized as "in the detent." On takeoff, the initial setting was 10-degrees detent (except in two cases which took off with 22 degrees) lasting about 0.13 percent of total time, followed by 4 degrees for about 0.70 percent of total time. By definition, the takeoff phase begins at lift-off and ends the first time the flap setting goes to zero. Subsequent operations with flaps down are in the landing phase. Flap deflection above 10,000 feet did not usually occur, except for one instance where 3-degree flap was selected while in a holding pattern at 15,000 feet at 210 knots CAS. Fourteen minutes later, the aircraft descended through 10,000 feet and the data were picked up in the regular computer analysis.

For landing, the most used detents were 4, 10, 22, and 42 degrees; the 18, 27, and 33 degree detents were generally transited rapidly.

For each of the most used detents, the gross weight, altitude above airport, and airspeed distributions are given separately for takeoff and landing, figures 17(a) through 17(f). For reference, the flap placard limit speed is also shown on the airspeed distributions. It can be seen that the airspeed distributions become more sharply peaked as the flap deflection increases.

Spoiler Deflections.- Data showing the operation of spoilers 2R and 5L (see fig. 1 for locations) are given in matrix form as a percent of total flight time in a given deflection band and within a given airspeed band in figures 18(a) and 18(b) and in plotted form in 18(c). Altitudes above which spoiler deflections are greater than 10 degrees are plotted in figure 19. These data indicate that most spoiler operations occur at about 240 to 260 knots at altitudes between 4,500 to 14,500 feet. They also show that spoiler 2R is used about 10 percent more often than spoiler 5L. These usages are as speed brakes only, with flaps up. Note that spoiler 2 moves linearly with speed brake handle position. Spoiler 5 moves nonlinearly with handle position, such that the spoiler angle for number 5 is much less than for number 2, until maximum spoiler deflection angle is approached. In addition, deflection of individual spoilers is limited by available control hinge movements; the full spoiler deflection of 60 degrees normally can be reached only at airspeeds below about 200 knots. In the

present data set, the maximum deflection of 55 to 60 degrees was reached only briefly (3 to 4 seconds at 200 to 220 knots).

Acceleration Derived Statistics

The acceleration level crossing counts per hour results, obtained within the given pressure altitude bands, are given as follows:

Quantity	Data Matrix	Plots for altitude
a_n	fig. 20(a)	d,e,f,g,h,i,j,k,l
a_{nM}	fig. 20(b)	d,e,f,g,h,i,j,k,l
a_{nG}	fig. 20(c)	d,e,f,g,h,i,j,k,l
a_y	fig. 21(a)	b,c,d,e,f,g,h,i,j

The following observations are noted for the normal acceleration results in figure 20:

1. The $a_n = 0$ level crossing counts/hour increase with altitude, generally.

2. The $a_n = 0$ level crossing counts/hour for a_{nG} are slightly higher than those for a_n because of the biasing induced in the a_n by the positive load factor in maneuvers as shown in the sketch below.

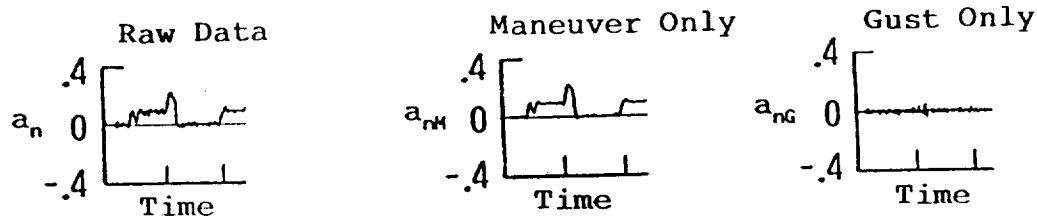

3. Approximate positive-negative symmetry of the data is observed

The a_y data, figures 21(a) through 21(j), show slightly higher rates at $a_y = 0$ at the higher altitudes.

The U_{de} exceedances derived from the a_{nG} are given in figures 22(a) through 22(j).

The maximum positive and negative normal accelerations experienced on each flight are shown in figures 23(a) through 23(f). The results indicate that for a_n, about 30 percent of the flights experienced between 0.25 and 0.30 plus g's, and 37 percent experienced between -0.20 and -0.25 g's. The most frequently experienced a_y was in the .04 to .06 interval both positive and negative. The 0.15 to 0.20 maximum gust g's per flight, figure 23(d), appear reasonably symmetric at about 35 percent of the flights. Interestingly enough, the most prevalent negative maneuver g's, figure 23(e), occurred significantly more often (57 percent of the number of flights) than the most prevalent positive (39 percent of the number of flights). These maximum g level data have been compiled in figure 23(f) to show the percent of flights to exceed a given g level. Thus, +0.3 a_n was exceeded on about 45 percent of the flights, +0.3 a_{nM} on about 5 percent of the flights, and +0.3 a_{nG} on 17 percent of the flights.

For each flap detent position, the a_n level crossing counts per hour are given in matrix form in figures 24(a) and 24(b) for take off and landing. Corresponding plots are given in figures 24(c) and 24(d). The dotted line in those plots is taken from figure 20(d) for a_n. The only significant difference in these results is that for takeoff with 4 and 10 degrees of flaps, negative normal accelerations are experienced somewhat more frequently than for the data from figure 20(d), which are for any flap setting, and at +0.4g, where the data indicate higher rates than with flaps down 4 and 10 degrees.

Comparison of DVGH and VGH Data

Previous published information by NACA/NASA on flight load experiences of transport airplanes during routine operations (i.e. refs. 1-5) were derived from analog type velocity-acceleration-height (VGH) recorders using manual data reduction techniques. The data in this report were obtained from digital recorders utilizing an automatic data reduction process. In both cases, the primary measurement is acceleration measured very near the airplane's center of gravity. Some of the differences between the two recording and processing techniques are listed in figure 25. Before comparing results, a short synopsis of the two systems is given.

VGH Program.- The frequency response of the VGH recorders were from near DC to 5 Hz. Reading accuracy and overall system errors combined to provide an accepted band width of 0.01 to 5 Hz for gust and maneuver load determination (ref. 14). Data were recorded as a continuous acceleration time history on 70mm photographic paper roll film. Peak accelerations were manually read in $\pm$0.01 g increments from the 1.0 g level flight reference line. Only the maximum peak occurring between successive crossings of the 1.0 g level flight reference line were read and counted (see fig. 7) Small oscillations of magnitude $\pm$0.05 g or less (and occasionally up to $\pm$0.3 g) about the zero level were not counted. The peaks were then cumulatively totaled from the highest level to the lowest to produce a frequency of exceedance distribution. Separation of gust and maneuver accelerations were dependent on the film reader's

experience but, generally, gusts were identified by their rapid rise and decay time, i.e., they had a relatively higher frequency than maneuver loads. The method of manual reading and representation of the analog data became known as the cumulative peak-between-means counting technique.

Digital Flight Data Program.- The process for reducing data from the digital recorders was more automated and, therefore, differs somewhat from that in the VGH Program. First of all, the sample rate was limited to 4 per second since that was already in use on the DFDR system. The maximum usable data frequency, therefore, would be near 2 Hz. Appendix A addresses the effect of sampling rate on determination of turbulence induced accelerations. It shows that during a 4.5-minute turbulence encounter of a B 57 airplane equipped with a high response gust measurement system (20 Hz accelerometer cutoff) there was a loss of 1/3 to 1/2 of the acceleration peaks as the data reduction sampling rate dropped from 40 per second to 20 per second to 4 per second. Also, the DFDR acceleration data were filtered to reject frequencies above 1.2 Hz to eliminate wing-body elastic response. Automatic separation of gusts and maneuver accelerations were accomplished using a low pass (maneuver) filter, DC to 0.09 Hz, and a high pass (gust) filter, 0.09 to 1.2 Hz.

Comparison of Results.- Figure 26 compares the derived gust velocity experience from 200 hours of L 1011 data with the VGH data from reference 4. Also shown are data from Volumes II, III, and IV of this report that included additional L 1011 data, B 727 and B 747 data. The two different L 1011 aircraft agree very well

despite an almost factor of 10 difference in the number of flight hours. The L 1011 data are noticeably higher at the lower gust values than the Boeing aircraft and the VGH gust curves derived from reference 4. All of the curves seem to converge at about 20 feet per second gust velocity except for the extrapolated B 747 curve from volume IV. The consistently lower values for that particular aircraft may be explained by the fact that it was used almost entirely on long overwater flights during the period of data collection.

The higher slope of the digital data may be related to differences between the manual and automatic data reduction processes. In the manual reading of VGH data, the acceleration peaks are increasingly more difficult to distinguish as they become smaller in the photographic time history traces. Thus, there may be a tendency to undercount VGH accelerations, whereas the digital process would provide an accurate count regardless of the peak magnitude, provided the sample rate were adequate. As previously discussed, the 4 sample per second rate used to obtain the present digital results may have missed counting a significant number of actual acceleration peaks. If this is the case, then the digital exceedance counts would be higher than shown.

Because of the many differences between the two data collection programs and because the current digital data suggests a change in slope of the derived gust velocity experience from previous VGH results, the author does not feel that it is practical to define a correlation factor to permit combining all of the data sets. It is recommended, however, that any future digital flight

loads program for transport airplanes consider increasing the frequency response of the gust measurement and analysis system to a level that, as a minimum, matches the VGH system. The new system should provide information at not only the aircraft short-period response frequency, but also at the higher frequencies associated with significant aeroelastic modes of the aircraft structure.

Autopilot Effects

Although autopilot status was not monitored in this test, some confirmation of some of the effects predicted by reference 15 was gleaned from the present results. Thus, the theoretical results of reference 15 indicate that the effects of the autopilot should be:

1. "...the introduction of multiple response modes at frequencies both below and above the controls-fixed short-period frequency...," and,

2. to reduce the gust response magnitude by 10 to 25 percent.

Some evidence of the existence of a resonance at a frequency below the controls--fixed short-period frequency may be seen in the sporadic appearance of a low amplitude limit cycle oscillation on a_n. A typical occurrence is shown in figure 27. The occurrence, magnitude, and frequency of this oscillation are more fully documented in the test reported in Volume II where autopilot status was monitored. The effect of the autopilot on the response above the controls-fixed short-period frequency is shown in figure 8 where the data intervals evidently overlapped autopilot "off" and "on" periods, resulting in some response at ~0.2 Hz and some at ~0.8 Hz. This too is more fully illustrated in Volume II.

However, the effects of the autopilot operation on the magnitude of the gust response and its effect on a_n and the U_{de} derivation could not be determined here, due to the lack of autopilot status and other information. Autopilot effects were not accounted for in the results of the VGH program, references 1-4.

CONCLUSIONS

Initial results of an effort to utilize a limited data set from existing aircraft Digital Flight Data Recorders to describe the aircraft operating conditions indicate:

1. A significant problem in Digital Flight Data Recorder data processing is data editing, particularly identification and replacement of wild points. A two-parameter algorithm has been developed and successfully applied to this problem, replacing the manual methods initially developed.

2. A large variety of Flight Profile Statistical Data useful to airline aircraft mission analysts and designers can be compiled from the few parameters selected.

3. An objective technique has been developed and applied to separate the maneuver and gust components of the normal acceleration data.

4. Acceleration gust exceedances derived from the DFDR system at 4 samples per second may be significantly less (approx. 50%) than if actual peak values were counted.

5. Improved data systems with sample rates and accelerometer natural frequencies higher than those used in the DFDR system will be needed to adequately describe the aircraft response to atmospheric turbulence.

APPENDIX A

ACCURACY CONSIDERATIONS

A complete study of the accuracy of each data type was not undertaken. However, due to its importance, some checks were performed on normal acceleration as described below. These results are also generally applicable to the lateral acceleration results given herein.

Accuracy

A basic DFDR system (ref. 6) was flown on a NASA DeHaviland Twin Otter aircraft to assess overall system performance by comparing its normal acceleration output with that of a NASA measuring and recording system. The overall accuracy of the NASA system was ± 0.12 g's, or about twice as accurate as the DFDR system at $\pm .2$ g's. The results of the test, shown in figure A-1, show that the DFDR system results had a standard deviation of about .055 g relative to the NASA system, with a correlation of 0.9790. In addition, figure A-2 indicates that the power spectrum from the DFDR system agrees well with that of the NASA system, with the largest discrepancy at around 0.02 Hz. Although data were obtained in a short time on only one flight, they indicate that the basic DFDR normal acceleration data are being accurately measured and recorded.

Sample Rate

The DFDR system described in reference 6 usually provides normal acceleration data at 4 samples per second. This provides adequate frequency response to about 2 Hz (based on the Nyquist rule), and was judged adequate to define the principal rigid-body

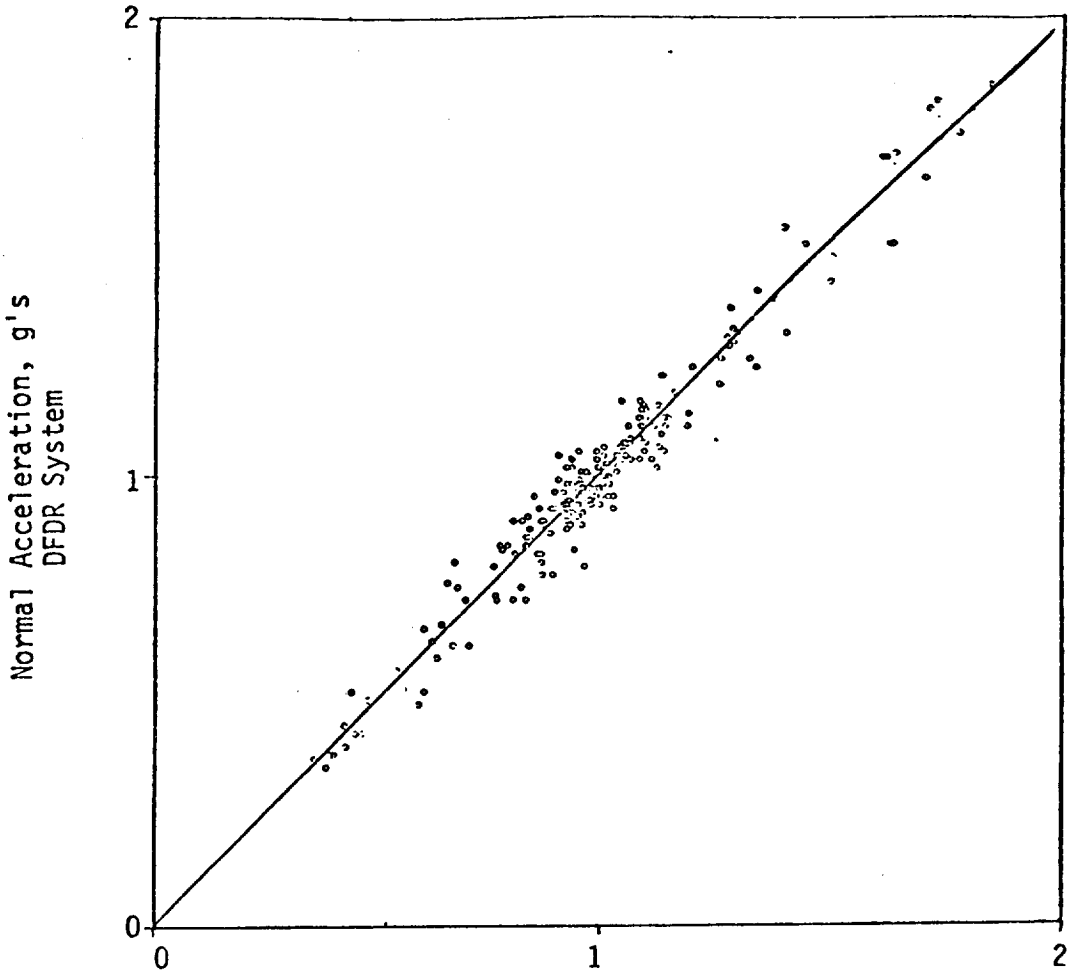

$$a_{n_{DFDR}} = .98865665\ a_{n_{NASA}} + .0061146752$$

Standard deviation = $\pm$.054772 g's

Correlation Coefficient = .9790

Figure A-1.- Comparison of DFDR system normal acceleration measurements with NASA system results.

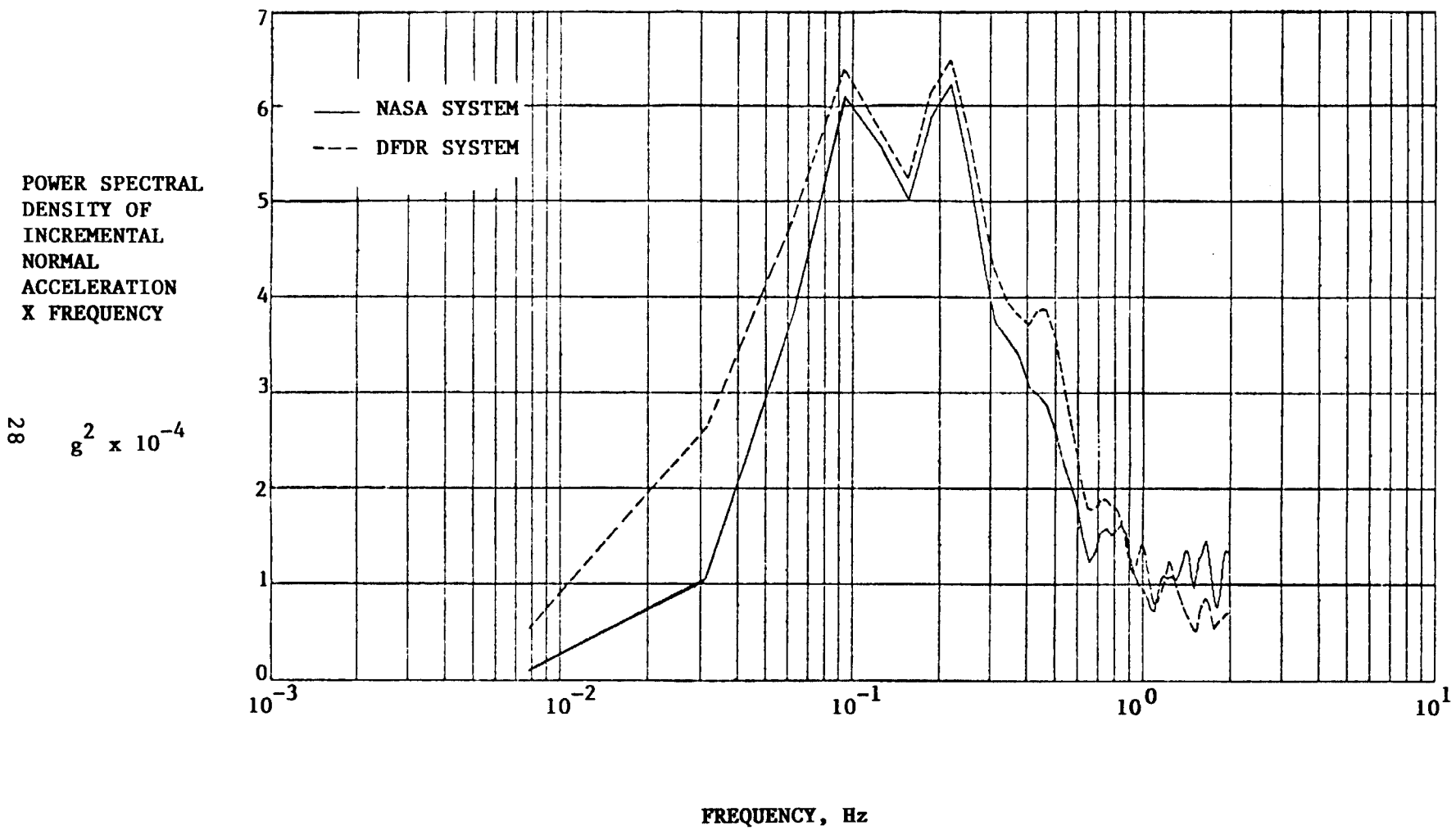

FIGURE A-2.- Comparison of normal acceleration power spectra measured by DFDR system and NASA measuring and recording system on a NASA DeHaviland Twin Otter aircraft.

gust response of large transports and for computing derived gust velocity, U_{de}. (Some data were obtained at 8 samples per second. The spectra for 4 and 8 samples per second, shown in figure A-3, are in good agreement up through about 2 Hz.) The question arises, however, about the effect of digital sampling on peak count since for previous analog VGH data the actual peaks were read--in other words--what is the reduction in peak count due to digital sampling? A recent unpublished analysis of a 200 samples per second digital cg normal acceleration record from a 1982 flight of a NASA B 57B aircraft in moderate turbulence is summarized in figure A-4. The results show that exceedances (both level crossing and peak count) increase significantly with sample rate up to 20 samples per second and only a slight increase when sample rate is increased from 20 to 40 samples per second. These results would indicate that exceedances reported herein may be 1/2 to 1/3 of those that would be determined from the previous method. This should be considered in the application of the acceleration data presented in Volumes I through V of this report.

If higher frequency response data are important in the future, consideration should be given to accelerometer frequency response characteristics. The so-called cutoff frequency (3 dB attenuation) typical to DFDR usage is 4 Hz. The accelerometer utilized for the research program with the B 57B aircraft had a cutoff frequency of 10 Hz.

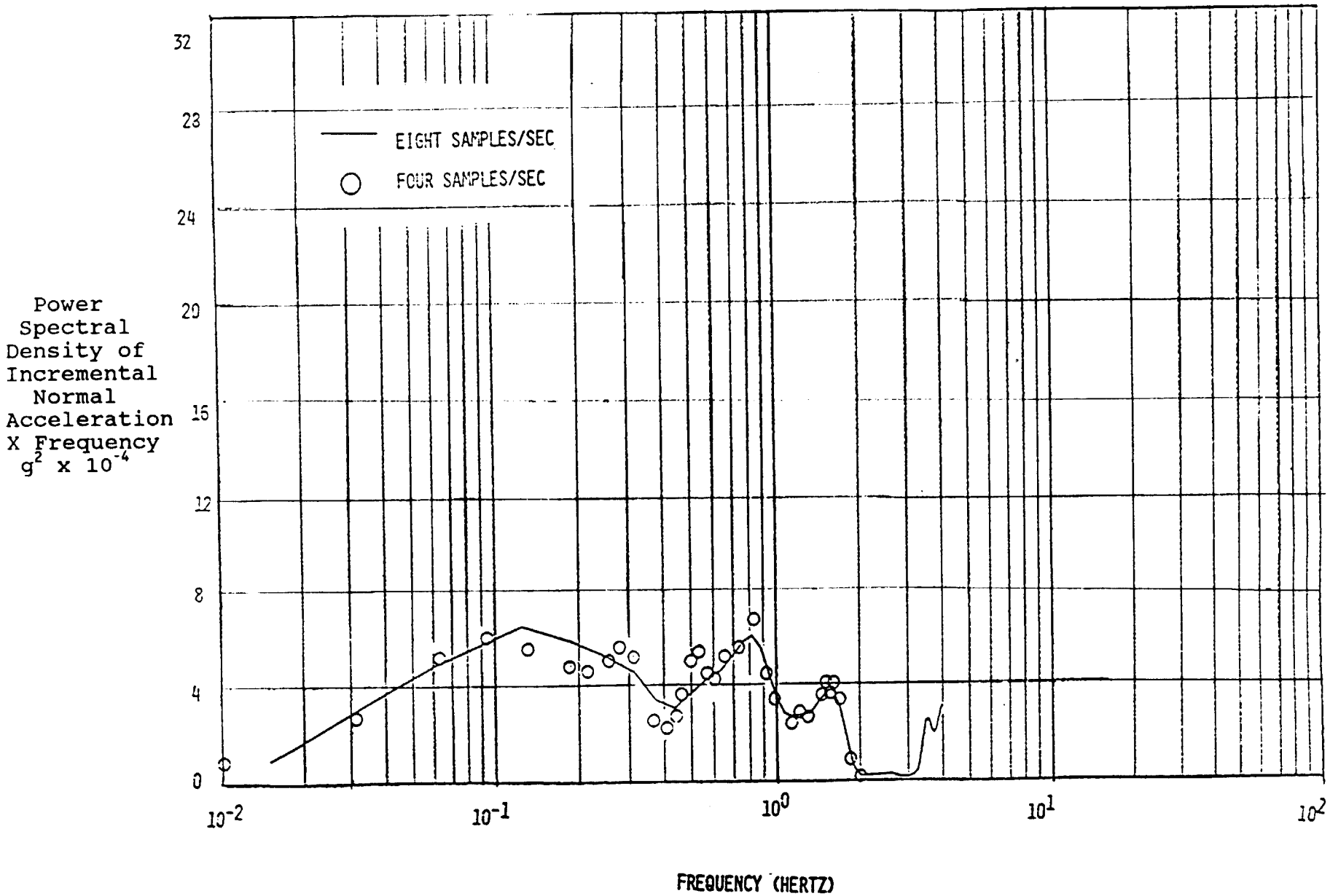

FIGURE A-3.- Effect of sample rate on definition of power spectra: L 1011.

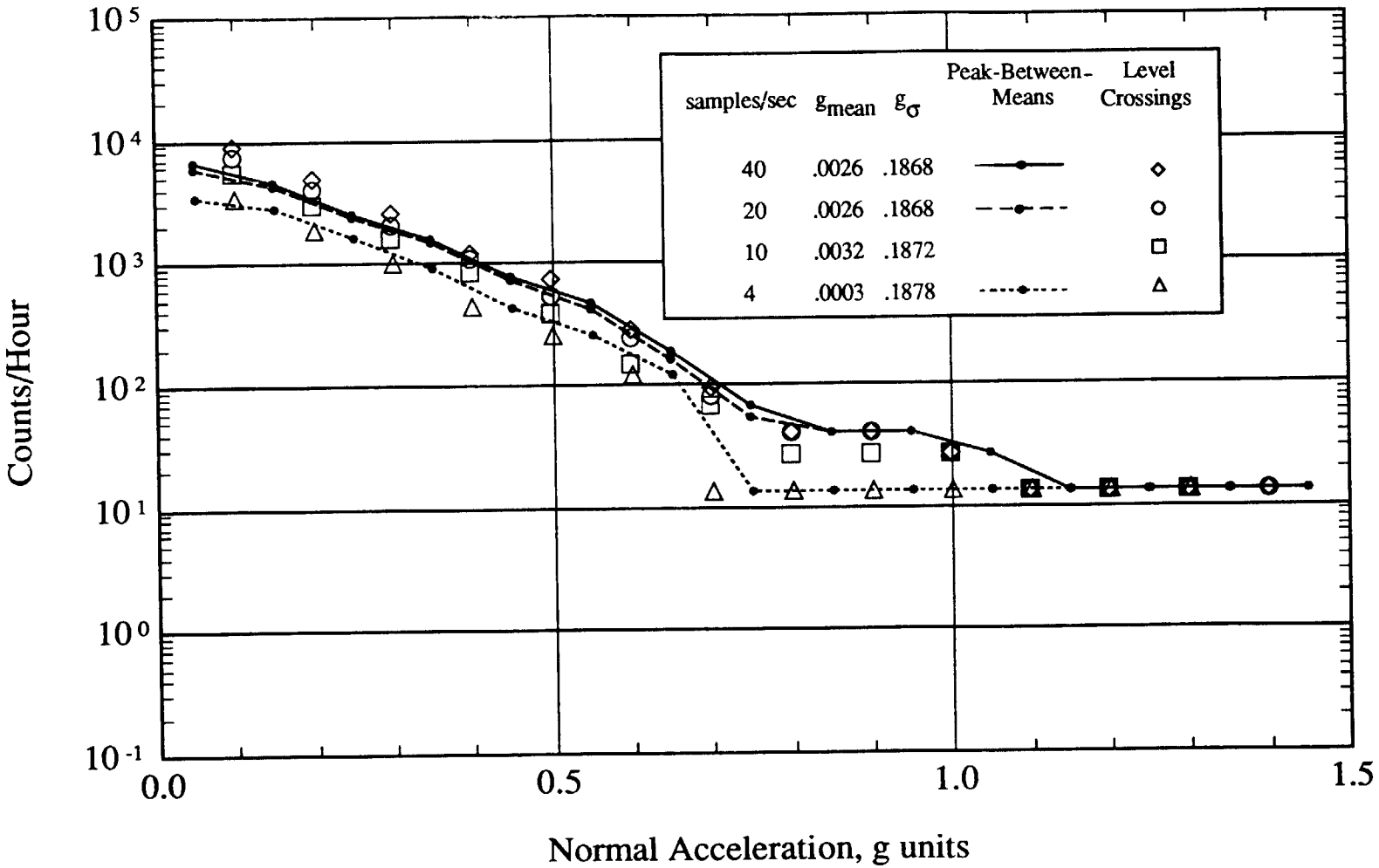

Figure A-4.- Comparison of acceleration exceedances obtained from unpublished NASA B57 4.5 minute run number 3113 using Level Crossing counting technique at 4, 10, 20, and 40 samples per second with exceedances obtained using the cummulative Peak-Between-Means counting technique.

APPENDIX B

WILD POINT EDITING ALGORITHM: KEDIT

This algorithm was developed in 1979 by D. A. Keskar of System Development Corporation Integrated Services, Inc. as part of contract NAS1-15400. The description given herein is based on that Company's document PDD-79-01, titled Program Description Document for Automatic Edit Program for Digital VGH Data Analysis.

OBJECTIVE

A software package needed to be developed for automatic data editing. It had to conform to the following restraints.

1. It should not replace any "good" data, with no artificial limit imposed on the magnitude of data excursions.
2. It should replace a "bad" point with the most probable data value at that point.
3. It should reconstruct data gaps caused by loss of frame synch.
4. The software package must be optimized as it will be used in editing hundreds of tapes, each 25 hours long, with sample rates as high as 4 per second.

PROBLEM SOLVING

The idea used in solving the problem is from basic statistics. Since the data are collected from the aircraft flying in a realistic physical environment, it must meet the tests based on moving average and standard deviation (fig. B-1).

The algorithm used is as follows:

For $i = p+1, p+2, \ldots . n-p$

calculate $\bar{x}_i = \frac{1}{2p} \sum_{\substack{j=-p \\ (j\neq 0)}}^{p} x_{i+j}$ mean

and $S^2_i = \frac{1}{2p} \left[\sum_{\substack{j=-p \\ (j\neq 0)}}^{+p} x^2_{i+j} \right] - (\bar{x}_i)^2$ variance

then

$$e_i = x_i - \bar{x}_i$$

If $| e_i | > K \cdot S_i$ perform "local mean" test

If $| e_i | \leq K \cdot S_i$ x_i is left unchanged.

The key to the success of this algorithm lies in proper selection of values of p and K.

Certain modifications must be done in the algorithm before it can be implemented. It should be noted that the concept of moving average fails if the point to be edited occurs just before a data drop out. To eliminate this problem, the points are temporarily replaced by the average of the previous 10 points. This results in a continuous record of data to be edited, (fig. B-2).

An analytical investigation was undertaken to find the most suitable values of constants p and K. As shown in figures B-3(a) and B-3(b), the decrease in the value of p below some threshold results in improper editing as the statistical information available is insufficient; while an increase in the value of p results in additional computational burden, as is obvious from the algorithm. For a reasonably good record (fig. B-4), values of $p \geq 4$ is sufficient as shown in figure B-3(a). On the other hand, for a record with a large number of noise spikes and out-of-synch points, figure B-5, p should be at least 8 as shown in figure B-3(b). Since the algorithm is used for editing many tapes, each 25 hours long, computational time requirement was a major consideration. For the data records considered, any value of p greater than 8 will edit the data satisfactorily, but will add significantly to computational cost by increasing the execution time. Based on this study, a value of $p = 8$ was found most suitable.

Similarly, a small value of K will replace some good points in the data while a large value of K will pass noise spikes in the data. The results of varying K in editing a typical data record are shown in figure B-5(a), B-5(b), and B-5(c). Thus, a few noise spikes were passed as good data with $K = 4$, while $K = 3$ replaced all the "bad" points by the most probable value at that point. This analysis resulted in choosing $K = 3$, which will insure replacing all "bad" data points while leaving most "good" data points unchanged.

The final algorithm computes mean and variance based on 8 points before and after the point in question. Since the points "after" are not edited as yet, the presence of noise spikes will add significant bias in mean and variance. To take care of this situation, the program checks the "after" points for unusually high values; for a point to be included in the statistics computation, it must be less than 25 times the value of previous point.

The objective of this algorithm is to replace all the "bad" points and retain almost all "good" data points. In a situation where mean and/or variance is close to zero, some "good" points may fail the edit test and eventually will get replaced. To alleviate this problem, one more test is done after the point in question fails the edit test.

Compute:

$$\bar{x}_{i_L} = \frac{| x_{i-1} | + | x_{i-2} |}{2} \qquad \text{(local mean)}$$

If $| x_i | > 2 \cdot \bar{x}_L$; replace x_i with $\bar{x}_i$

If $| x_i | \leq 2 \cdot \bar{x}_L$; $\bar{x}_i$ is left unchanged

This modification significantly improves the chance of retaining almost all "good" data points.

The final flow chart for the algorithm is given in figure B-6.

KEDIT SUMMARY

A software package has been developed for automatic editing of data obtained from airline aircraft Digital Data Flight Recorders. The algorithm has been tested on several data records to insure that all "bad" data points are replaced by the most probable data value at that point and almost all "good" data points are left unchanged. The algorithm also reconstructs the data gap of 4 seconds due to loss of frame synch. The algorithm is computationally efficient and takes about 6 seconds of CPU time to edit a record 10 minutes long sampled at the rate of 4 per second on a CDC-6000 series computer. The implementation has resulted in savings of 8 to 10 man hours per tape and has also improved the quality of editing since "human errors" are eliminated. Finally, the algorithm compiles statistics of types and numbers of points edited in each channel. This could be a vital piece of information in interpreting the final results. For example, if the number of points edited in one particular tape is too high, the confidence in the subsequent results obtained from the data of this tape should be low.

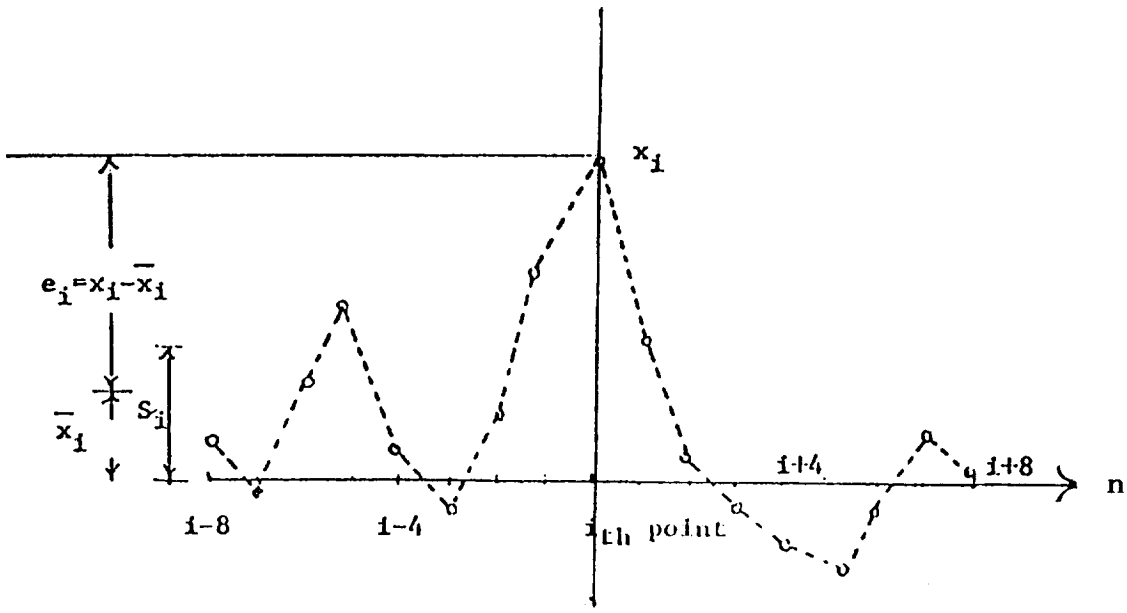

Figure B-1. - Illustration of algorithm.

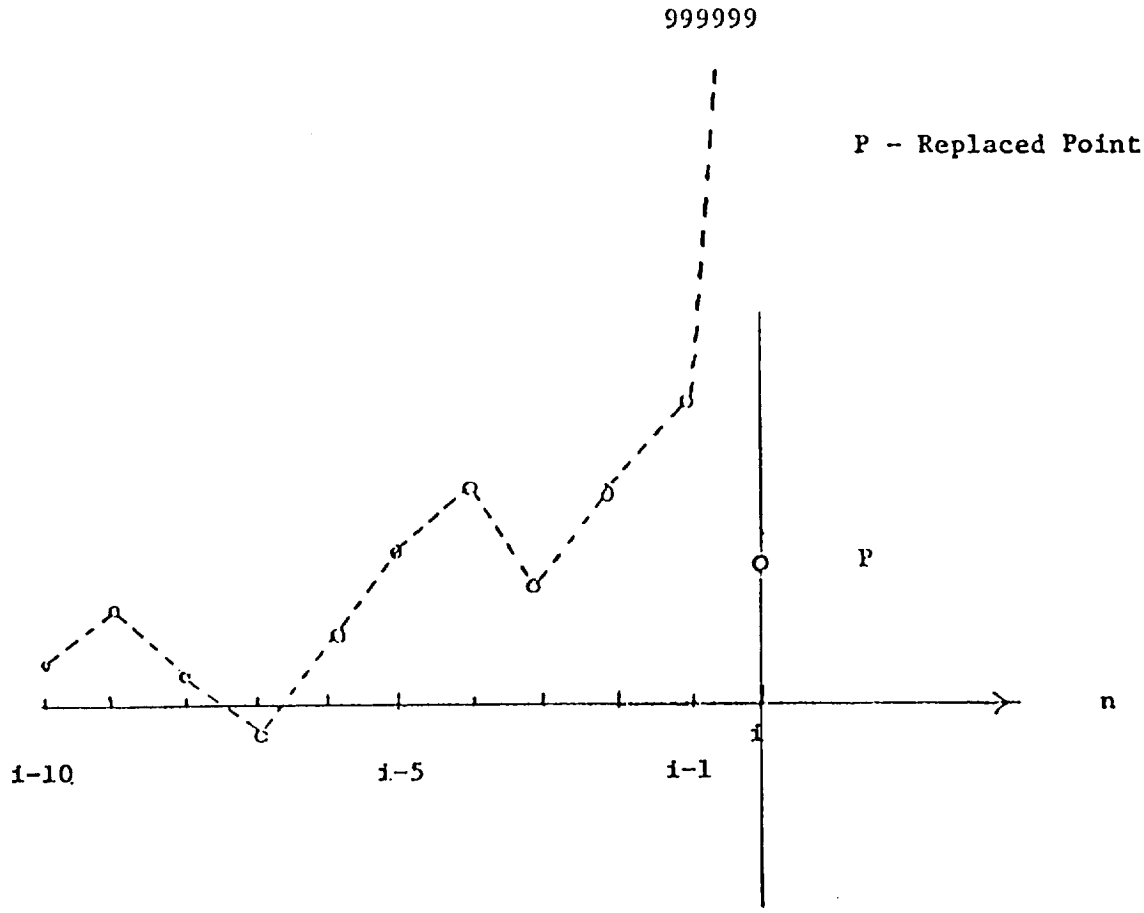

Figure B-2. - Temporary replacement of loss of synch data.

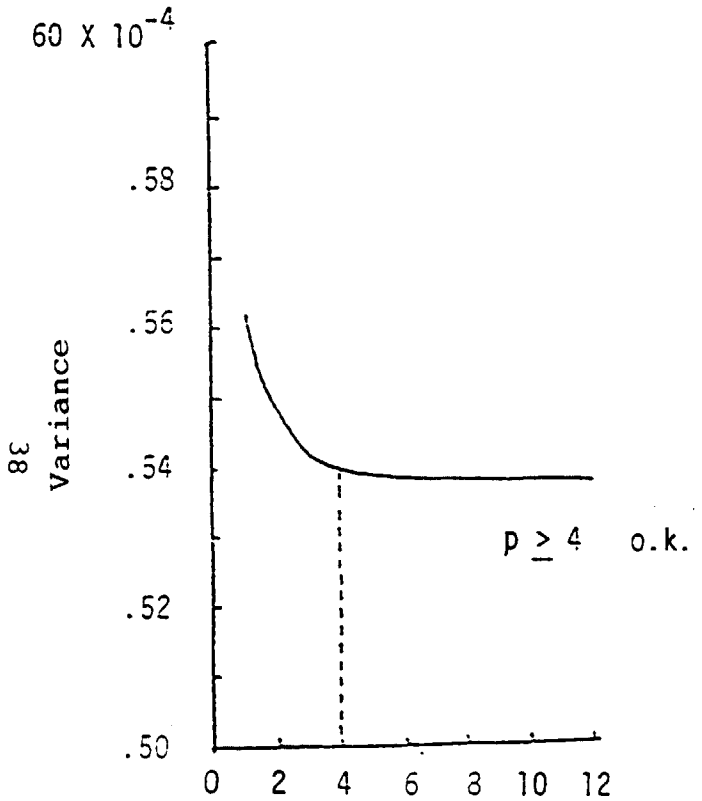

(a) A "good" record (figure B-4a)

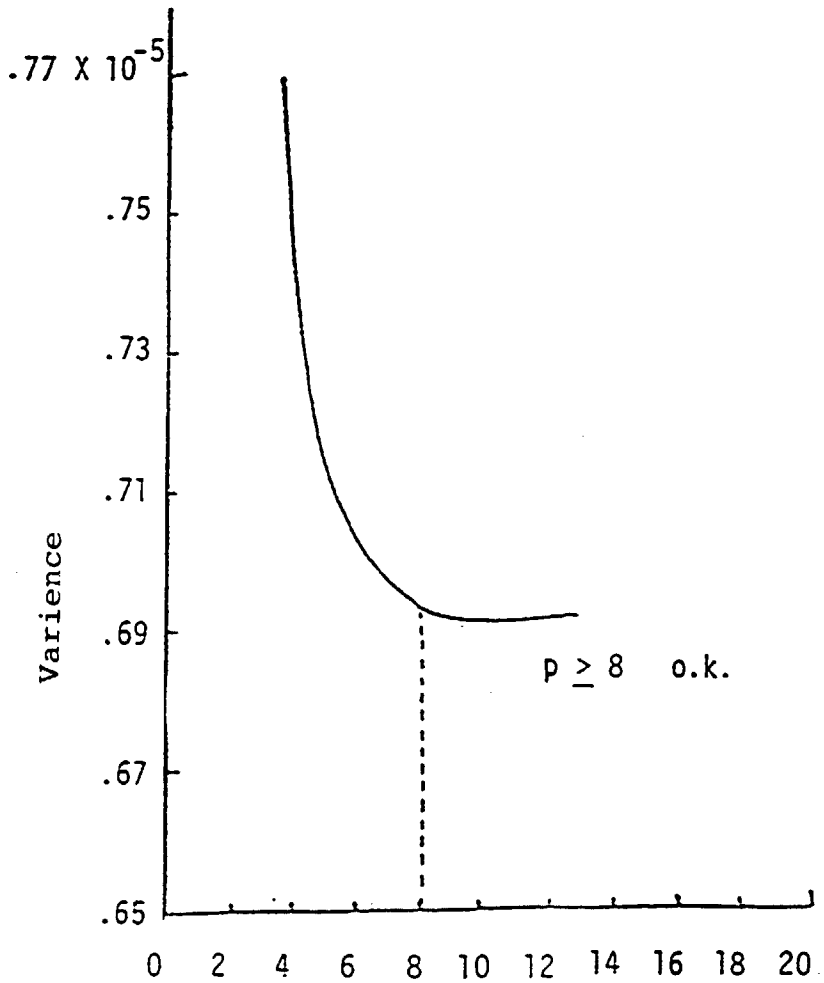

(b) A "bad" record (figure B-5a)

FIGURE B-3.- Effect of varying p on goodness of fit.

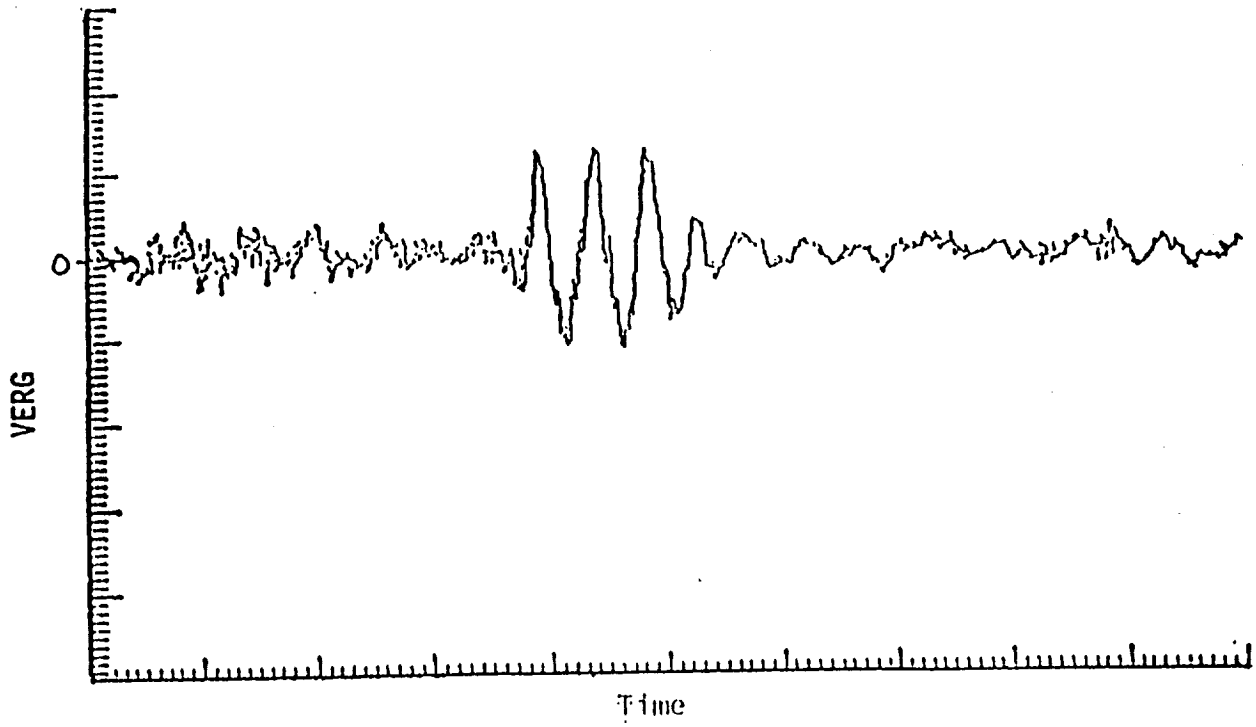

(a) Original "good" record

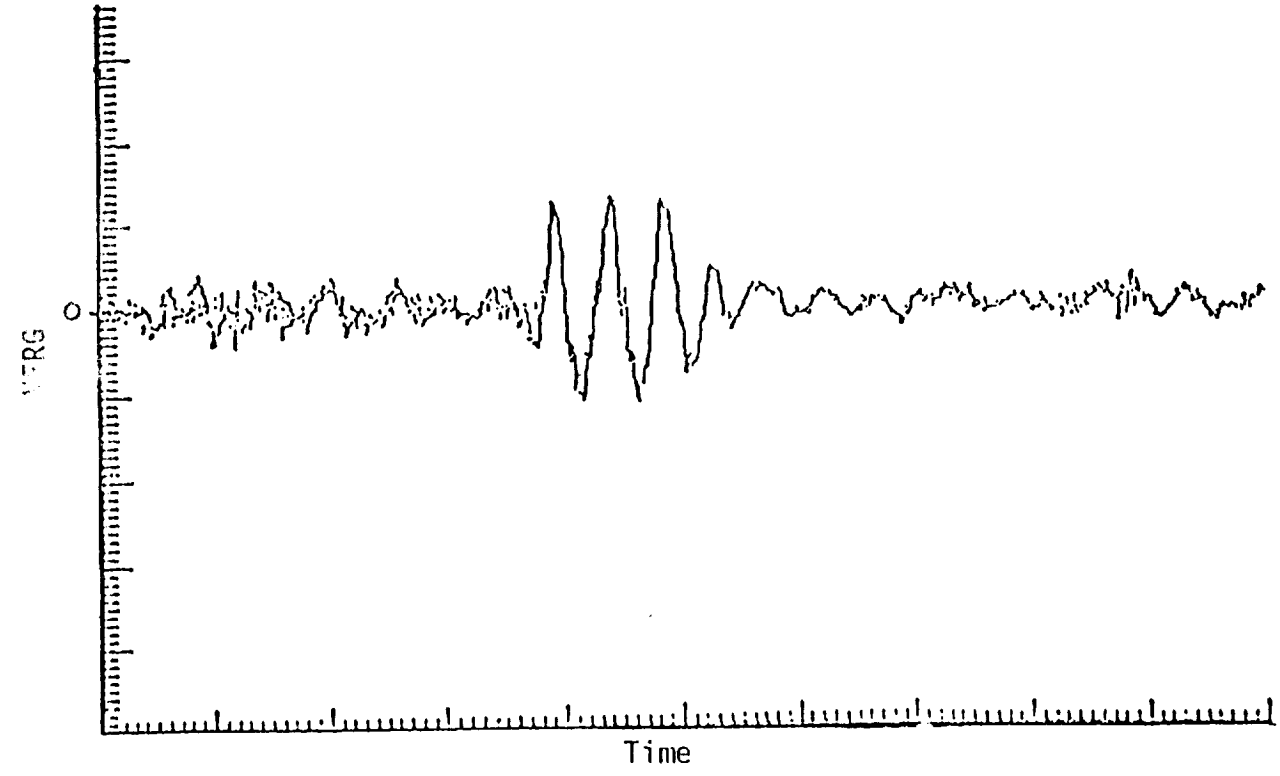

(b) Edited record with p=3 - no change

FIGURE B-4.- Illustration that algorithm does not alter good record.

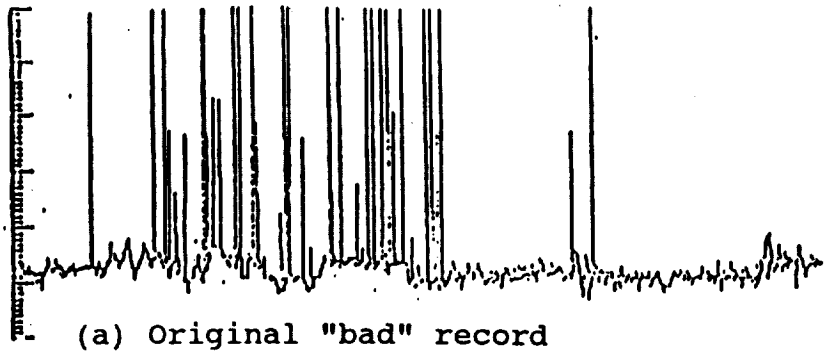

(a) Original "bad" record

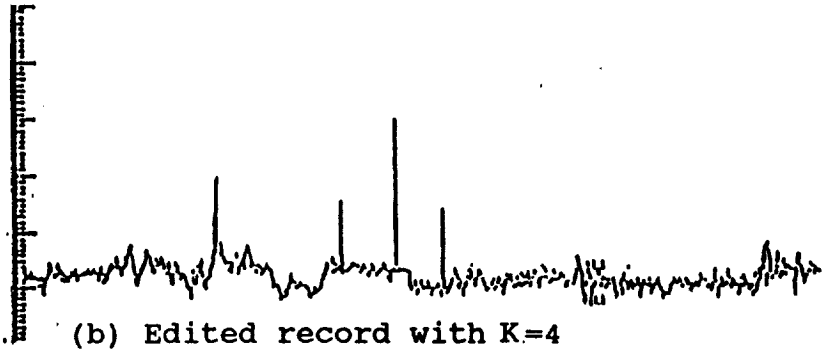

(b) Edited record with K=4

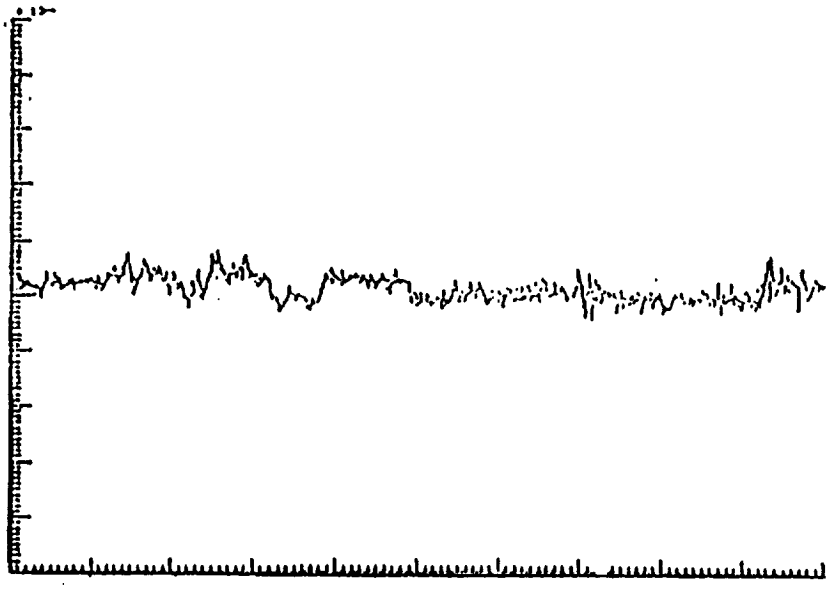

(c) Edited record with K=3

FIGURE B-5.- Illustration of effect of K on editing "bad" record.

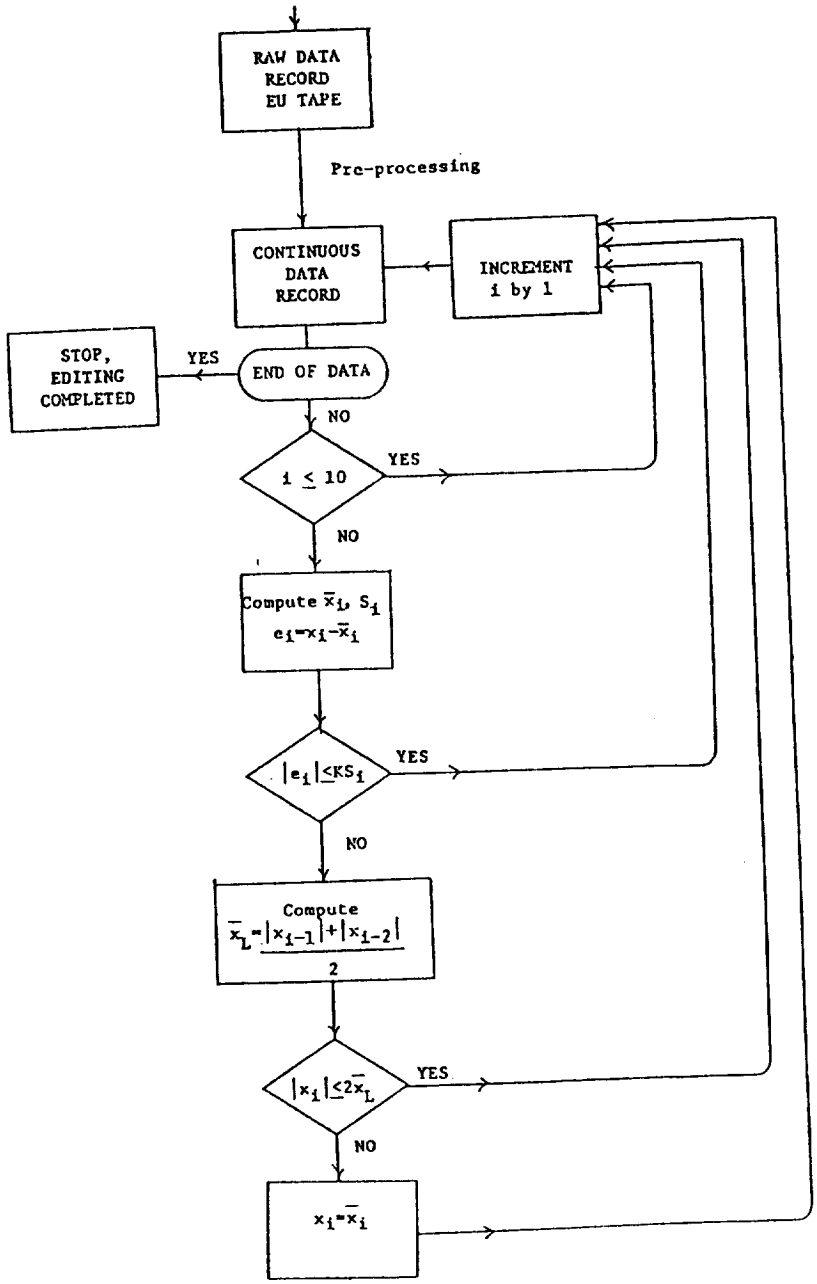

FIGURE B-6.- Flow chart of completed algorithm.

APPENDIX C

WEIGHT CALCULATION

Since the fuel weight on the L 1011 aircraft can amount to 30 percent of the gross weight (130,000 lbs out of 430,000 lbs), it was deemed necessary to determine a reasonably accurate aircraft weight at each instant of flight to permit accurate computation of the derived gust velocities. To permit this, the airline operator supplied for each flight the following support data:

Gross weight leaving the terminal
Gross weight at beginning of takeoff roll
Fuel weight at beginning of takeoff roll
Fuel burned terminal to terminal
Airborne time
Taxi-in time

It was further determined that the average fuel burn during the takeoff roll was 328 pounds.

These data were used to compute the gross weight at lift-off and at touch-down as shown in figure C-1. The gross weight at any time in between was computed assuming a linear variation with time. This linear assumption was found to be, for one flight, within 2 percent of the weight computed using fuel-burn equations supplied by the manufacturer. This comparison is shown in figure C-2.

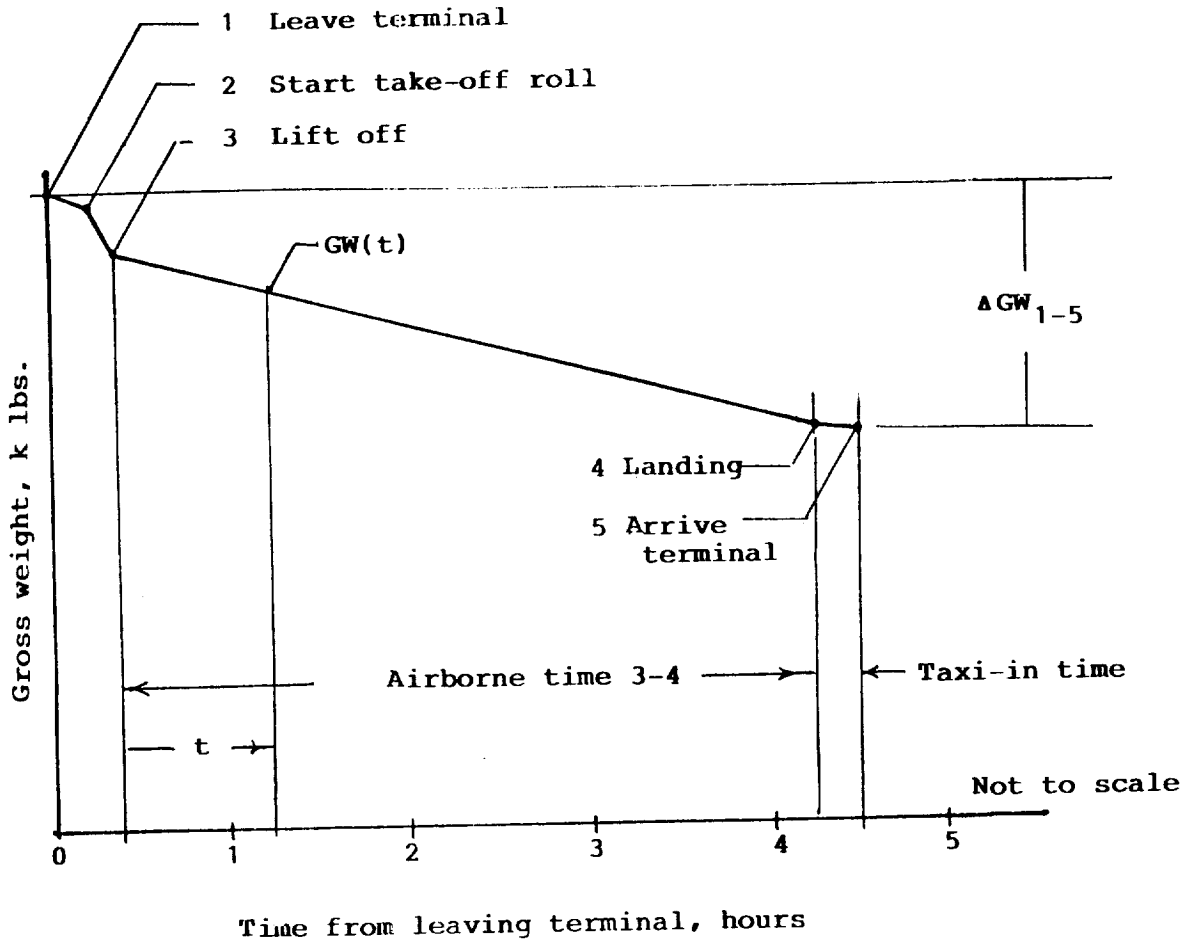

- Airline Operator Supplied for Each Flight
  - Gross weight @ 1
  - Gross weight @ 2
  - Fuel weight @ 2
  - Fuel burned terminal to terminal = ΔGW_{1-5}
  - Airborne time = t_{3-4}
  - Taxi-in time = t_{4-5} in minutes; x 100 lbs/min = ΔGW_{4-5}
  - Takeoff fuel burn = 328 lbs

- NASA Calculated
  - Gross weight @ 3 = GW @ 2 - 328 lbs
  - Gross weight @ 5 = GW @ 1 - ΔGW_{1-5}
  - Gross weight @ 4 = GW @ 5 + ΔGW_{4-5}
  - Burn $rate_{3-4}$ $= \dfrac{GW\ @\ 3 - GW\ @\ 4}{t_{3-4}}$
  - Gross weight (t) = GW @ 3 - BR_{3-4} x t

Figure C-1.- Scheme for gross weight calculation.

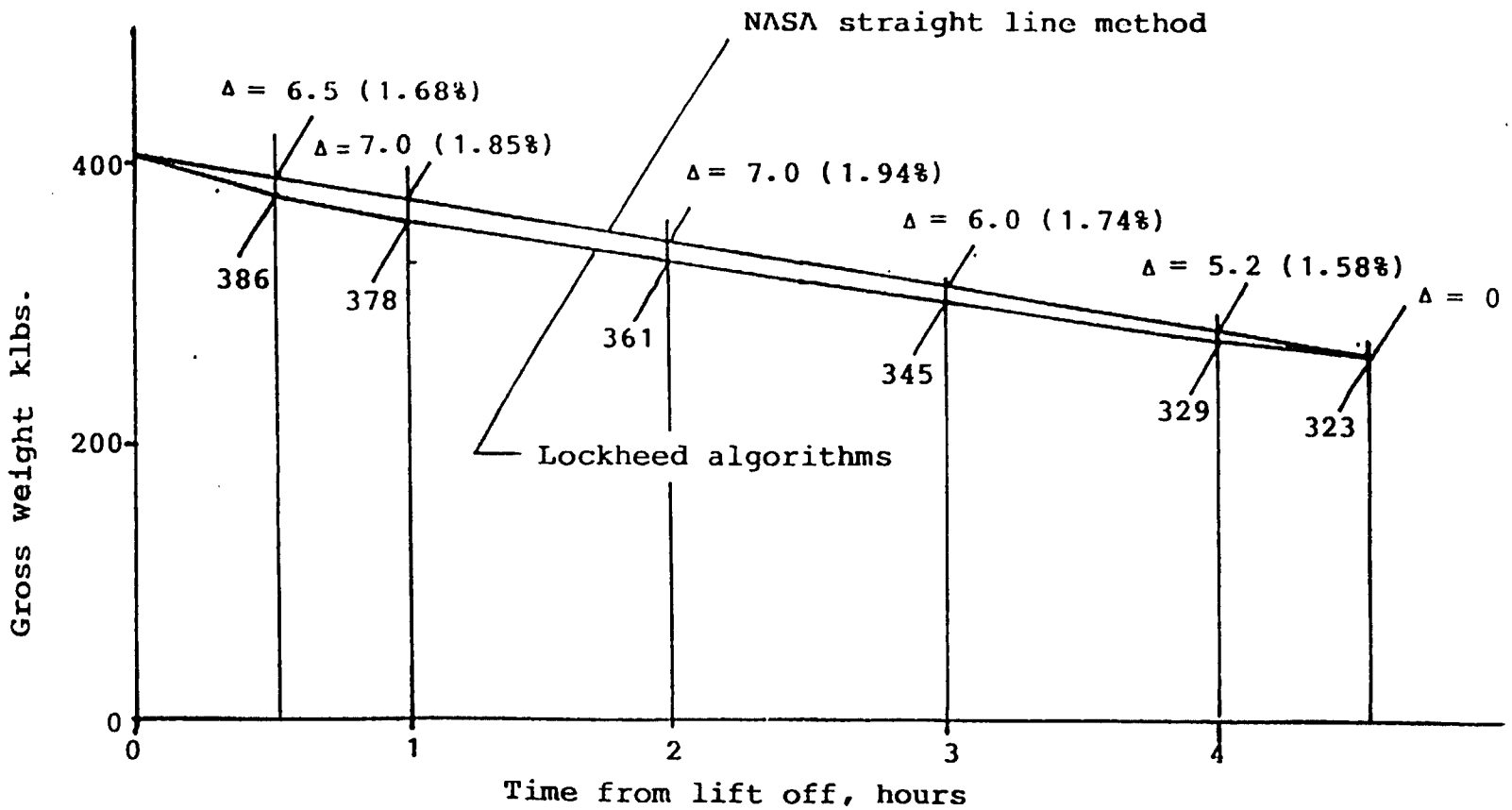

Figure C-2.- Comparison of NASA staightline method of calculating gross weight variation with time versus Lockheed fuel flow algorithms methods.

APPENDIX D

DESIGN OF NUMERICAL FILTER TO SEPARATE GUST AND MANEUVER ACCELERATIONS

The $\frac{\sin x}{x}$ filter of reference 11 has been applied to separate and high frequency components of the normal acceleration response as indicated on page 13. The application of that technique to this problem was performed by Dwight W. Smith, formerly of System Development Corporation Integrated Services, Inc., as part of contract NAS1-15400, and is described in that Company's document PDD 77-2, August 24, 1977. The design parameters and resulting numerical weighting functions are given in figures D-1, D-2, and D-3.

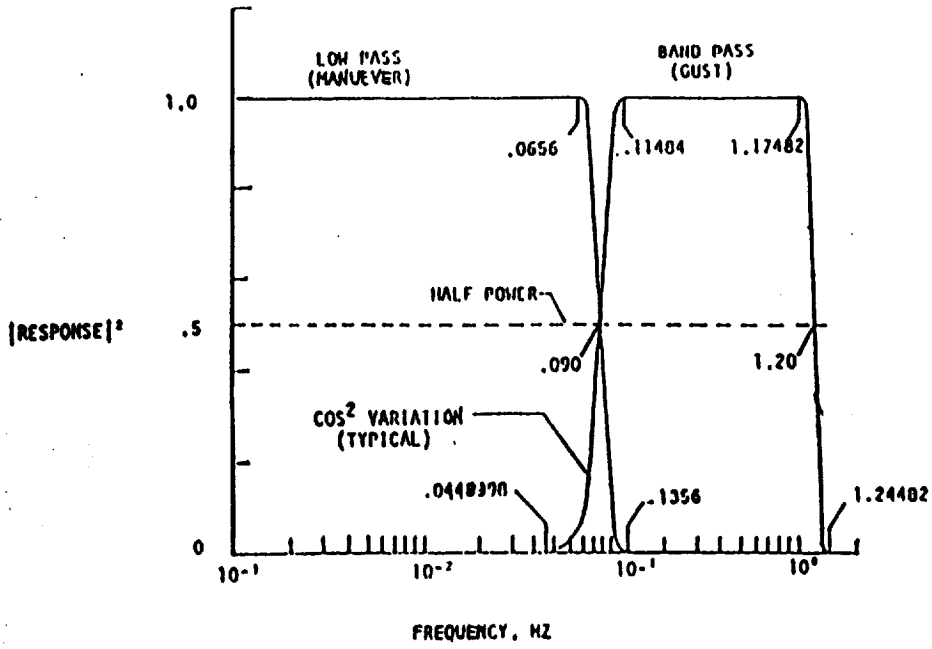

(a) Desired frequency response of filters and definition of critical frequencies.

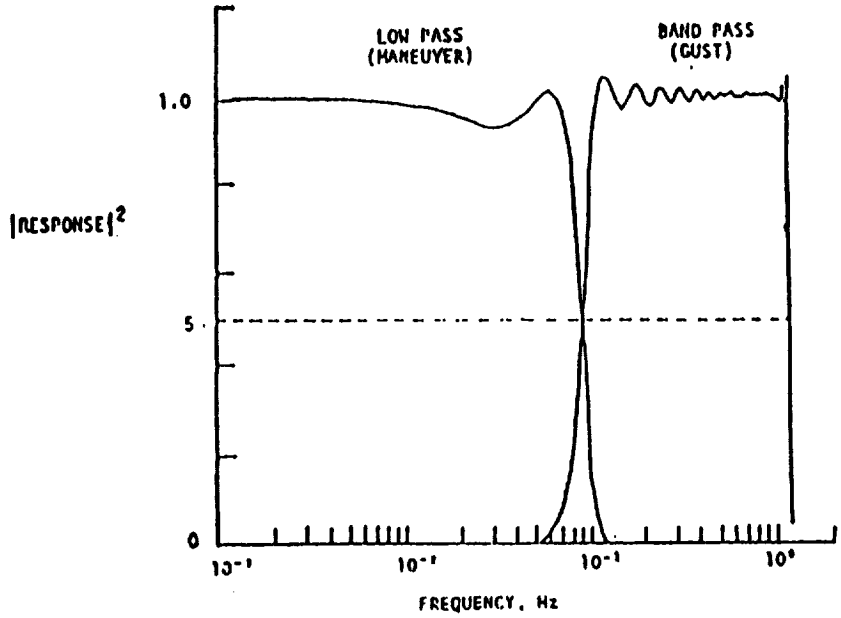

(b) Actual frequency response of filters with 62 weighting functions at 4 samples per second.

Figure D-1. - Numerical filters used in separating gust and maneuver accelerations.

$$a_{nM}\ (t_i) = a_n\ (t_i)\ \times\ W_{1_{LP}} + \sum_{j=2}^{NWTS} W_{j_{LP}} [an\ (t_{i-j+1}) + a_n\ (t_{i+j-1})]$$

$$a_{nG}\ (t_i) = a_n\ (t_i)\ \times\ W_{1_{BP}} + \sum_{j=2}^{NWTS} W_{j_{BP}} [a_n\ (t_{i-j+1}) + a_n\ (t_{i+j-1})]$$

where:

t_i = ith time point

W_j = filter weights $W_{1,2,3,\ldots}$ given in figure D-3

NWTS = Number of weighting constants = 62

LP = Low Pass

BP = Band Pass

Figure D-2.- Time history weighting function format.

$W_i = W_1 , W_2 , W_3 , \ldots W_{62}$

W_i
LP

1	.49463E-01	16	.13630E-01	31	-.79834E-02	47	.29154E-02
2	.49244E-01	17	.10456E-01	32	-.74532E-02	48	.30151E-02
3	.48588E-01	18	.74454E-02	33	-.67819E-02	49	.30230E-02
4	.47509E-01	19	.46357E-02	34	-.60000E-02	50	.29482E-02
5	.46023E-01	20	.20579E-02	35	-.51380E-02	51	.28011E-02
6	.44158E-01	21	-.26264E-03	36	-.42255E-02	52	.25933E-02
7	.41943E-01	22	-.23065E-02	37	-.32909E-02	53	.23367E-02
8	.39418E-01	23	-.40603E-02	38	-.23606E-02	54	.20440E-02
9	.36623E-01	24	-.55171E-02	39	-.14584E-02	55	.17274E-02
10	.33605E-01	25	-.66758E-02	40	-.60535E-03	56	.13985E-02
11	.30413E-01	26	-.75410E-02	41	.18061E-03	57	.10685E-02
12	.27098E-01	27	-.81231E-02	42	.88500E-03	58	.74719E-03
13	.23711E-01	28	-.84372E-02	43	.14967E-02	59	.44321E-03
14	.20305E-01	29	-.85027E-02	44	.20083E-02	60	.16377E-03
15	.16928E-01	30	-.83427E-02	45	.24154E-02	61	-.85417E-04
				46	.27171E-02	62	-.30021E-03

(a) Low Pass

W_i
BP

1	.56487	16	-.23620E-02	31	.82254E-02	47	-.22518E-03
2	.26116	17	-.32516E-01	32	.01527E-01	48	.44415E-02
3	-.13695	18	-.13160E-02	33	-.11178E-02	49	.34913E-03
4	-.97187E-01	19	-.70445E-02	34	.48938E-02	50	-.24366E-02
5	.38487E-01	20	-.25586E-01	35	.12307E-01	51	.18992E-02
6	-.42083E-01	21	-.42077E-02	36	.26061E-02	52	.79207E-03
7	-.84234E-01	22	.40994E-02	37	.18795E-02	53	-.32414E-02
8	-.45115E-02	23	-.15160E-01	38	.10832E-01	54	-.52614E-03
9	-.14169E-01	24	-.63422E-02	39	.54931E-02	55	.77549E-03
10	-.65382E-01	25	.95904E-02	40	.43064E-05	56	-.29427E-02
11	-.24764E-01	26	-.41775E-02	41	.73435E-02	57	-.22346E-02
12	-.28227E-02	27	-.65077E-02	42	.67874E-02	58	.31915E-03
13	-.44010E-01	28	.10402E-01	43	-.59443E-03	59	-.20560E-02
14	-.33080E-01	29	.48957E-02	44	.32631E-02	60	-.29623E-02
15	.13860E-03	30	-.45374E-02	45	.63120E-02	61	-.25083E-03
				46	-.28507E-03	62	-.10833E-02

(b) Band Pass

Figure D-3 Filter weights

REFERENCES

1. Donely, Philip: Summary of Information Relating to Gust Loads on Airplanes. NACA Report 997, 1950.

2. Press, Harry; and McDougal, Robert L: The Gust and Gust-Load Experience of a Twin-Engine Low-Altitude Transport Airplane in Operation on a Northern Transcontinental Route. NACA TN 2663, 1952.

3. Donely, Philip; Jewel, Joseph W., Jr.; and Hunter, Paul A.: An Assessment of Repeated Loads on General Aviation and Transport Aircraft. NASA Paper at 5th ICAF Symposium Aircraft Fatigue-Design, Operational and Economic Aspects; Melbourne, Australia, May 22-24, 1967.

4. Zalovcik, John A.; Jewel, Joseph W., Jr.; and Morris, Garland J.: Comparison of VGH Data From Wide-Body and Narrow-Body Long-Haul Turbine-Powered Transport. NASA TN D-8481, 1977.

5. Jewel, Joseph W., Jr.: Flight Duration, Airspeed Practices, and Altitude Management of Airplanes Involved in the NASA VGH General Aviation Program. NASA TM 89074, 1987.

6. Mark 2 Aircraft Integrated Data System (AIDS Mark 2) Aeronautical Radio, Inc. ARINC 573-6, December, 1974.

7. Crabill, Norman L.; and Morris, Garland J.: The NASA Digital VGH Program--Early Results. Presented at the 1980 NASA Aircraft Safety and Operating Problems Conference, NASA CP 2170, Part II, compiled by J. W. Stickle, November 1980.

8. White, J. Harold; and Finger, John F.: Development of a Multipurpose Smart Recorder for General Aviation Aircraft. NASA CR 168353, 1988.

9. van Dijk, G.M.: Statistical Load Data Processing in the Sixth ICAF Symposium on Advanced Approaches to Fatigue Evaluation. NASA SP 309, Miami, 1971.

10. Crooks, W. M.; Hoblit, F. M; and Mitchel, F. A.: Project HICAT. High Altitude Clear Air Turbulence Measurements and Meteorological Correlations AFFDL TR 68-127, Vol. 1. Final Report, March 13, 1967 to July 31, 1968.

11. Graham, R. J.: Determination and Analysis of Numerical Smoothing Weights. NASA TRR 179, 1963.

12. Coleman, Thomas L.; and Copp, Martin: Maneuver Accelerations Experienced by Five Types of Commercial Transport Airplanes During Routine Operations. NACA TN 3086, 1954.

13. Pratt, Kermit G.; and Walker, Walter G.: A Revised Gust-Load Formula and a Re-Evaluation of V-G Data Taken on Civil Transport Airplanes From 1933 to 1950. NACA Report 1206, 1954.

14. Richardson, Norman R.: NACA VGH Recorder. NACA TN 2265, February 1951.

15. Goldberg, Joseph H.: Gust Response of Commercial Jet Aircraft Including Effects of Autopilot Operation. NASA CR 165919, June 1982.

TABLE I.- WEIGHT AND GEOMETRY OF THE L 1011 AIRCRAFT.

Weights	
Maximum takeoff	430,000 lbs
Empty weight	247,500 lbs
Areas	
Wing	3,456 ft^2
Stabilizer and elevator	1,282 ft^2
Mean chord	
Wing	22.3 ft
Stabilizer and elevator	19.42 ft
Sweepback quarter chord	
Wing	35°
Stabilizer and elevator	35°
Fuselage Stations of Mean Aerodynamic Chord Leading Edge	
Wing	1143
Stabilizer and elevator	1885
Accelerometer location (see figure 1)	
Fuselage station	1243
Waterline	182

TABLE II.- LIFT-CURVE SLOPES USED IN CALCULATING U_{de} FROM a_{nG} FOR THE L-1011-1 AIRCRAFT

LIFT-CURVE SLOPE C_{L_α}, PER DEGREE

Flaps up $C_{L_\alpha} = f(M, HP)$

M	HP = 0	10	20	40 kft
.20	.0923	.0928	.0929	.0936
.35	.0923	.0928	.0930	.0938
.50	.0913	.0920	.0929	.0946
.60	.0918	.0928	.0940	.0963
.70	.0940	.0954	.0970	.1003
.80	-	.1038	.1058	.1100
.89	-	.1210	.1240	.1305
.91	-	-	.1227	.1286
.95	-	-	.1030	.1081

Flaps Down $C_{L_\alpha} = f(FLP)$

FLP, deg	HP = 0
0	.0925
4	.0973
10	.0980
18	.0975
22	.0971
27	.0962
33	.0948
45	.0912

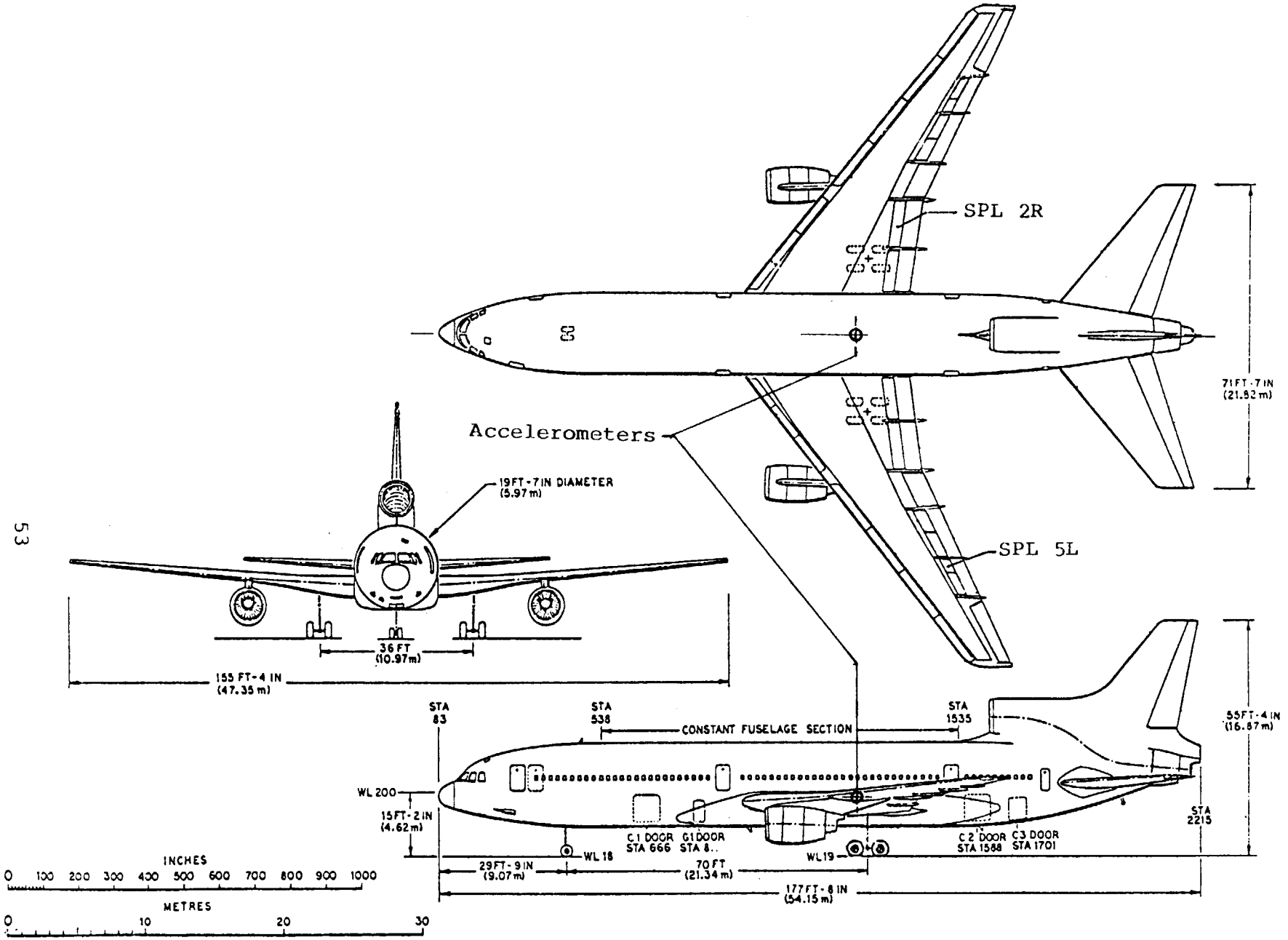

FIGURE 1.- Aircraft three-view with locations of accelerometers and spoilers.

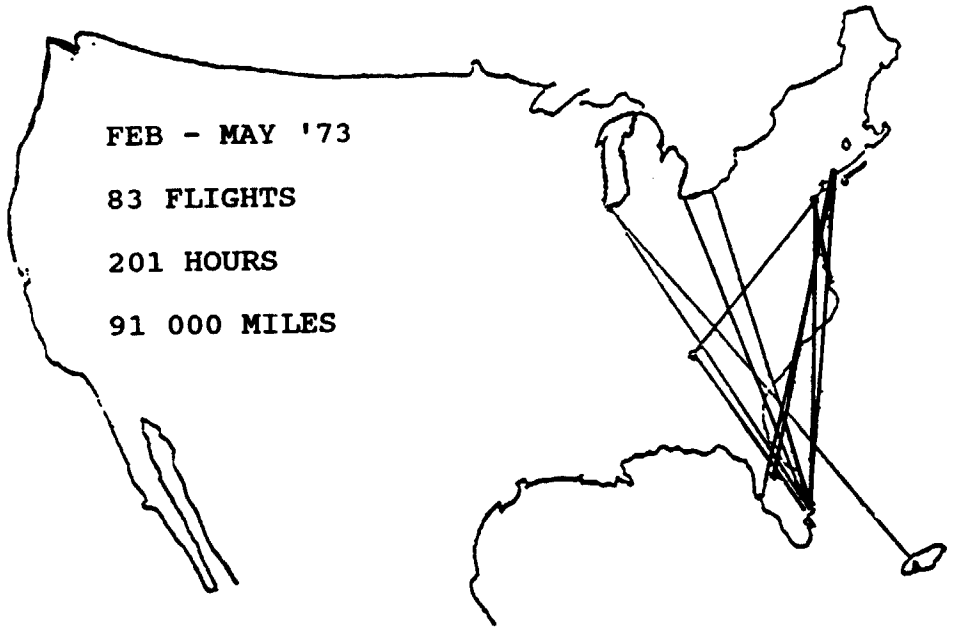

Figure 2. - Location of service area and scope of data base.

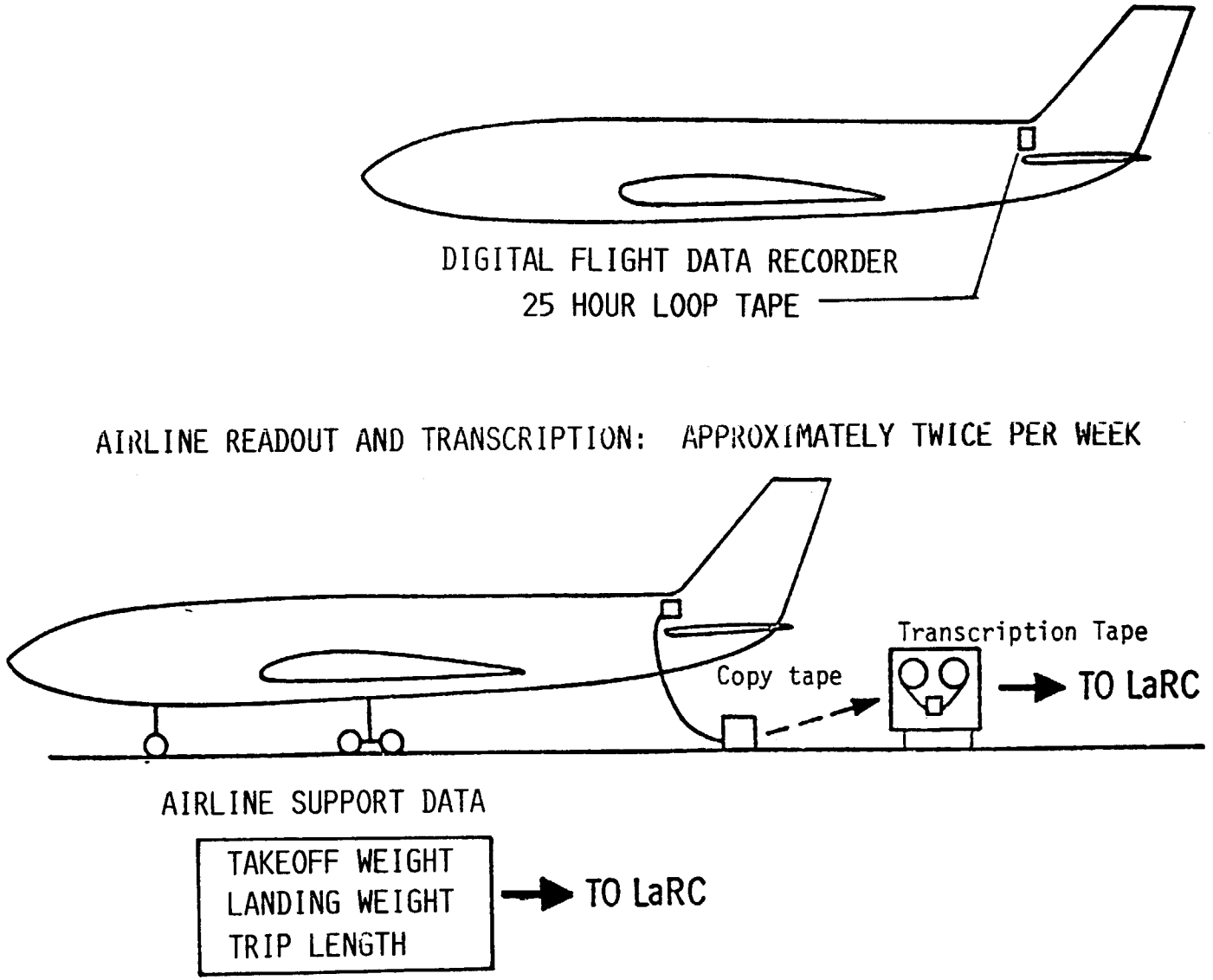

Figure 3. - Digital VGH program data sources and handling.

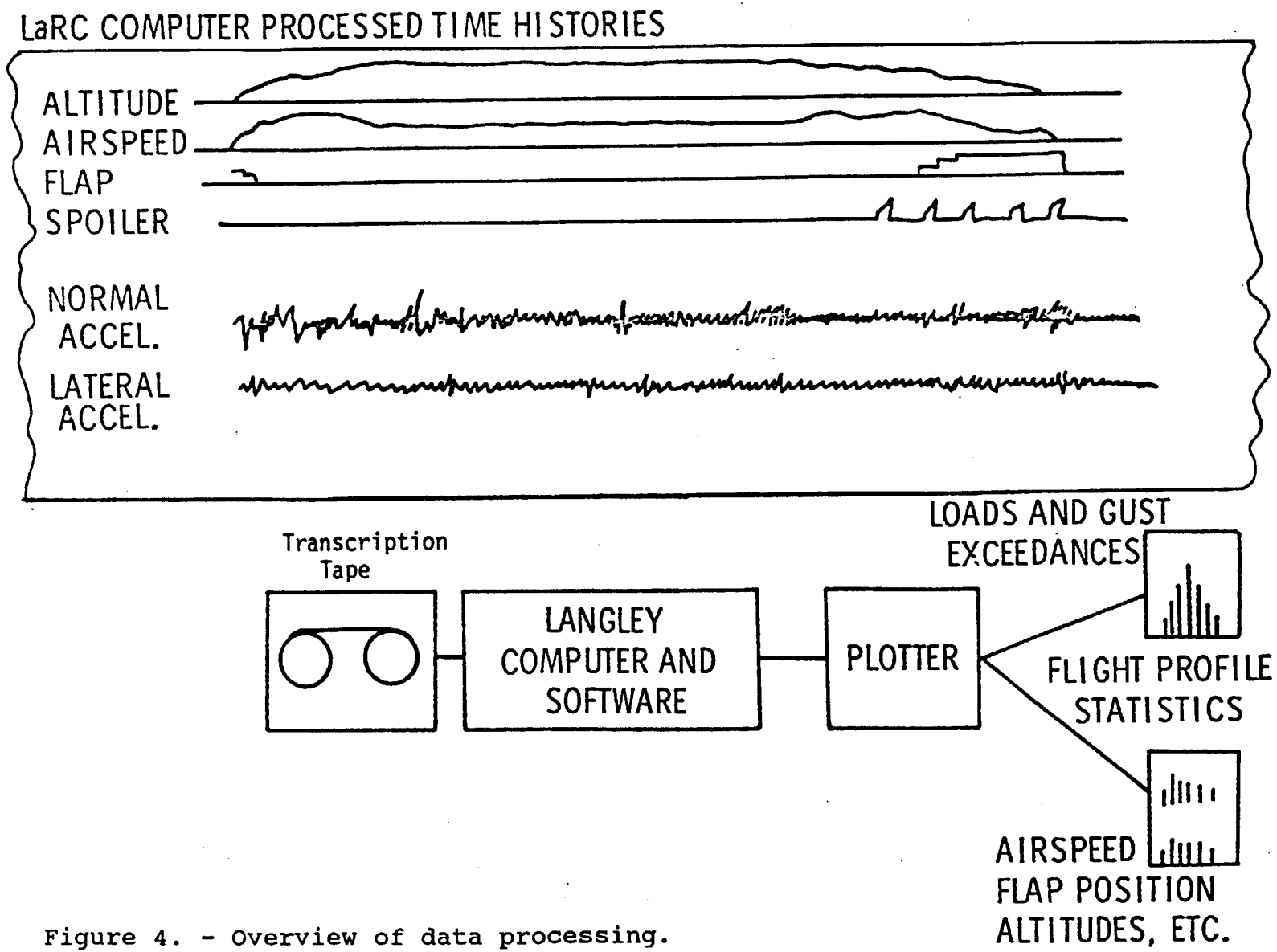

Figure 4. - Overview of data processing.

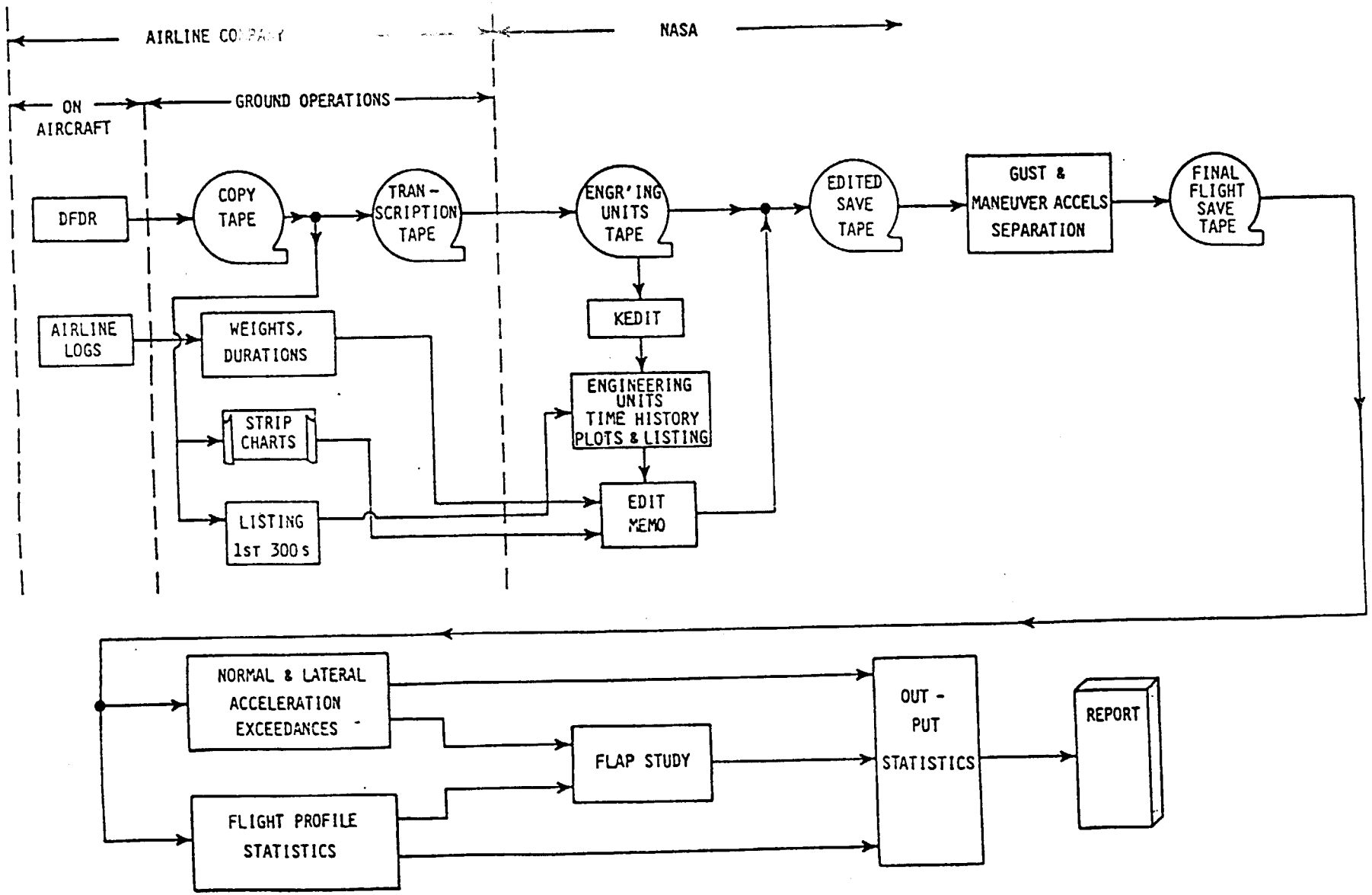

Figure 5. - Simplified data flow.

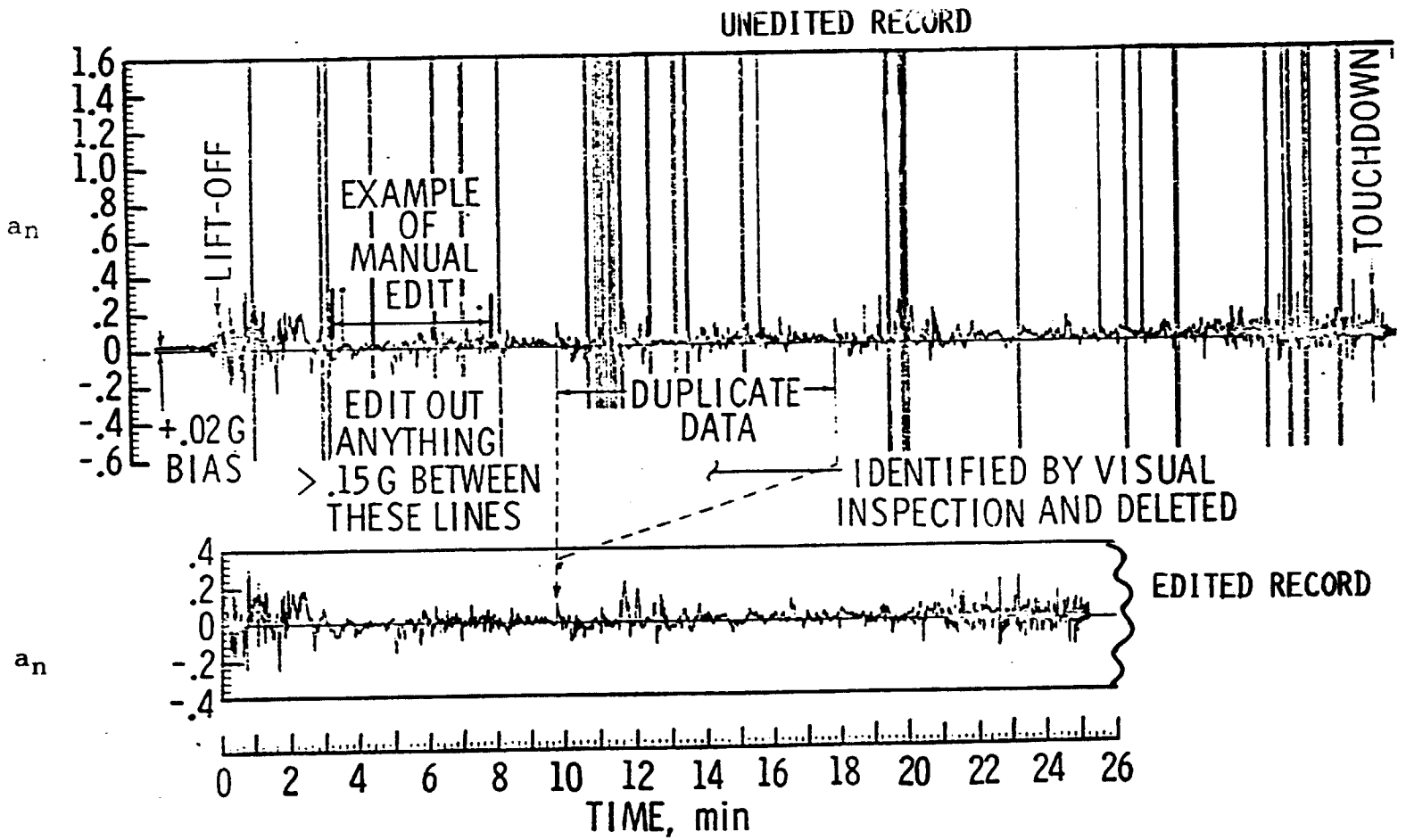

Figure 6. - Example of editing process.

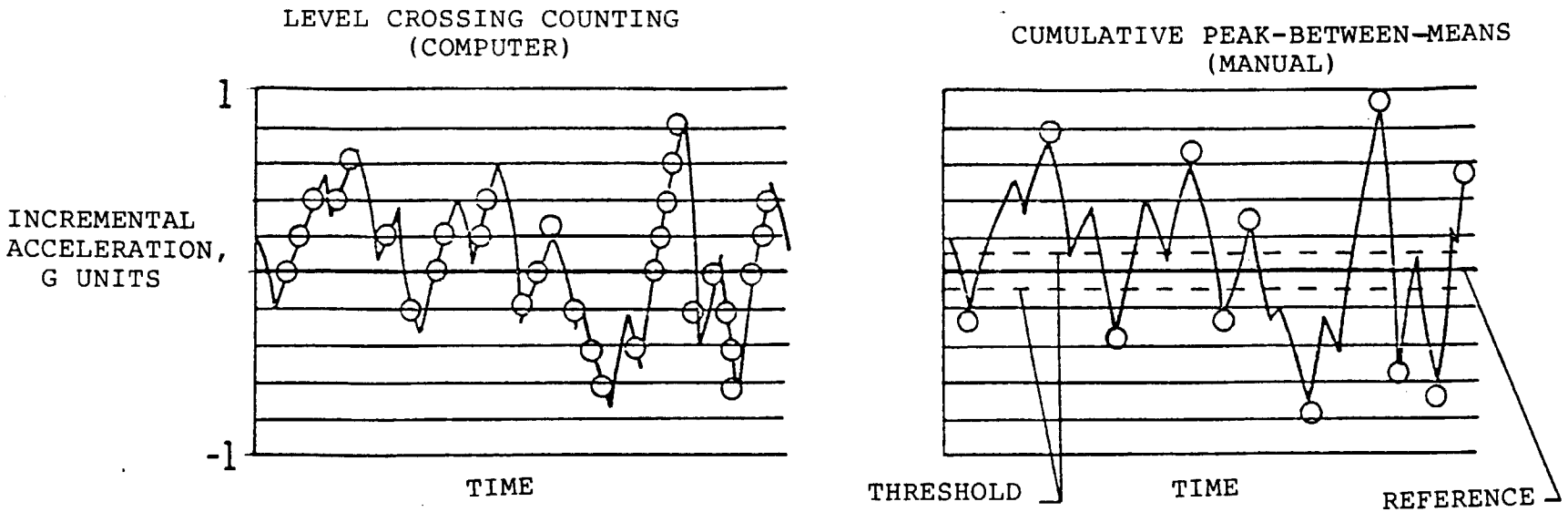

Note that the zero level incremental (= 1.0g absolute) is only counted once, that is when crossed with a positive slope. Also, these data have had all frequencies above 1.2 Hz removed, so that zero level jitter is reduced without using a threshold.

In the previous analog VGH program, threshold values of ± 0.2 and ± 0.3 g were frequently employed. Exceedances were derived by summing the counts from the largest value to the lowest.

Figure 7. - Level crossing and peak counting techniques.

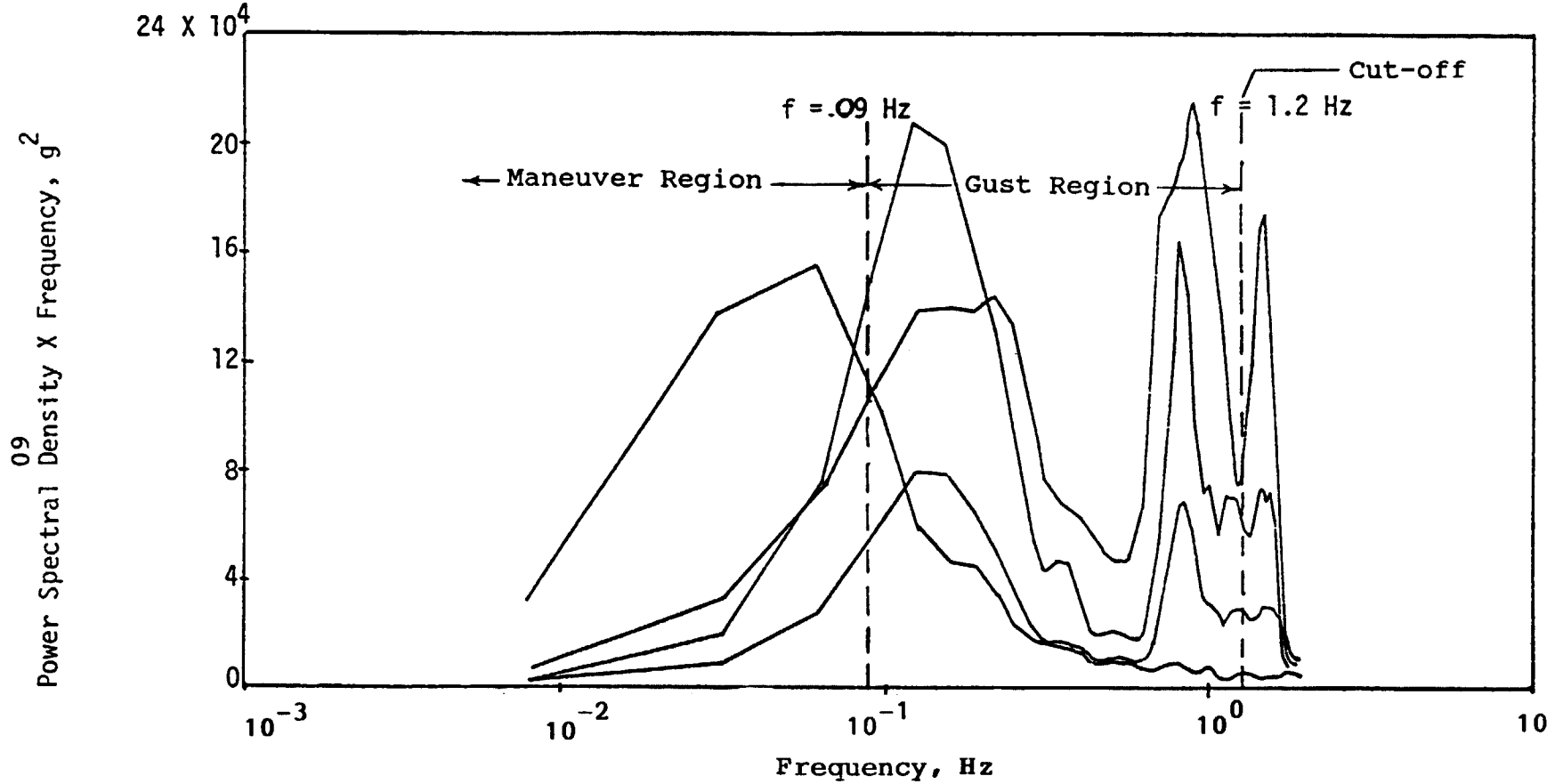

Figure 8. - Sample L1011 normal acceleration power spectra.

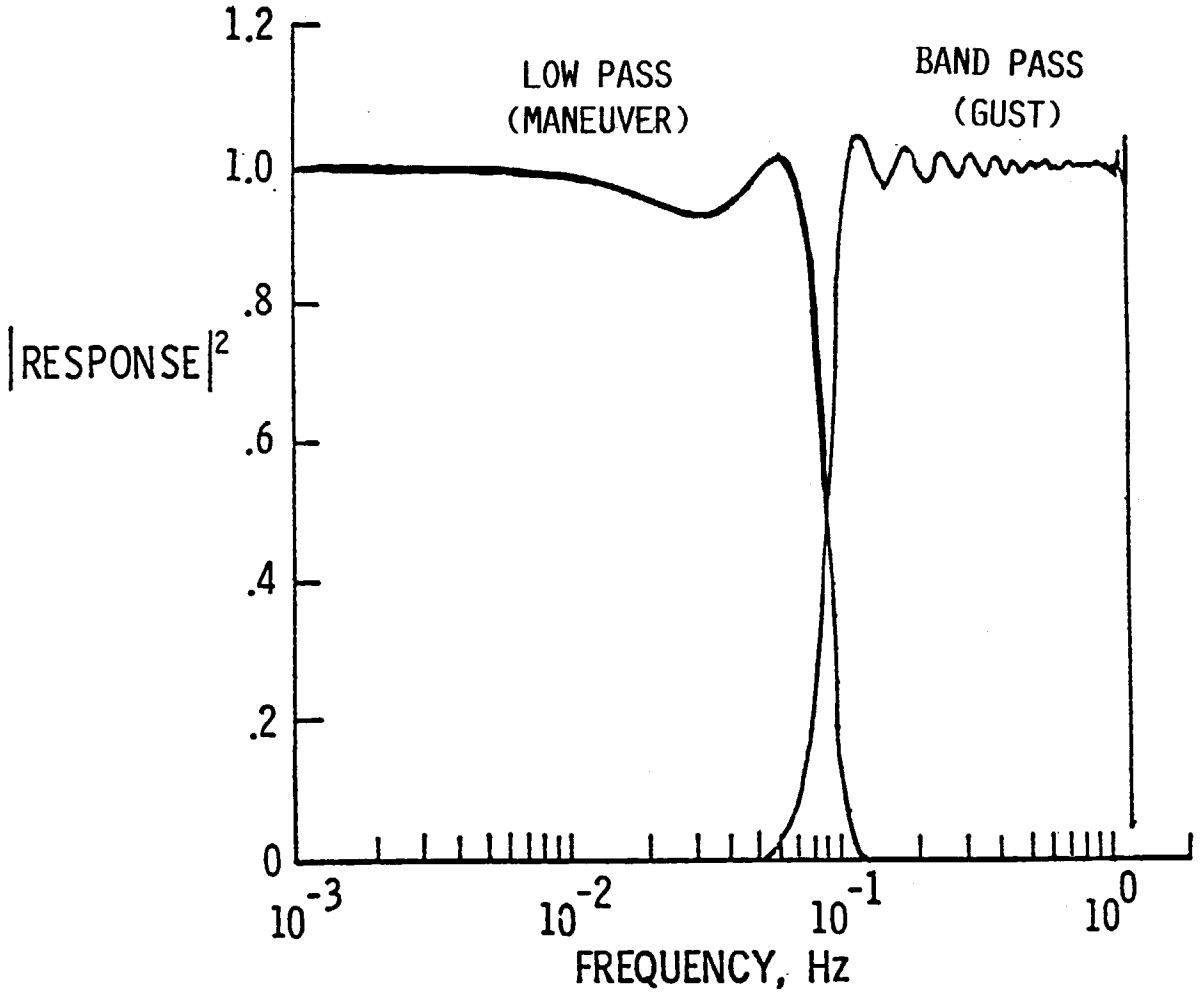

Figure 9.- Frequency response of numerical filters used to separate gust and maneuver accelerations, and to eliminate elastic responses above 1.2 Hz.

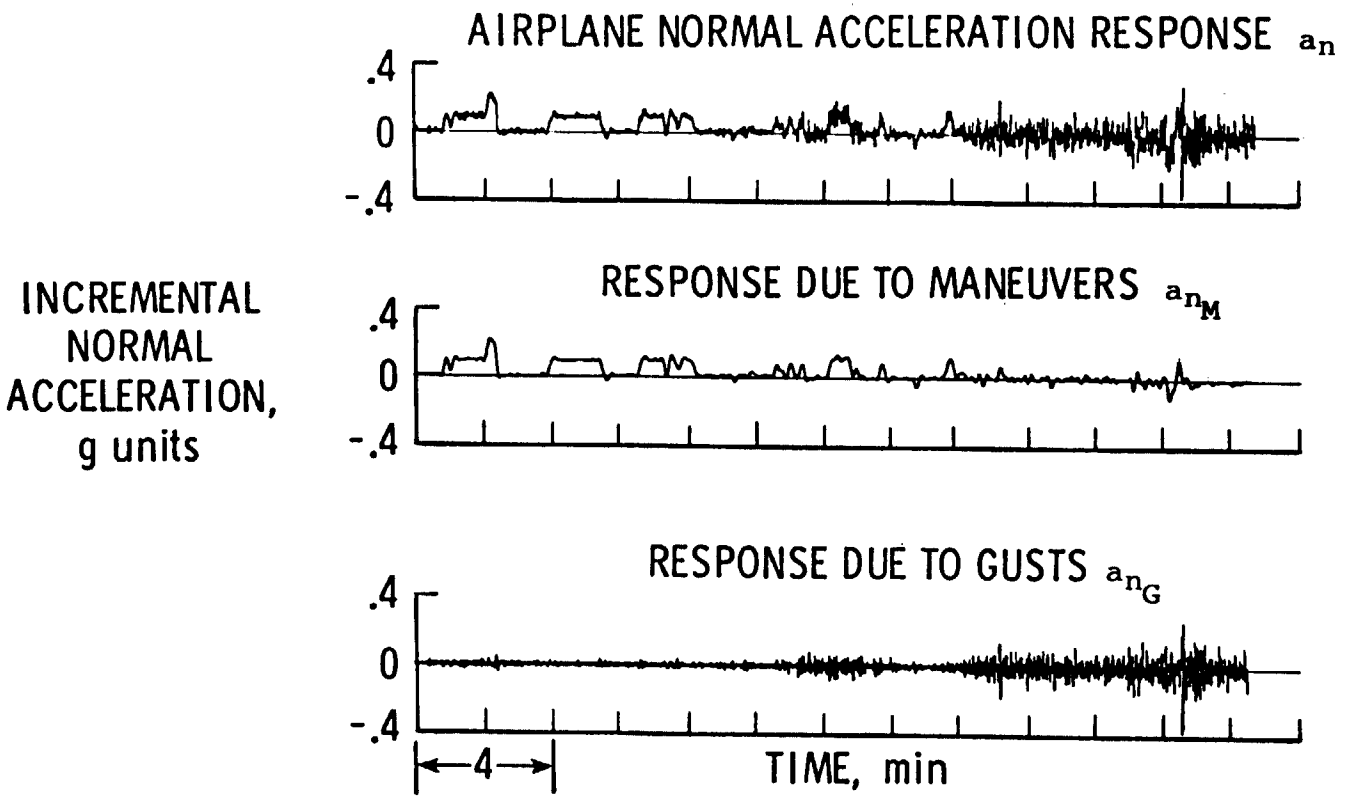

Figure 10.- Filter separation of normal acceleration time history.

• Flight Profile Statistics	**• Percent of Total Flight Time**	**• Percent of Total Flights**
o Entire Flight (flaps up or down)	o Fig.13- GW & HP for Flight Modes o Fig.14- CAS & HP for Flight Modes	o Fig.12- Weight Stats @ TO & landing o Fig.15- Max HP vs. duration
o Flaps Down Only	o Fig.16- Flap Detents in take off and landing o Fig.17- GW, AGL, CAS vs. detents in take off and landing	Not Applicable
o Spoiler Deflections	o Fig.18- Spoiler deflections vs. CAS o Fig.19- Spoiler > 10° vs. Hp	Not Applicable
• Acceleration Derived Statistics	**• Counts Per Hour**	**• Percent of Total Flights**
o Entire Flight	o Fig.20- Normal acceleration exceedances o Fig.21- Lateral acceleration exceedances o Fig.22- U_{de} exceedances	o Fig. 23- Maximum Acceleration
o Flaps Down Only	o Fig.24- Normal acceleration vs. detents, take off and landing	Not Applicable

Figure 11- Organization of the Numerical Results and Discussion.

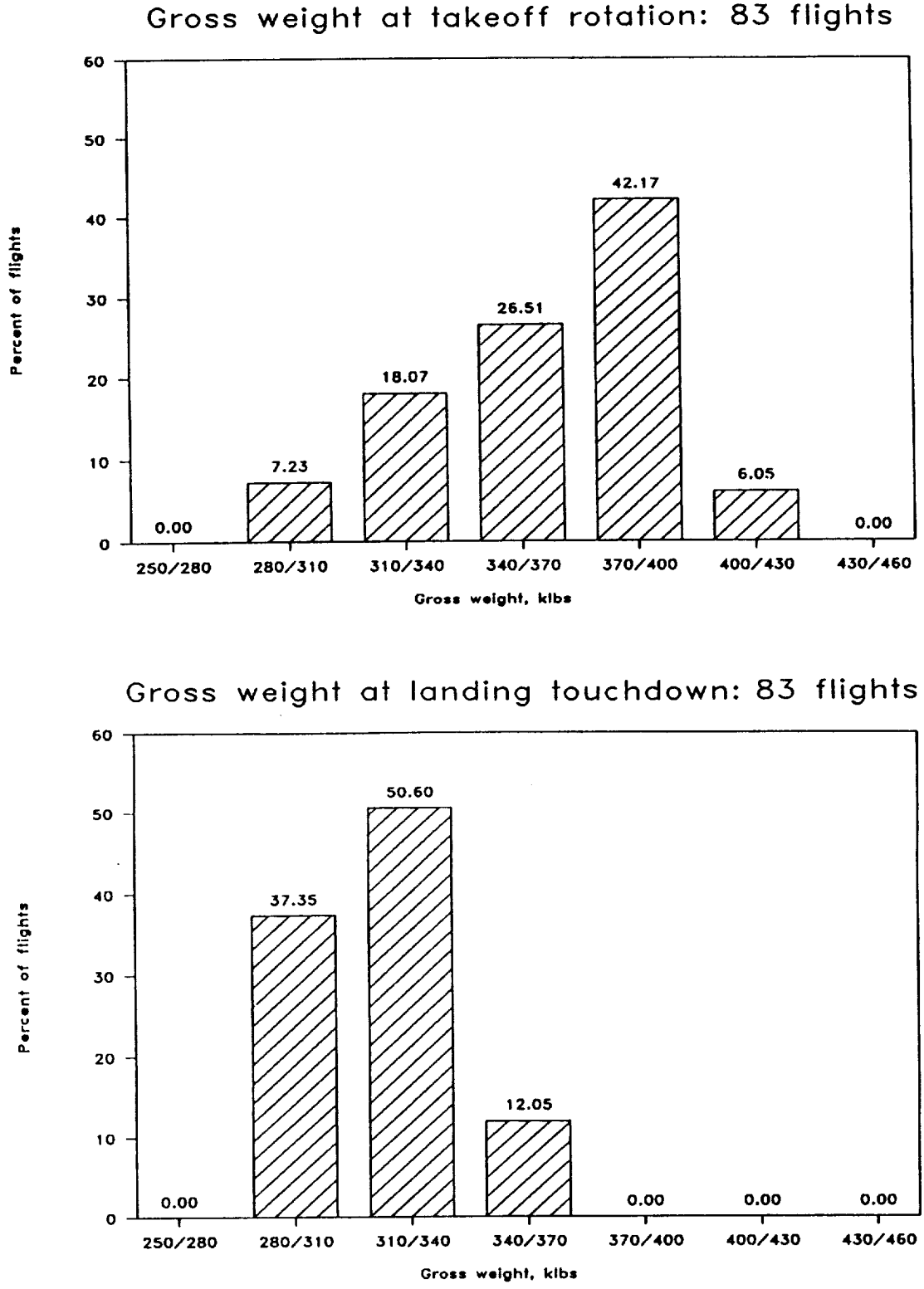

(a) Percent of take-offs and landings made at various gross weights

Figure 12.- Weight statistics for take-off and landing.

FUEL WEIGHT AT TAKEOFF ROTATION

Flight Duration Hours	10 TO 40 KLB	40 TO 70 KLB	70 TO 100 KLB	100 TO 130 KLB	130 TO 160 KLB	160 TO 190 KLB	10 TO 190 KLB
0 - .5	0	2.4	0	0	0	0	2.4
.5 - 1.0	0	3.6	3.6	0	0	0	7.2
1.0 - 1.5	0	4.8	2.4	0	0	0	7.2
1.5 - 2.0	0	0	3.6	0	0	0	3.6
2.0 - 2.5	0	1.2	31.3	3.6	0	0	36.1
2.5 - 3.0	0	1.2	9.6	1.2	0	0	12.0
3.0 - 3.5	0	0	18.1	4.8	0	0	22.9
3.5 - 4.0	0	1.2	0	3.6	0	0	4.8
4.0 - 4.5	0	0	0	3.6	0	0	3.6
4.5 - 5.0	0	0	0	0	0	0	0.0
Totals	0	14.4	68.6	16.8	0	0	99.8

FUEL WEIGHT AT LANDING TOUCHDOWN

0 - .5	1.2	1.2	0	0	0	0	2.4
.5 - 1.0	0	4.8	2.4	0	0	0	7.2
1.0 - 1.5	3.6	3.6	0	0	0	0	7.2
1.5 - 2.0	0	3.6	0	0	0	0	3.6
2.0 - 2.5	22.9	12.0	1.2	0	0	0	36.1
2.5 - 3.0	3.6	7.2	1.2	0	0	0	12.0
3.0 - 3.5	4.8	18.1	0	0	0	0	22.9
3.5 - 4.0	1.2	3.6	0	0	0	0	4.8
4.0 - 4.5	0	3.6	0	0	0	0	3.6
4.5 - 5.0	0	0	0	0	0	0	0.0
Totals	37.3	57.7	4.8	0	0	0	99.8
					TOTAL FLIGHTS		83

(b) Percent of flights at various fuel weights and durations for takeoff and landing

Figure 12. - Concluded.

PRESSURE ALTITUDE BANDS

Weight klbs	-500 TO 4500 FT	4500 TO 9500 FT	9500 TO 14500 FT	14500 TO 19500 FT	19500 TO 24500 FT	24500 TO 29500 FT	29500 TO 34500 FT	34500 TO 39500 FT	39500 TO 44500 FT	-500 TO 44500 FT
250 - 280	0	0	0	0	0	0	0	0	0	0
280 - 310	0.0726	0.0403	0.0376	0.0340	0.0377	0.0846	0.0699	0	0	0.3767
310 - 340	0.2285	0.2552	0.3656	0.3052	0.4753	0.5388	0.4267	0.2008	0	2.7865
340 - 370	0.4291	0.4864	0.6440	0.7124	0.8635	0.9639	0.9084	0.1101	0	4.9138
370 - 400	0.7550	0.7083	0.8462	0.8580	1.0956	1.2645	0.9664	0.0724	0	6.5664
400 - 430	0.1147	0.1091	0.1064	0.0916	0.1284	0.1485	0.2291	0.0168	0	0.9446
Percent time climb	1.6	1.6	2.0	2.0	2.6	3.0	2.6	0.4	0	15.8
250 - 280	0	0	0	0	0	0	0	0	0	0
280 - 310	0.5954	0.8689	0.1182	0.1331	0.0166	1.1699	1.0131	0.3860	0	4.3012
310 - 340	0.7347	0.6648	0.3905	0.1606	0.1247	3.1113	9.2169	6.7380	0	21.1450
340 - 370	0.2194	0.3538	0.1806	0.3063	0.1586	5.1659	17.4801	9.1180	0	32.9827
370 - 400	0.0510	0.0038	0.0049	0	0	1.6528	5.1216	3.7500	0	10.5841
400 - 430	0	0.0087	0.0059	0	0	0	0.1650	0.0080	0	0.1876
Percent time level	1.6	1.9	0.7	0.6	0.3	11.1	33.0	20.0	0	69.2
250 - 280	0	0	0	0	0	0	0	0	0	0
280 - 310	1.1210	0.6410	0.4416	0.4176	0.4624	0.5160	0.2353	0.0735	0	3.9084
310 - 340	1.7256	1.2000	1.0265	0.8901	0.8559	0.9008	0.6661	0.0609	0	7.3259
340 - 370	0.4528	0.5590	0.6323	0.4923	0.4817	0.5636	0.4288	0.0595	0	3.6700
370 - 400	0	0	0	0	0	0.0198	0.0697	0.0065	0	0.0960
400 - 430	0	0	0	0	0	0	0	0	0	0
Percent time descent	3.3	2.4	2.1	1.8	1.8	2.0	1.4	0.2	0	15.0
Total Percent Time In Altitude Band	6.5	5.9	4.8	4.4	4.7	16.1	37.0	20.6	0	100.0

$$\text{Percent time} = \frac{\text{Hours in altitude and climb (level, descent) and gross weight bands}}{\text{Total hours}} \times 100$$

(a) Percent time in gross weight and altitude band matrix

Figure 13. - Gross weight and altitude statistics for climb, level, and descent Flight Modes.

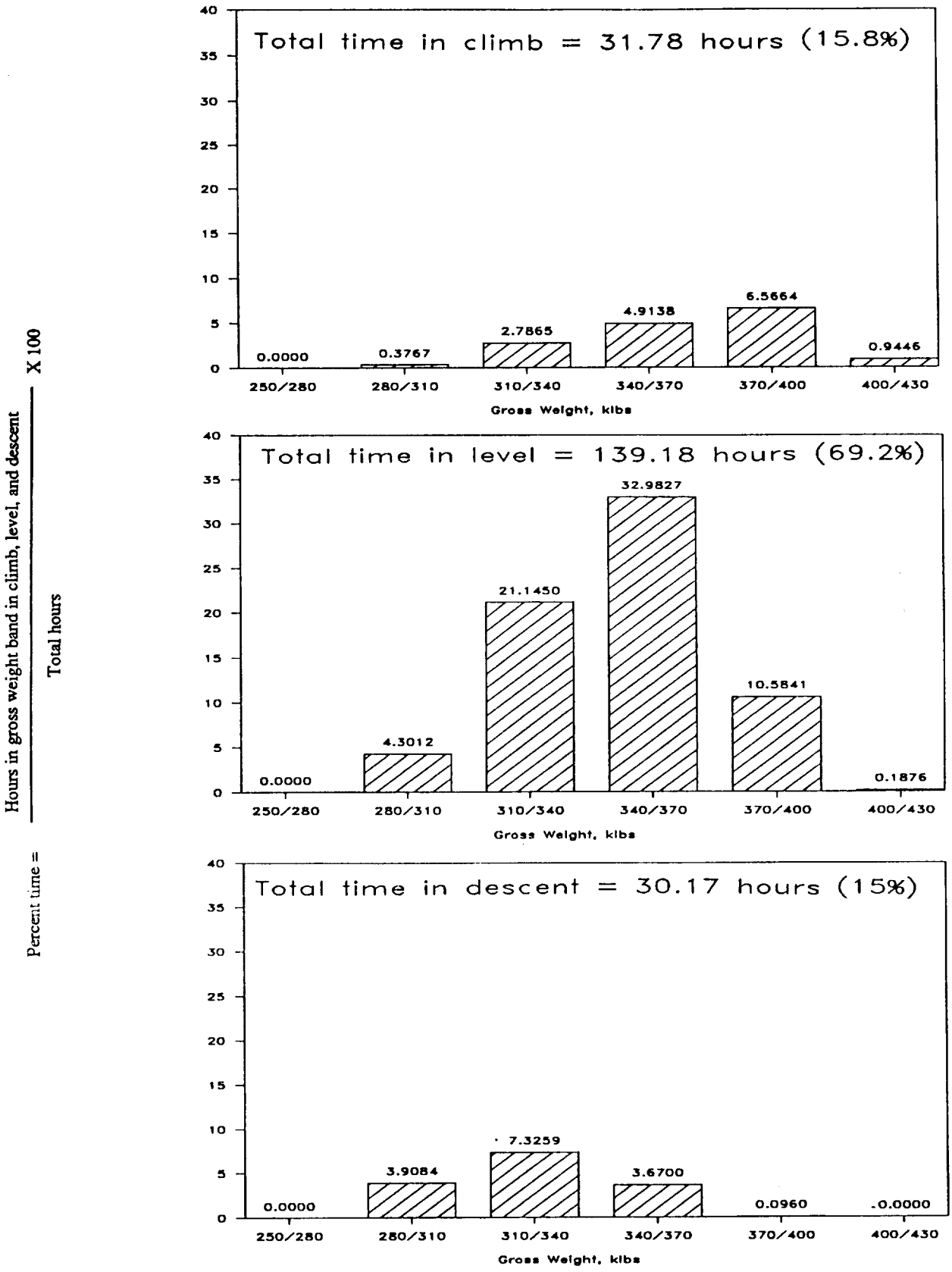

(b) Percent time vs. gross weight for climb, level, and descent

Figure 13.- Continued.

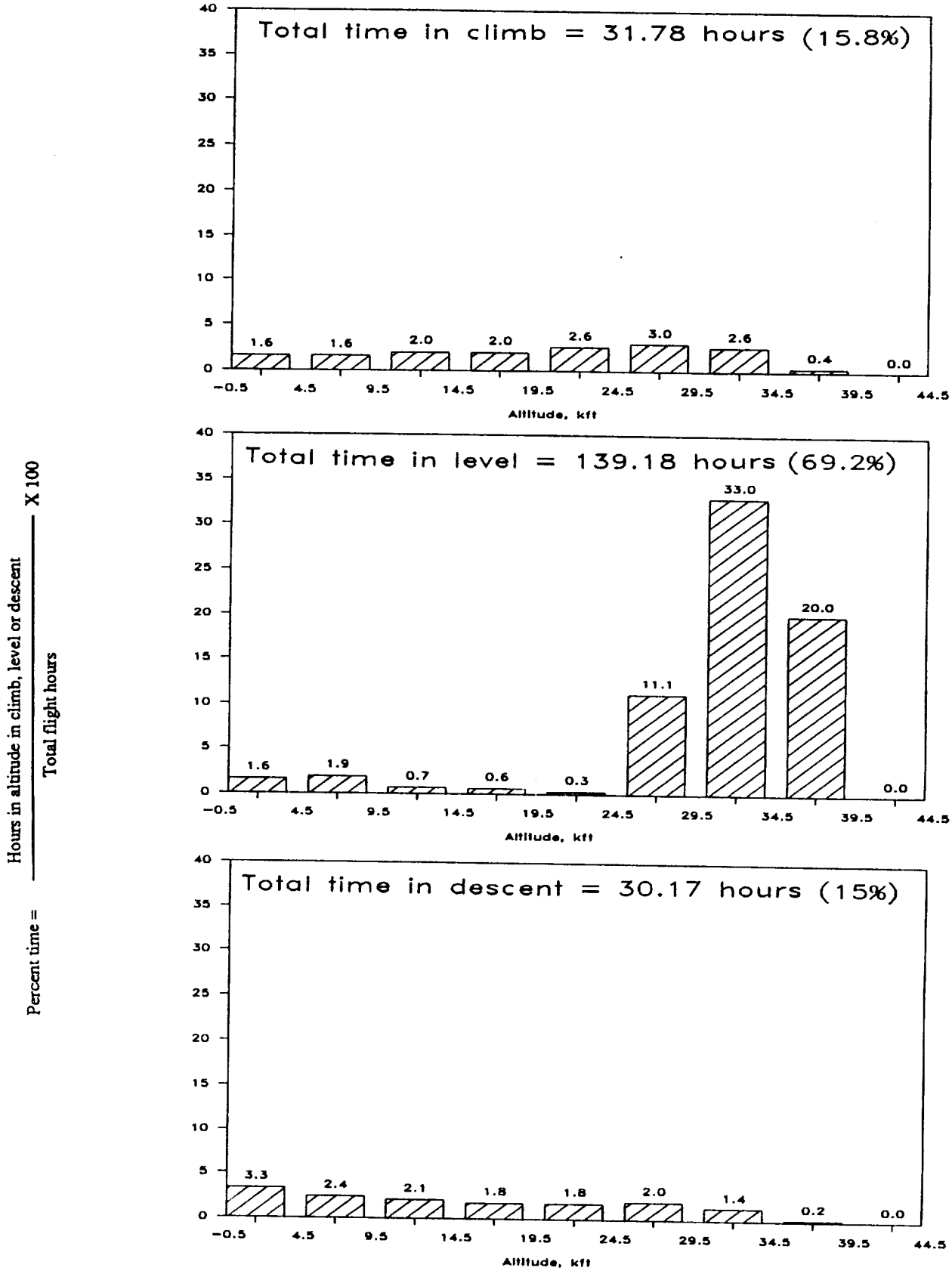

(c) Percent time vs. altitude for climb, level, and descent

Figure 13.- Concluded.

CAS Interval KTS	-500 TO 4500 FT	4500 TO 9500 FT	9500 TO 14500 FT	14500 TO 19500 FT	19500 TO 24500 FT	24500 TO 29500 FT	29500 TO 34500 FT	34500 TO 39500 FT	39500 TO 44500 FT	-500 TO 44500 FT
	PRESSURE ALTITUDE BANDS						Entire Flights			
120 - 130	0	0	0	0	0	0	0	0	0	0
130 - 140	0	0	0	0	0	0	0	0	0	0
140 - 150	0	0	0	0	0	0	0	0	0	0
150 - 160	0	0	0	0	0	0	0	0	0	0
160 - 170	0.0091	0	0	0	0	0	0	0	0	0.0091
170 - 180	0.0930	0.0040	0	0	0	0	0	0	0	0.0970
180 - 190	0.1858	0.0014	0	0	0	0	0	0	0	0.1872
190 - 200	0.2331	0	0	0	0	0	0	0	0	0.2331
200 - 210	0.2259	0.0054	0	0	0	0	0.0031	0	0	0.2344
210 - 220	0.1682	0.0064	0	0	0	0	0.0065	0	0	0.1811
220 - 230	0.1416	0.0344	0.0026	0	0	0	0.0055	0	0	0.1841
230 - 240	0.1219	0.0518	0.0066	0.0010	0	0	0.0039	0.0016	0	0.1868
240 - 250	0.1208	0.2826	0.0610	0.0274	0.0112	0.0081	0.0517	0.0094	0	0.5722
250 - 260	0.0986	0.3134	0.0856	0.0106	0.0172	0.0159	0.0699	0.0488	0	0.6600
260 - 270	0.0642	0.1406	0.0876	0.0160	0.0195	0.0150	0.0712	0.0687	0	0.4728
270 - 280	0.0208	0.0842	0.0676	0.0374	0.0382	0.0726	0.1240	0.0938	0	0.5386
280 - 290	0.0168	0.0518	0.0860	0.0670	0.0785	0.1011	0.4170	0.1405	0	0.9587
290 - 300	0.0182	0.0862	0.1354	0.0880	0.1633	0.3255	0.7361	0.0378	0	1.5905
300 - 310	0.0254	0.0952	0.2852	0.2170	0.3032	0.5328	0.7337	0	0	2.1925
310 - 320	0.0234	0.0573	0.1736	0.1130	0.1368	0.2865	0.3102	0	0	1.1008
320 - 330	0.0101	0.0464	0.1272	0.0930	0.1732	0.4662	0.0634	0	0	0.9795
330 - 340	0.0096	0.0853	0.1482	0.1816	0.2345	0.5562	0.0036	0	0	1.2190
340 - 350	0.0173	0.1899	0.4190	0.6478	0.8317	0.5433	0	0	0	2.6490
350 - 360	0.0045	0.0627	0.2872	0.4672	0.5704	0.0705	0	0	0	1.4625
360 - 370	0.0026	0	0.0224	0.0316	0.0200	0.0054	0	0	0	0.0846
370 - 380	0	0	0.0056	0.0014	0.0023	0	0	0	0	0.0093
380 - 390	0	0	0	0	0	0	0	0	0	0
390 - 400	0	0	0	0	0	0	0	0	0	0
Percent time in alt. & climb	1.6	1.6	2.0	2.0	2.6	3.0	2.6	0.4	0	15.8

$$\text{Percent Time} = \frac{\text{Hours in Altitude and Climb and Airspeed Bands}}{\text{Total Flight Hours}} \times 100$$

(a) Percent time in airspeed and altitude bands, for climb

Figure 14. - Airspeed and altitude statistics for climb, level, and descent Flight Modes.

	PRESSURE ALTITUDE BANDS									Entire Flights
CAS Interval KTS	-500 TO 4500 FT	4500 TO 9500 FT	9500 TO 14500 FT	14500 TO 19500 FT	19500 TO 24500 FT	24500 TO 29500 FT	29500 TO 34500 FT	34500 TO 39500 FT	39500 TO 44500 FT	-500 TO 44500 FT
120 - 130	0	0	0	0	0	0	0	0	0	0
130 - 140	0.0010	0	0	0	0	0	0	0	0	0.0010
140 - 150	0.0254	0	0	0	0	0	0	0	0	0.0254
150 - 160	0.1467	0	0	0	0	0	0	0	0	0.1467
160 - 170	0.2650	0	0	0	0	0	0	0	0	0.2650
170 - 180	0.2248	0.0315	0	0	0	0	0	0	0	0.2563
180 - 190	0.1653	0.0150	0	0	0	0	0	0	0	0.1803
190 - 200	0.0451	0.0391	0	0	0	0	0	0	0	0.0842
200 - 210	0.0480	0.1222	0.0102	0.0266	0	0	0.0010	0	0	0.2080
210 - 220	0.0766	0.1851	0.0225	0.0280	0	0	0.0297	0	0	0.3419
220 - 230	0.0710	0.0726	0.0591	0.0042	0	0	0.0198	0	0	0.2267
230 - 240	0.1096	0.1032	0.0239	0.0032	0.0731	0	0.0165	0.0004	0	0.3299
240 - 250	0.0981	0.2810	0.0405	0.0042	0.0024	0.0067	0.0132	0.0420	0	0.4881
250 - 260	0.1272	0.4885	0.0468	0.0042	0.0047	0	0.0396	0.1200	0	0.8310
260 - 270	0.0560	0.1178	0.0400	0.0052	0.0024	0.0011	0.0627	0.8720	0	1.1572
270 - 280	0.0165	0.0998	0.0400	0.0112	0.0042	0.0056	0.0660	1.3920	0	1.6353
280 - 290	0.0245	0.0528	0.0635	0.0089	0.0024	0.0666	0.2112	4.9500	0	5.3799
290 - 300	0.0165	0.0465	0.0488	0.0187	0	0.0810	3.2043	12.4540	0	15.8698
300 - 310	0.0125	0.0522	0.0425	0.0191	0.0119	0.0233	15.9600	0.1680	0	16.2895
310 - 320	0.0106	0.0479	0.0435	0.0163	0.0101	0.2042	9.2895	0	0	9.6221
320 - 330	0.0090	0.0403	0.0561	0.0425	0.0065	2.3243	3.9864	0	0	6.4651
330 - 340	0.0090	0.0319	0.0468	0.1186	0.0077	4.2080	0.1023	0	0	4.5243
340 - 350	0.0382	0.0294	0.0493	0.0870	0.0053	3.3866	0	0	0	3.5965
350 - 360	0.0030	0.0359	0.0322	0.1223	0.0250	0.7437	0	0	0	0.9621
360 - 370	0	0.0068	0.0244	0.0710	0.1307	0.0466	0	0	0	0.2795
370 - 380	0	0	0.0073	0.0089	0.0136	0	0	0	0	0.0298
380 - 390	0	0	0.0015	0	0	0	0	0	0	0.0015
390 - 400	0	0	0	0	0	0	0	0	0	0
Percent time in alt. & level	1.6	1.9	0.7	0.6	0.3	11.1	33.0	20	0	69.2

$$\text{Percent Time} = \frac{\text{Hours in Altitude and Level and Airspeed Bands}}{\text{Total Flight Hours}} \times 100$$

(b) Percent time in airspeed and atitude bands, for level flight

Figure 14. - Continued.

PRESSURE ALTITUDE BANDS Entire Flights

CAS Interval KTS	-500 TO 4500 FT	4500 TO 9500 FT	9500 TO 14500 FT	14500 TO 19500 FT	19500 TO 24500 FT	24500 TO 29500 FT	29500 TO 34500 FT	34500 TO 39500 FT	39500 TO 44500 FT	-500 TO 44500 FT
120 - 130	0.0082	0	0	0	0	0	0	0	0	0.0082
130 - 140	0.2673	0	0	0	0	0	0	0	0	0.2673
140 - 150	0.7448	0	0	0	0	0	0	0	0	0.7448
150 - 160	0.4788	0.0098	0	0	0	0	0	0	0	0.4886
160 - 170	0.3359	0.0379	0	0	0	0	0	0	0	0.3738
170 - 180	0.2069	0.0550	0	0	0	0	0	0	0	0.2619
180 - 190	0.2069	0.0910	0	0	0	0	0	0	0	0.2979
190 - 200	0.1848	0.1102	0	0	0	0	0	0	0	0.2950
200 - 210	0.1630	0.1464	0.0227	0.0014	0	0	0.0015	0	0	0.3350
210 - 220	0.0828	0.1512	0.0491	0.0056	0	0	0.0049	0	0	0.2936
220 - 230	0.1030	0.0674	0.0244	0	0.0034	0.0172	0.0055	0	0	0.2209
230 - 240	0.1247	0.1253	0.0361	0.0387	0.0437	0.0142	0.0088	0	0	0.3915
240 - 250	0.1551	0.3499	0.0664	0.0056	0	0.0010	0.0137	0.0009	0	0.5926
250 - 260	0.0917	0.3883	0.1031	0	0	0	0.0094	0.0014	0	0.5939
260 - 270	0.0271	0.1711	0.0510	0	0	0.0026	0.0020	0.0112	0	0.2650
270 - 280	0.0323	0.0478	0.0401	0.0014	0	0.0014	0.0157	0.0186	0	0.1573
280 - 290	0.0142	0.0235	0.0412	0.0106	0	0.0056	0.0354	0.0684	0	0.1969
290 - 300	0.0059	0.0343	0.0722	0.0092	0	0.0156	0.1553	0.0833	0	0.3758
300 - 310	0.0122	0.0590	0.0491	0.0412	0.0256	0.0318	0.3675	0.0163	0	0.6027
310 - 320	0.0089	0.0516	0.0649	0.0248	0.0506	0.0922	0.3419	0	0	0.6349
320 - 330	0.0079	0.0550	0.1149	0.1017	0.0698	0.2502	0.3041	0	0	0.9036
330 - 340	0.0079	0.0708	0.1180	0.1064	0.1303	0.4546	0.1120	0	0	1.0000
340 - 350	0.0182	0.1087	0.2518	0.2777	0.2952	0.5898	0.0225	0	0	1.5639
350 - 360	0.0099	0.1061	0.4395	0.5117	0.4727	0.3432	0	0	0	1.8831
360 - 370	0	0.1294	0.4887	0.5584	0.5717	0.1646	0	0	0	1.9128
370 - 380	0	0.0098	0.0638	0.1048	0.1373	0.0162	0	0	0	0.3319
380 - 390	0	0	0.0019	0	0	0	0	0	0	0.0019
390 - 400	0	0	0	0	0	0	0	0	0	0
Percent Time in alt. & descent	3.3	2.4	2.1	1.8	1.8	2.0	1.4	0.2	0	15.0

$$\text{Percent Time} = \frac{\text{Hours in Altitude and Descent and Airspeed Bands}}{\text{Total Flight Hours}} \times 100$$

(c) Percent time in airspeed and altitude bands, for descent

Figure 14. - Concluded.

PERCENT OF FLIGHTS

Flight Duration Hours	-.5 TO 4.5 KFT	4.5 TO 9.5 KFT	9.5 TO 14.5 KFT	14.5 TO 19.5 KFT	19.5 TO 24.5 KFT	24.5 TO 29.5 KFT	29.5 TO 34.5 KFT	34.5 TO 39.5 KFT	39.5 TO 44.5 KFT	-.5 TO 44.5 KFT
0 - .5	1.2	1.2	0	0	0	0	0	0	0	2.4
.5 - 1.0	0	2.4	0	2.4	0	1.2	1.2	0	0	7.2
1.0 - 1.5	0	0	0	0	0	2.4	4.8	0	0	7.2
1.5 - 2.0	0	0	0	0	0	2.4	0	1.2	0	3.6
2.0 - 2.5	0	0	0	0	0	4.8	8.4	22.8	0	36.0
2.5 - 3.0	0	0	0	0	0	1.2	9.6	1.2	0	12.0
3.0 - 3.5	0	0	0	0	0	2.4	13.2	7.2	0	22.8
3.5 - 4.0	0	0	0	0	0	1.2	2.4	1.2	0	4.8
4.0 - 4.5	0	0	0	0	0	0	2.4	1.2	0	3.6
4.5 - 5.0	0	0	0	0	0	0	0	0	0	0
Totals	1.2	3.6	0	2.4	0	15.6	42.0	34.8	0	99.6

TOTAL FLIGHTS	83
TOTAL HOURS	201.4
TOTAL MILES	91487

(a) Percent of flights to maximum altitude versus flight duration

Figure 15. - Maximum altitude and flight duration statistics.

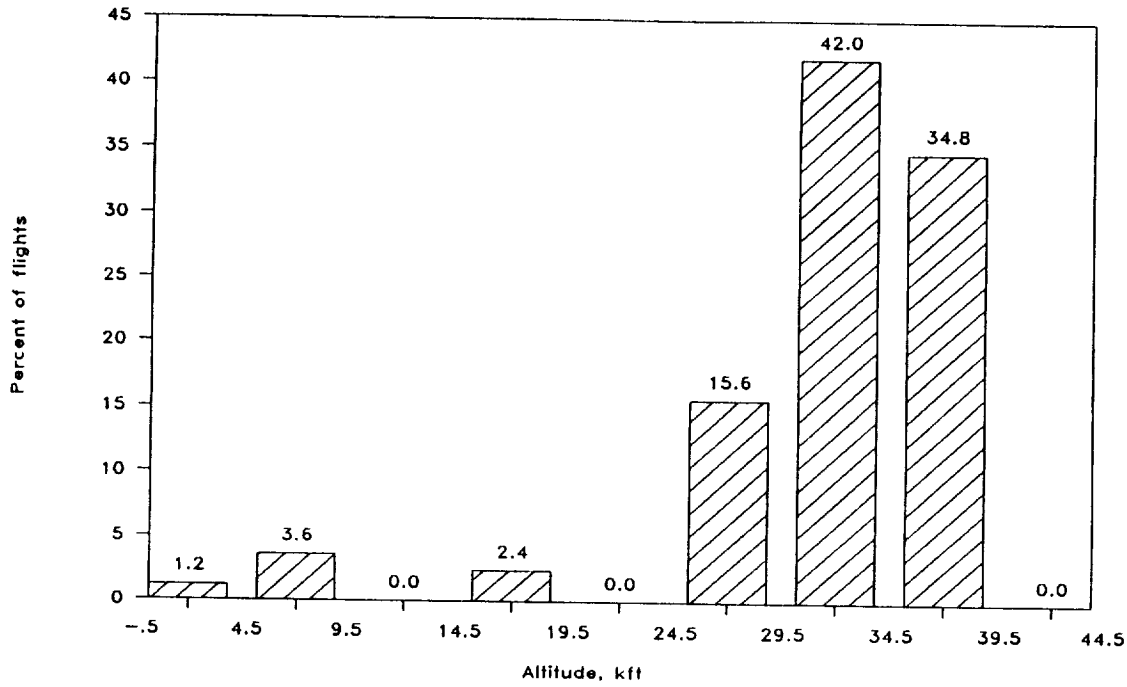

(b) Percent of flights to maximum altitude distribution

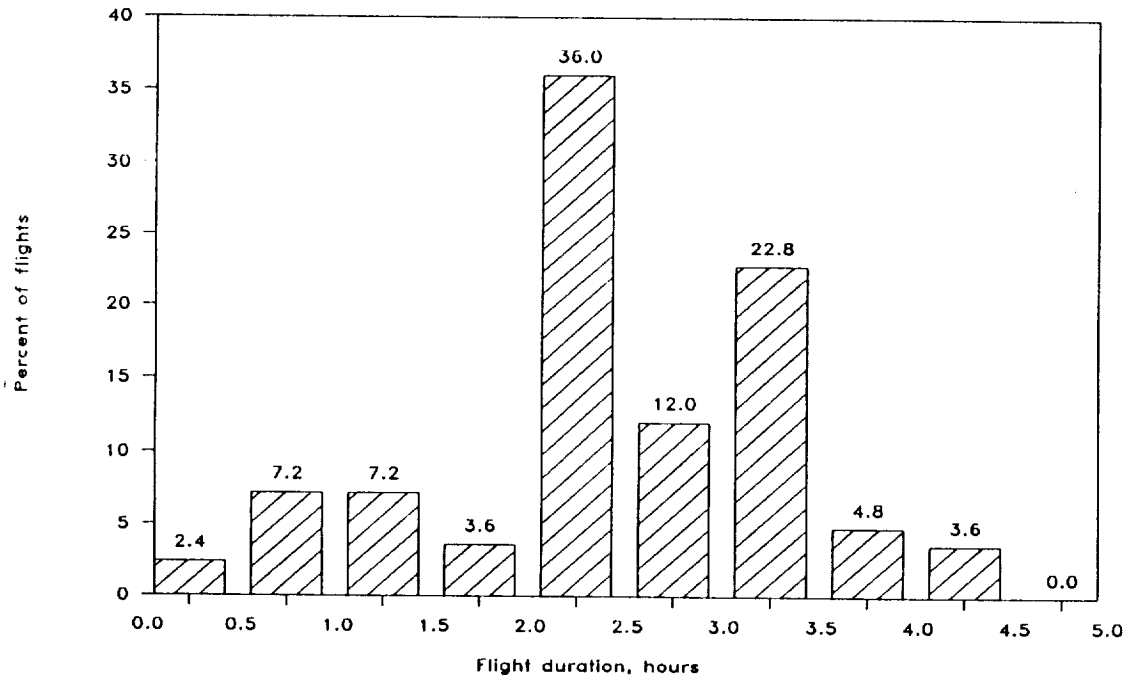

(c) Percent of flights for flight duration distribution

Figure 15.- Concluded.

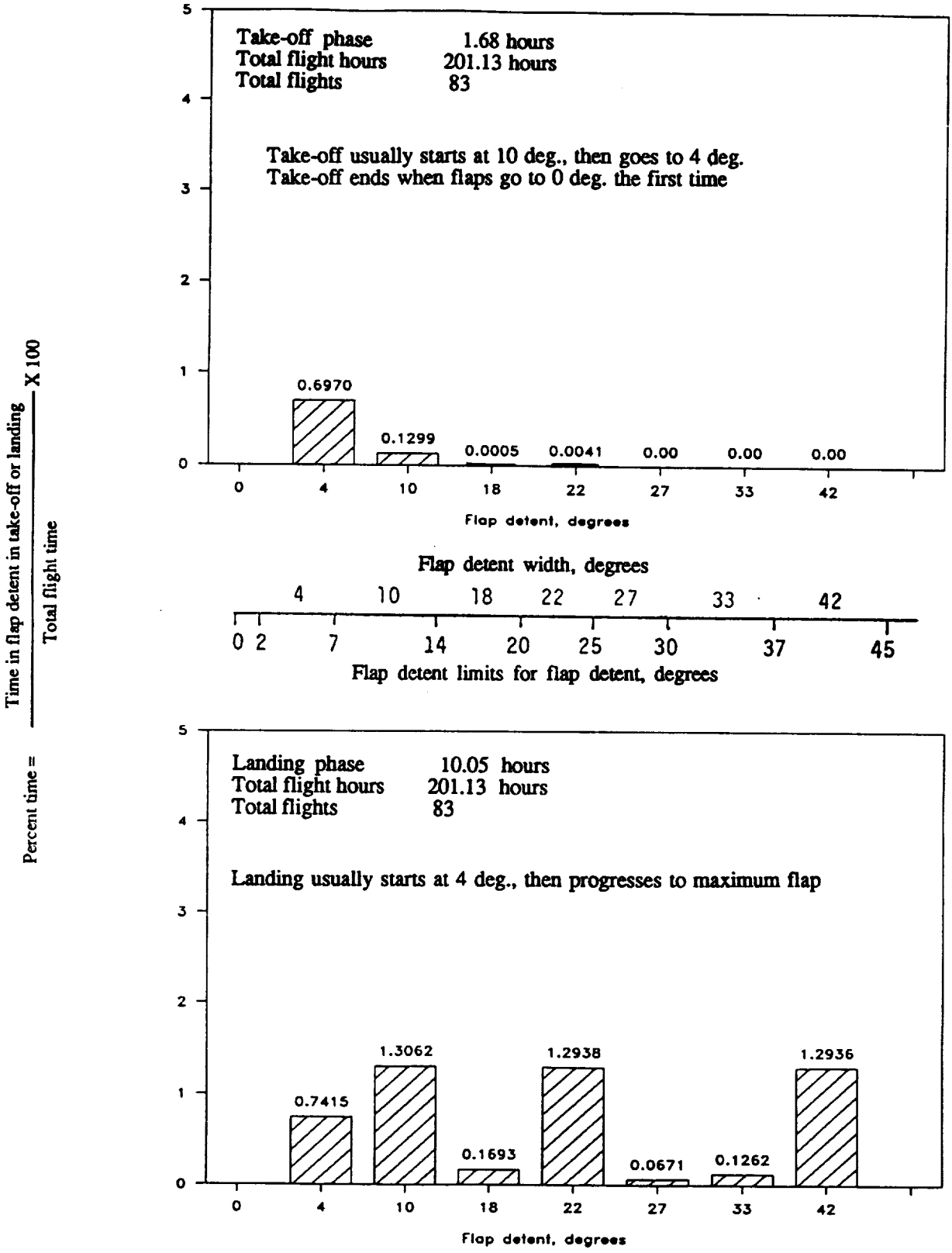

Figure 16.- Percent of time of flap detent usage in take-off and landing.

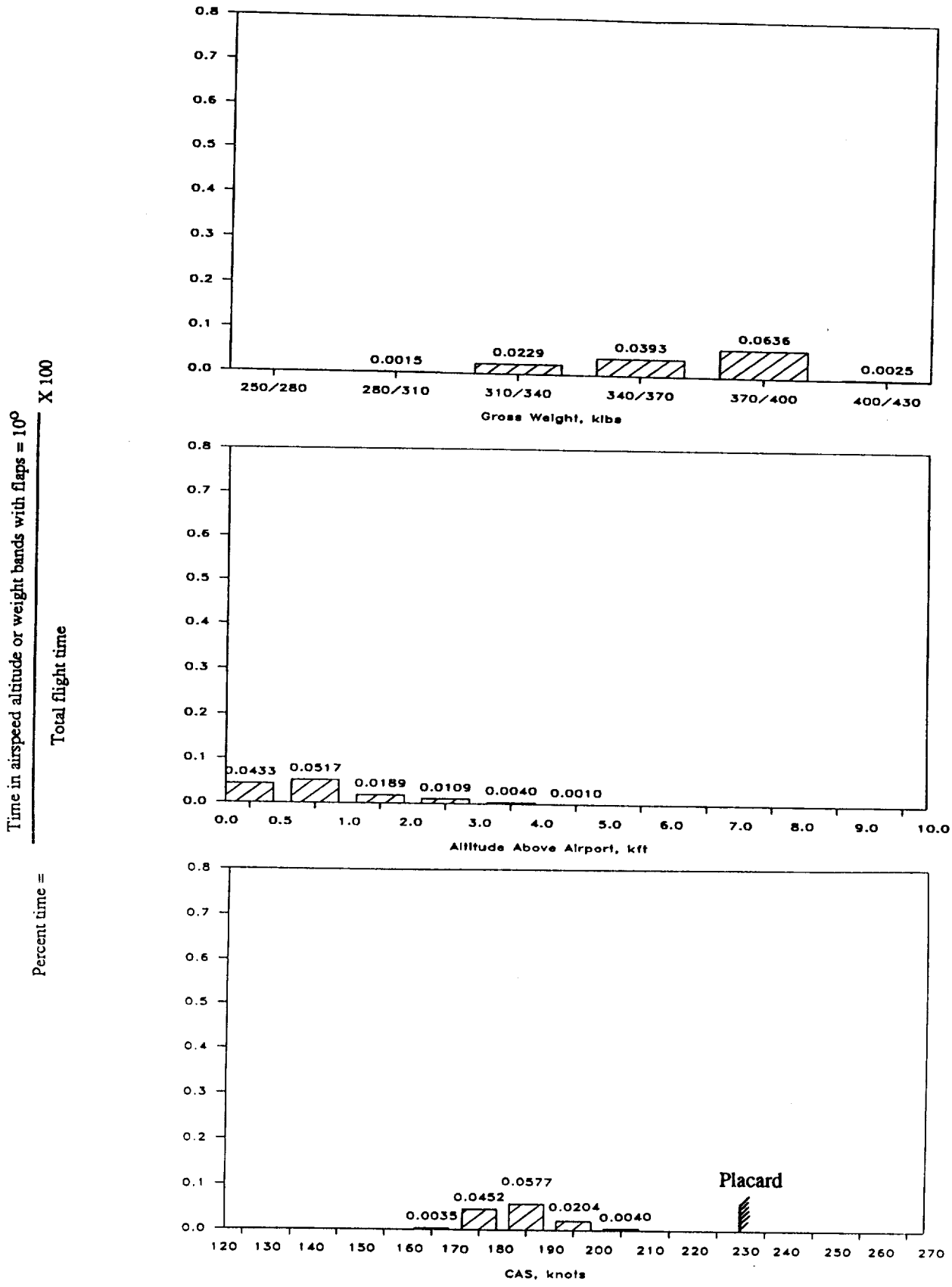

(a) Take-off with flaps = 10 deg. (.2620 hours)

Figure 17.- Percent time in gross weight, altitude above airport, and airspeed bands

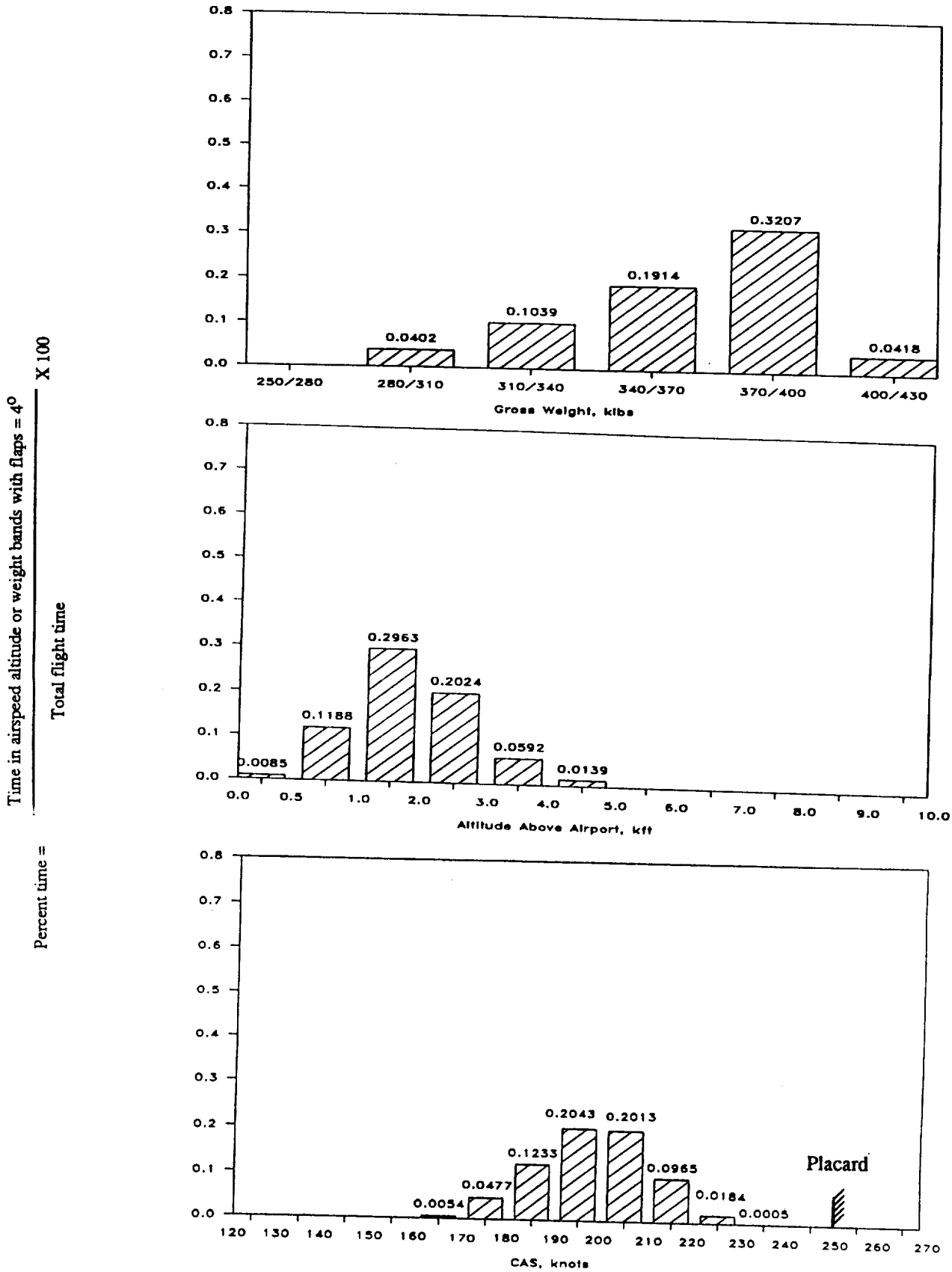

(b) Take-off with flaps = 4 deg. (1.4050 hours)

Figure 17.- Continued.

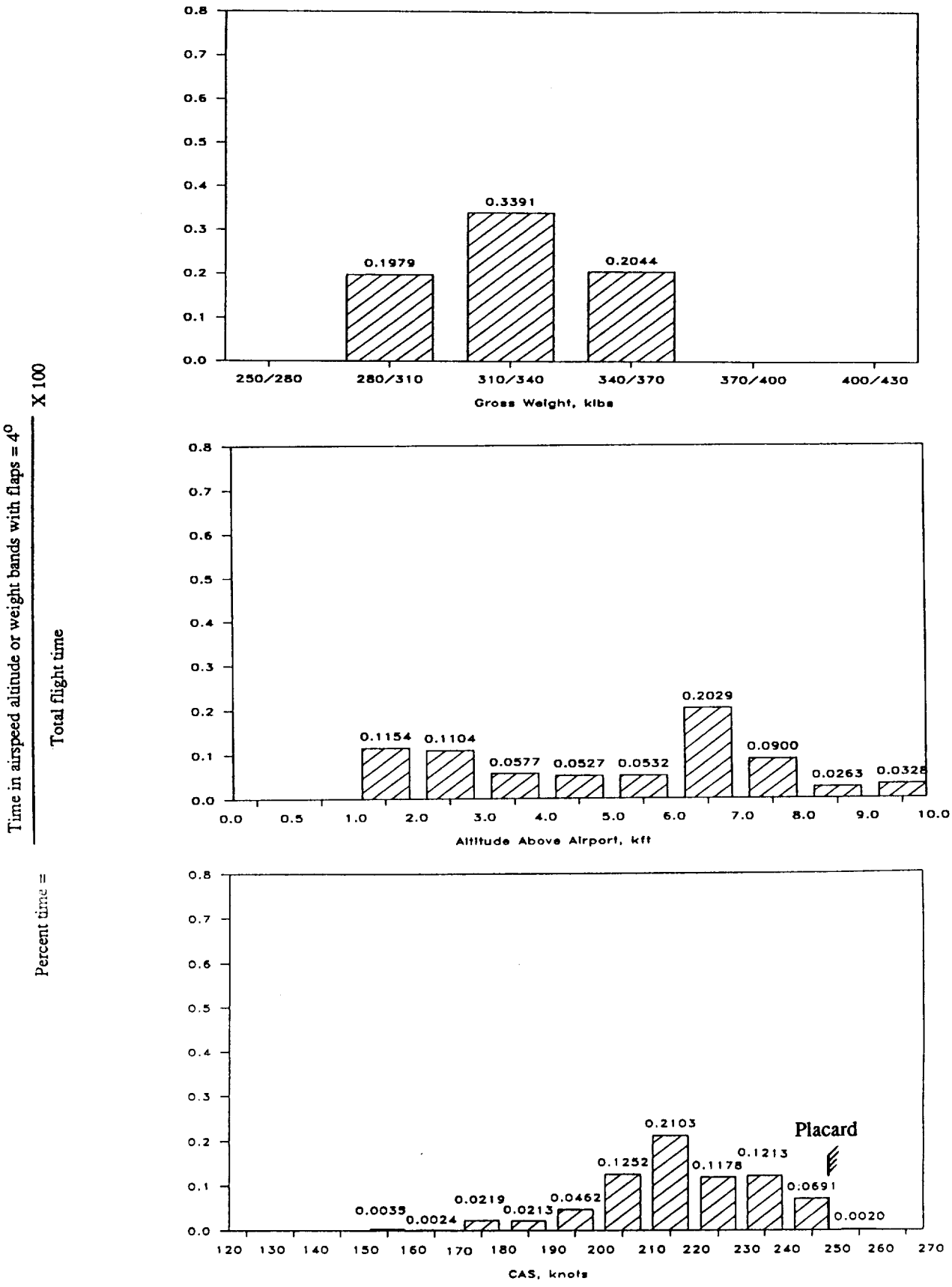

(c) Landing with flaps = 4 deg. (1.4914 hours)

Figure 17.- Continued.

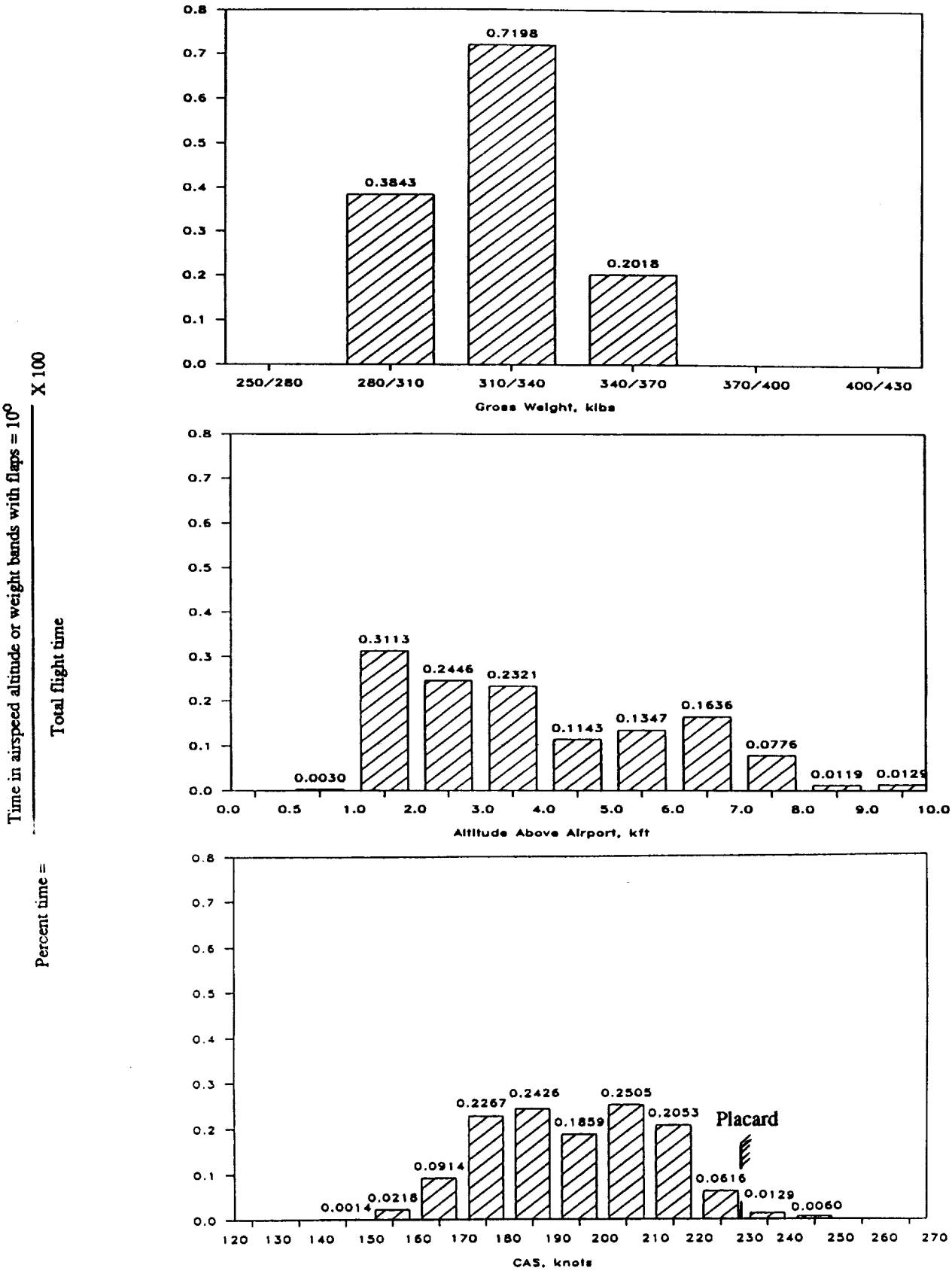

(d) Landing with flaps = 10 deg. (2.6272 hours)

Figure 17.- Continued.

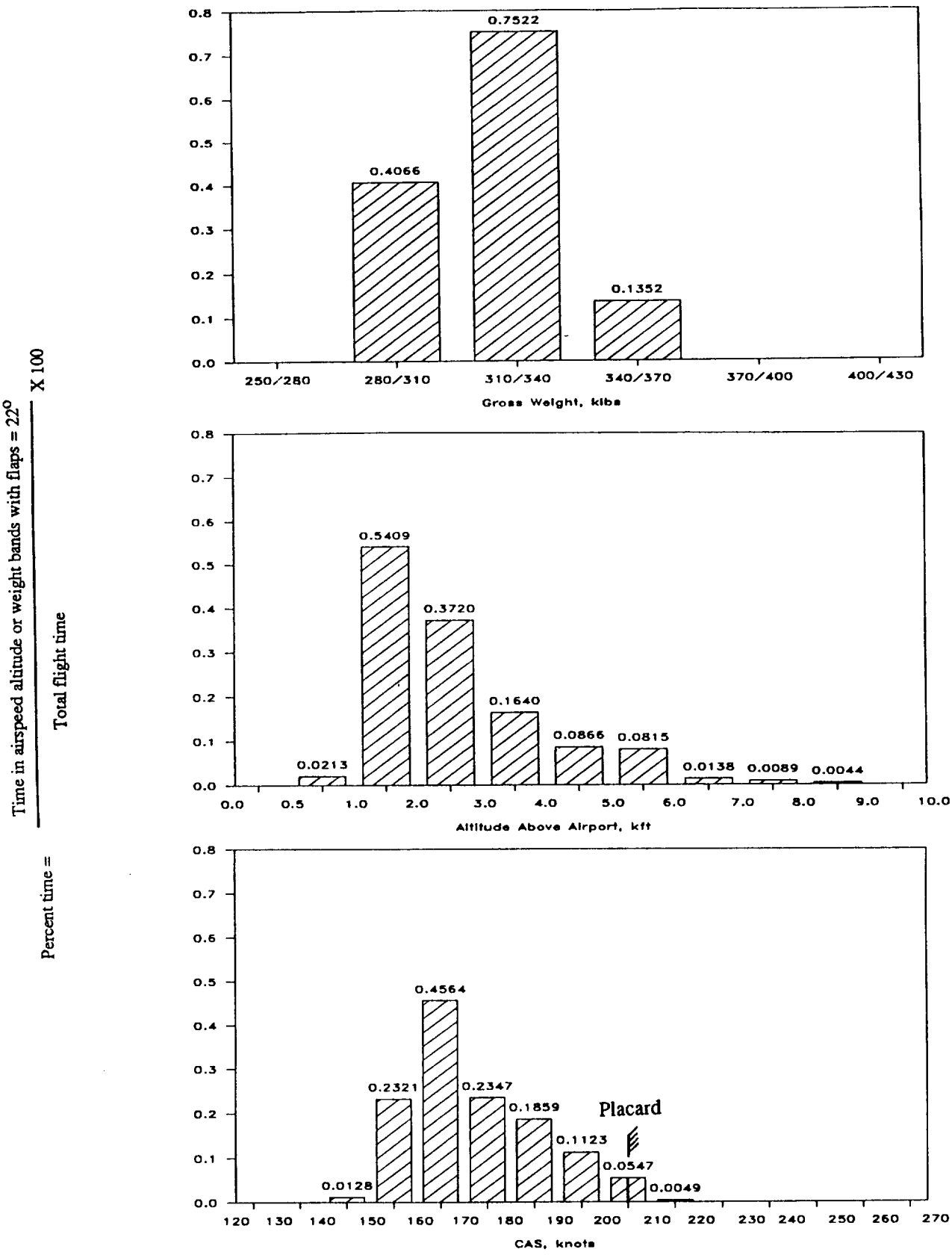

(e) Landing with flaps = 22 deg. (2.6022 hours)

Figure 17.- Continued.

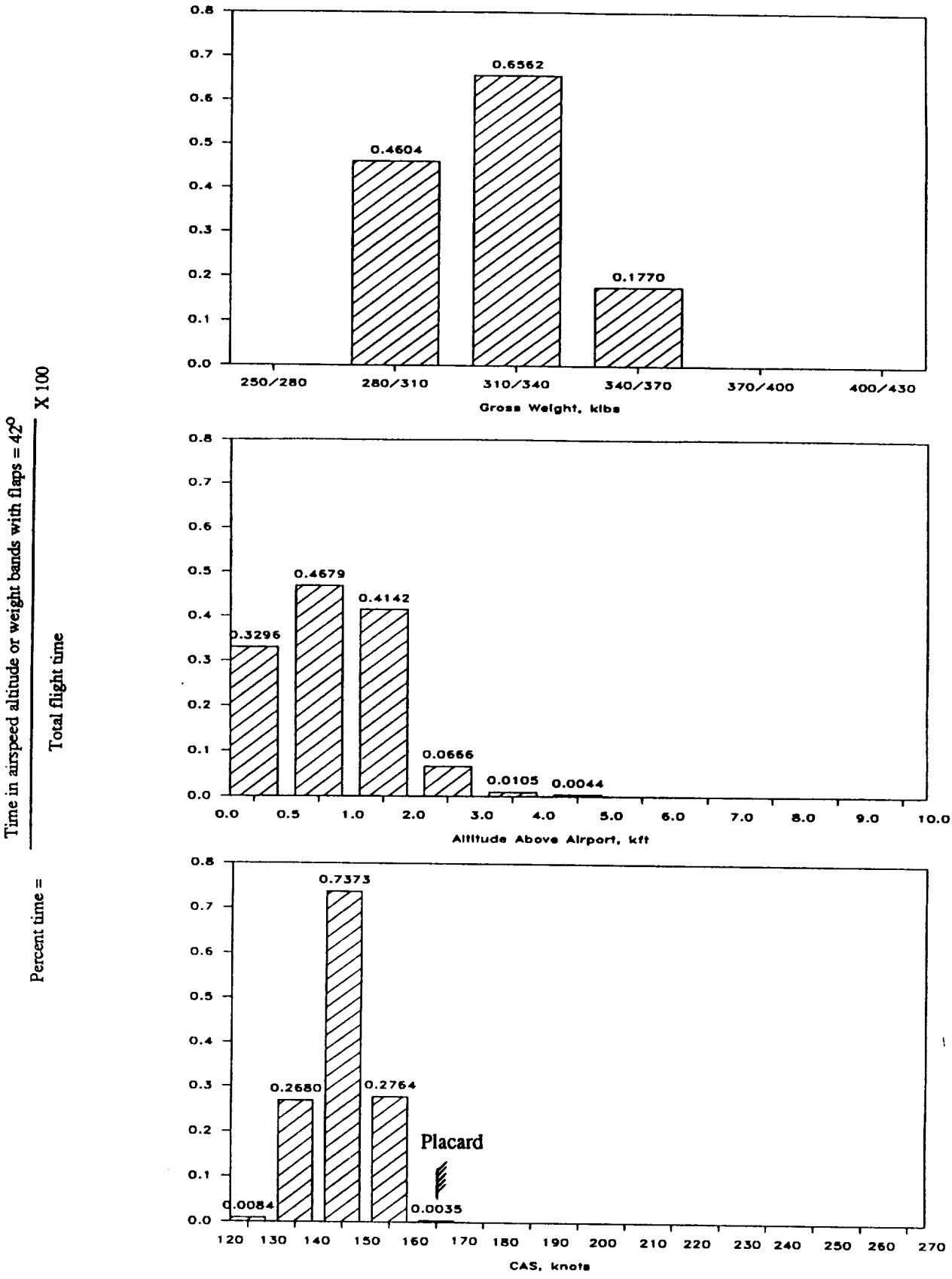

(f) Landing with flaps = 42 deg. (2.6018 hours)

Figure 17.- Concluded.

CAS, KNOTS Flaps up

Deflection degrees	180 TO 200 KTS	200 TO 220 KTS	220 TO 240 KTS	240 TO 260 KTS	260 TO 280 KTS	280 TO 300 KTS	300 TO 320 KTS	320 TO 340 KTS	340 TO 360 KTS	360 TO 380 KTS	380 TO 400 KTS
2 - 5	0	0.0005	0.0005	0.0085	0.0005	0	0.0040	0.0015	0.0020	0.0015	0
5 - 10	0	0.0005	0.0085	0.0380	0.0070	0.0005	0.0850	0.0065	0.0079	0.0094	0
10 - 15	0	0	0.0055	0.0490	0.0130	0.0130	0.0130	0.0110	0.0360	0.0470	0
15 - 20	0	0.0005	0.0040	0.0310	0.0180	0.0080	0.0130	0.0500	0.0930	0.0380	0
20 - 25	0	0.0080	0.0065	0.0190	0.0150	0.0085	0.0950	0.0470	0	0	0
25 - 30	0	0.0005	0.0015	0.0140	0.0085	0.0900	0.0220	0	0	0	0
30 - 35	0	0.0005	0.0085	0.0630	0.0860	0.0015	0	0	0	0	0
35 - 40	0	0.0005	0.0290	0.1800	0.0005	0	0	0	0	0	0
40 - 45	0	0.0119	0.0661	0.0010	0	0	0	0	0	0	0
45 - 50	0.0040	0.0144	0.0015	0	0	0	0	0	0	0	0
50 - 55	0	0	0	0	0	0	0	0	0	0	0
55 - 60	0	0	0	0	0	0	0	0	0	0	0
Totals	0.0040	0.0373	0.1316	0.4035	0.1485	0.1215	0.1555	0.1160	0.1389	0.0959	0

$$\text{Percent Time} = \frac{\text{Time Spoiler is Deflected}}{\text{Total Flight Time}} \times 100$$

(a) Spoiler 2 right - Matrix

Figure 18. - Percent time spoiler is deflected vs. airspeed.

CAS, KNOTS Flaps up

Deflection degrees	180 TO 200 KTS	200 TO 220 KTS	220 TO 240 KTS	240 TO 260 KTS	260 TO 280 KTS	280 TO 300 KTS	300 TO 320 KTS	320 TO 340 KTS	340 TO 360 KTS	360 TO 380 KTS	380 TO 400 KTS
2 - 5	0	0.0010	0.0075	0.0606	0.0150	0.0150	0.0190	0.0160	0.0280	0.0290	0
5 - 10	0	0.0079	0.0075	0.0390	0.0310	0.0130	0.0350	0.0140	0.0094	0.0170	0
10 - 15	0	0.0005	0.0020	0.0120	0.0020	0.0045	0.0070	0.0020	0.0160	0.0010	0
15 - 20	0	0.0005	0.0025	0.0180	0.0055	0.0020	0.0045	0.0270	0.0740	0.0250	0
20 - 25	0	0	0.0010	0.0230	0.0015	0.0065	0.0600	0.0490	0	0	0
25 - 30	0	0	0.0020	0.0180	0.0015	0.0360	0.0170	0	0	0	0
30 - 35	0	0	0.0045	0.0025	0.0280	0.0460	0	0	0	0	0
35 - 40	0	0.0005	0.0005	0.0210	0.0570	0	0	0	0	0	0
40 - 45	0	0	0.0045	0.1500	0.0010	0	0	0	0	0	0
45 - 50	0	0	0.0690	0.0184	0	0	0	0	0	0	0
50 - 55	0	0.0260	0.0170	0	0	0	0	0	0	0	0
55 - 60	0	0.0005	0	0	0	0	0	0	0	0	0
Totals	0	0.0369	0.1180	0.3625	0.1425	0.1230	0.1425	0.0108	0.1274	0.0720	0

$$\text{Percent Time} = \frac{\text{Time Spoiler is Deflected}}{\text{Total Flight Time}} \times 100$$

(b) Spoiler 5 left - Matrix

Figure 18. - Continued

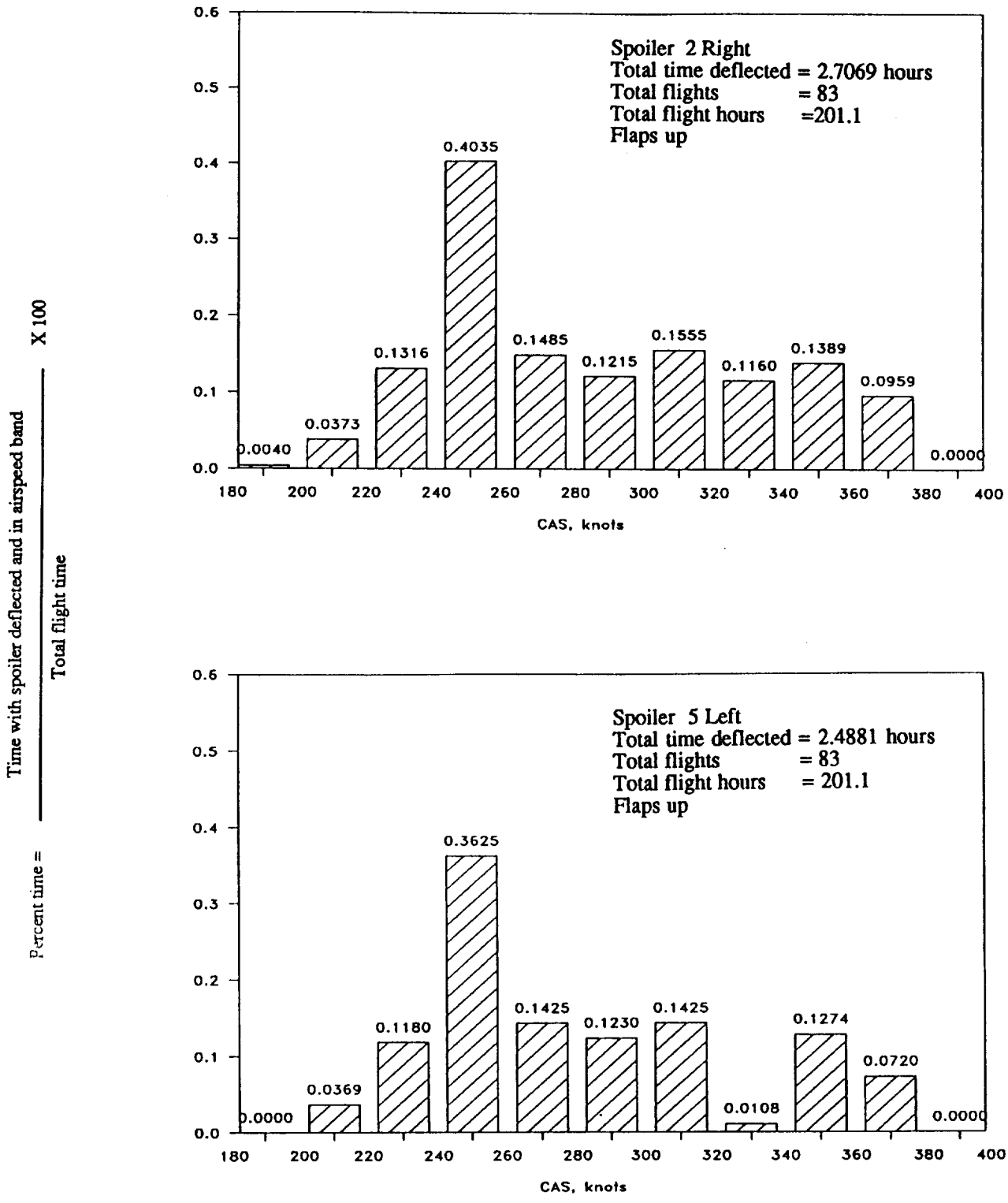

(c) Spoiler use vs. airspeed, histograms

Figure 18.- Concluded.

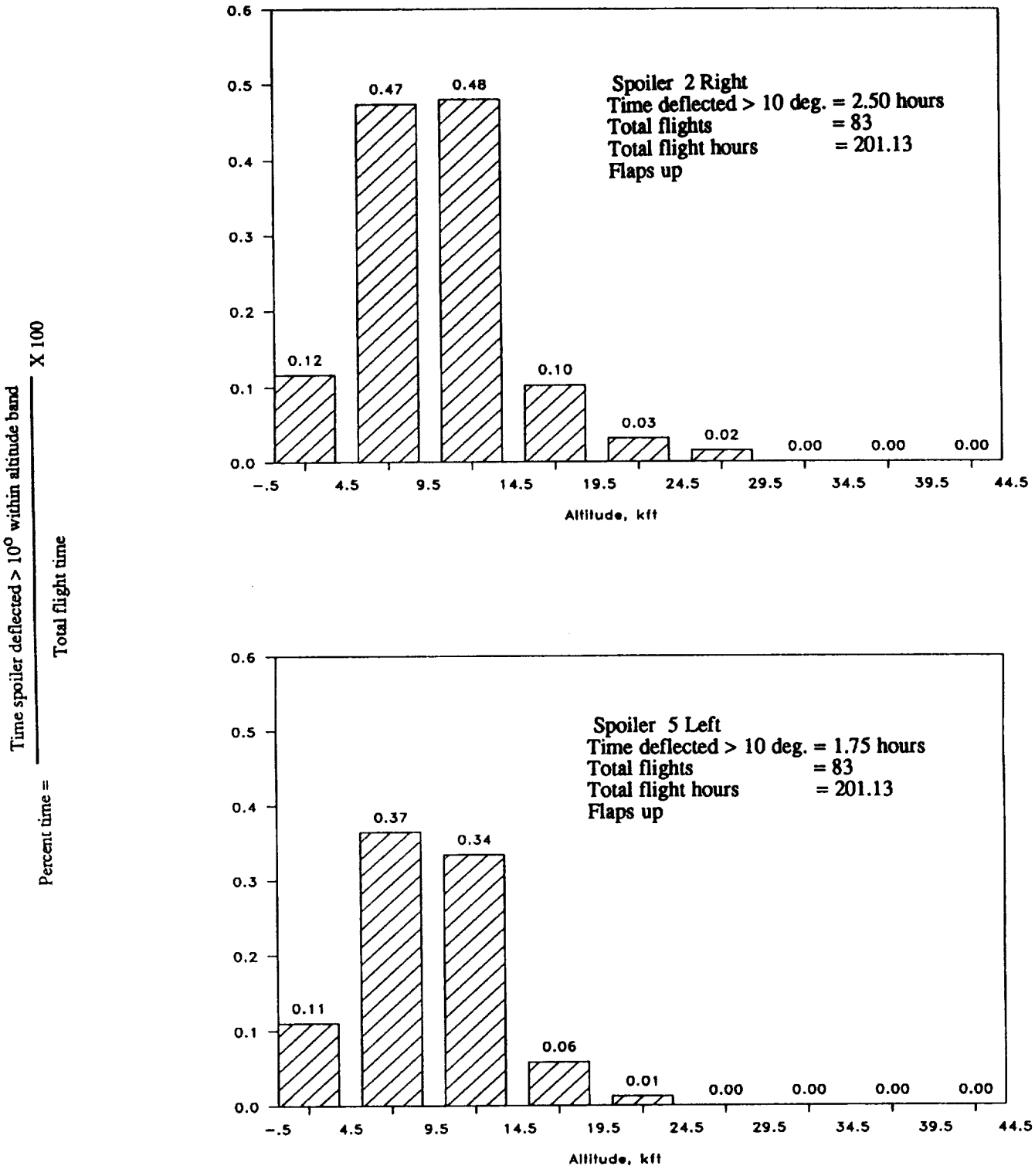

Figure 19.- Percent time of spoiler use vs. altitude histograms.

PRESSURE ALTITUDE BANDS

a_n g's	-500 TO 4500 FT	4500 TO 9500 FT	9500 TO 14500 FT	14500 TO 19500 FT	19500 TO 24500 FT	24500 TO 29500 FT	29500 TO 34500 FT	34500 TO 39500 FT	39500 TO 44500 FT	-500 TO 44500 FT
1.60	0	0	0	0	0	0	0	0	0	0
1.40	0	0	0	0	0	0	0	0	0	0
1.20	0	0	0	0	0	0	0	0	0	0
1.00	0	0	0	0	0	0	0	0	0	0
.80	0	0	0	0	0	0	0	0	0	0
.70	0	0	0	0	0	0	0	0	0	0
.60	0	0	0	0	0	0	0	0	0	0
.50	0	0.08	0	0	0	0	0	0	0	0
.40	0.08	0.82	0	0	0.21	0.03	0.01	0	0	0.07
.30	0.61	3.05	0.31	0.57	0.53	0.06	0.04	0.07	0	0.33
.20	14.43	11.52	6.13	3.97	1.59	0.93	0.43	0.70	0	2.63
.15	41.46	30.29	16.20	13.39	5.29	3.66	2.23	2.92	0	8.19
.10	142.22	87.57	73.62	49.82	25.79	17.38	12.63	18.31	0	32.72
.05	409.72	264.20	214.23	204.31	150.74	116.11	97.22	103.77	0	144.90
0	890.89	938.77	964.07	1128.60	1171.99	1656.77	1682.94	1569.31	0	1476.05
-.05	359.53	206.50	169.16	158.68	128.75	103.56	92.47	114.51	0	131.41
-.10	96.05	51.69	37.07	27.13	15.86	13.76	9.85	15.90	0	22.22
-.15	22.85	17.03	8.93	6.81	3.07	3.19	1.62	3.07	0	5.14
-.20	4.94	6.09	2.80	1.59	1.16	0.99	0.24	0.58	0	1.32
-.30	0.15	1.32	0.10	0.11	0	0.06	0.01	0.10	0	0.13
-.40	0	0.25	0	0	0	0.03	0	0.02	0	0.02
-.50	0	0.08	0	0	0	0	0	0	0	0
-.60	0	0	0	0	0	0	0	0	0	0
-.70	0	0	0	0	0	0	0	0	0	0
-.80	0	0	0	0	0	0	0	0	0	0
-1.00	0	0	0	0	0	0	0	0	0	0
-1.20	0	0	0	0	0	0	0	0	0	0
-1.40	0	0	0	0	0	0	0	0	0	0
-1.60	0	0	0	0	0	0	0	0	0	0
FLIGHT HOURS @ ALT	13.2	12.1	9.6	8.8	9.5	32.3	74.5	41.4	0	201.4
FLIGHT MILES @ ALT	2684.9	3549.1	3609.7	3791.7	4396.4	16102.9	36983.4	20369.4	0	91487.0

TOTAL FLIGHTS	83
TOTAL FLIGHT HOURS FLAPS UP AND DOWN	201.4
TOTAL FLIGHT MILES FLAPS UP AND DOWN	91487

(a) a_n Level crossing counts per hour within pressure altitude bands

Figure 20. - Normal acceleration exceedances

PRESSURE ALTITUDE BANDS

a_{nM} g's	-500 TO 4500 FT	4500 TO 9500 FT	9500 TO 14500 FT	14500 TO 19500 FT	19500 TO 24500 FT	24500 TO 29500 FT	29500 TO 34500 FT	34500 TO 39500 FT	39500 TO 44500 FT	-500 TO 44500 FT
1.60	0	0	0	0	0	0	0	0	0	0
1.40	0	0	0	0	0	0	0	0	0	0
1.20	0	0	0	0	0	0	0	0	0	0
1.00	0	0	0	0	0	0	0	0	0	0
.80	0	0	0	0	0	0	0	0	0	0
.70	0	0	0	0	0	0	0	0	0	0
.60	0	0	0	0	0	0	0	0	0	0
.50	0	0	0	0	0	0	0	0	0	0
.40	0	0	0	0	0	0	0	0	0	0
.30	0	0.16	0	0	0.11	0.03	0	0	0	0.02
.20	0.84	0.91	0.73	0.22	0.21	0.03	0	0	0	0.17
.15	3.95	2.96	1.66	1.25	0.85	0.15	0.03	0.05	0	0.65
.10	16.02	11.85	7.89	3.97	3.07	0.93	0.12	0.14	0	2.68
.05	51.94	43.95	33.44	23.50	18.39	5.98	2.77	2.44	0	12.02
0	147.22	130.86	119.73	113.39	117.86	174.37	182.09	182.00	0	165.46
-.05	37.59	30.53	26.90	18.04	10.99	4.46	2.05	2.10	0	8.80
-.10	6.45	6.67	4.57	2.16	1.06	0.50	0.09	0.05	0	1.31
-.15	0.84	0.99	0.52	0.45	0.11	0.12	0	0	0	0.18
-.20	0.08	0.25	0.10	0	0	0.03	0	0	0	0.03
-.30	0	0	0.10	0	0	0	0	0	0	0
-.40	0	0	0	0	0	0	0	0	0	0
-.50	0	0	0	0	0	0	0	0	0	0
-.60	0	0	0	0	0	0	0	0	0	0
-.70	0	0	0	0	0	0	0	0	0	0
-.80	0	0	0	0	0	0	0	0	0	0
-1.00	0	0	0	0	0	0	0	0	0	0
-1.20	0	0	0	0	0	0	0	0	0	0
-1.40	0	0	0	0	0	0	0	0	0	0
-1.60	0	0	0	0	0	0	0	0	0	0
FLIGHT HOURS @ ALT	13.2	12.1	9.6	8.8	9.5	32.3	74.5	41.4	0.0	201.4
FLIGHT MILES @ ALT	2684.9	3549.1	3609.7	3791.7	4396.4	16102.9	36983.4	20369.4	0.0	91487.0

TOTAL FLIGHTS	83
TOTAL FLIGHT HOURS FLAPS UP AND DOWN	201.4
TOTAL FLIGHT MILES FLAPS UP AND DOWN	91487

(b) a_{nM} Level crossing counts per hour within pressure altitude bands

Figure 20. - Continued

PRESSURE ALTITUDE BANDS

a_{nG} g's	-500 TO 4500 FT	4500 TO 9500 FT	9500 TO 14500 FT	14500 TO 19500 FT	19500 TO 24500 FT	24500 TO 29500 FT	29500 TO 34500 FT	34500 TO 39500 FT	39500 TO 44500 FT	-500 TO 44500 FT
1.60	0	0	0	0	0	0	0	0	0	0
1.40	0	0	0	0	0	0	0	0	0	0
1.20	0	0	0	0	0	0	0	0	0	0
1.00	0	0	0	0	0	0	0	0	0	0
.80	0	0	0	0	0	0	0	0	0	0
.70	0	0	0	0	0	0	0	0	0	0
.60	0	0	0	0	0	0	0	0	0	0
.50	0	0	0	0	0	0	0	0	0	0
.40	0	0.25	0	0	0	0.03	0	0	0	0.02
.30	0.08	1.40	0	0.23	0	0.03	0.03	0.02	0	0.12
.20	2.20	3.87	0.73	0.68	0.32	0.25	0.17	0.24	0	0.61
.15	8.66	7.57	2.29	2.95	1.06	0.99	0.82	1.35	0	2.05
.10	48.14	25.51	13.60	13.51	5.71	6.41	6.00	9.30	0	11.36
.05	280.56	119.42	80.79	73.78	44.29	54.76	53.95	65.58	0	77.15
0	1187.02	1373.91	1570.51	1780.70	1814.16	1899.88	1833.43	1784.85	0	1748.30
-.05	280.33	122.30	79.96	73.89	43.97	55.60	54.85	67.09	0	77.83
-.10	48.52	23.79	13.81	12.15	5.60	6.26	5.10	8.24	0	10.65
-.15	7.59	8.15	2.80	2.95	1.06	1.23	0.64	1.28	0	2.00
-.20	1.60	4.36	0.93	0.23	0.11	0.31	0.09	0.14	0	0.54
-.30	0.15	1.40	0.10	0	0	0	0	0.02	0	0.10
-.40	0	0.16	0	0	0	0	0	0	0	0.01
-.50	0	0.08	0	0	0	0	0	0	0	0
-.60	0	0	0	0	0	0	0	0	0	0
-.70	0	0	0	0	0	0	0	0	0	0
-.80	0	0	0	0	0	0	0	0	0	0
-1.00	0	0	0	0	0	0	0	0	0	0
-1.20	0	0	0	0	0	0	0	0	0	0
-1.40	0	0	0	0	0	0	0	0	0	0
-1.60	0	0	0	0	0	0	0	0	0	0
FLIGHT HOURS @ ALT	13.2	12.1	9.6	8.8	9.5	32.3	74.5	41.4	0.0	201.4
FLIGHT MILES @ ALT	2684.9	3549.1	3609.7	3791.7	4396.4	16102.9	36983.4	20369.4	0.0	91487.0

TOTAL FLIGHTS	83
TOTAL FLIGHT HOURS FLAPS UP AND DOWN	201.4
TOTAL FLIGHT MILES FLAPS UP AND DOWN	91487

(c) a_{nG} Level crossing counts per hour within pressure altitude bands

Figure 20.- Continued.

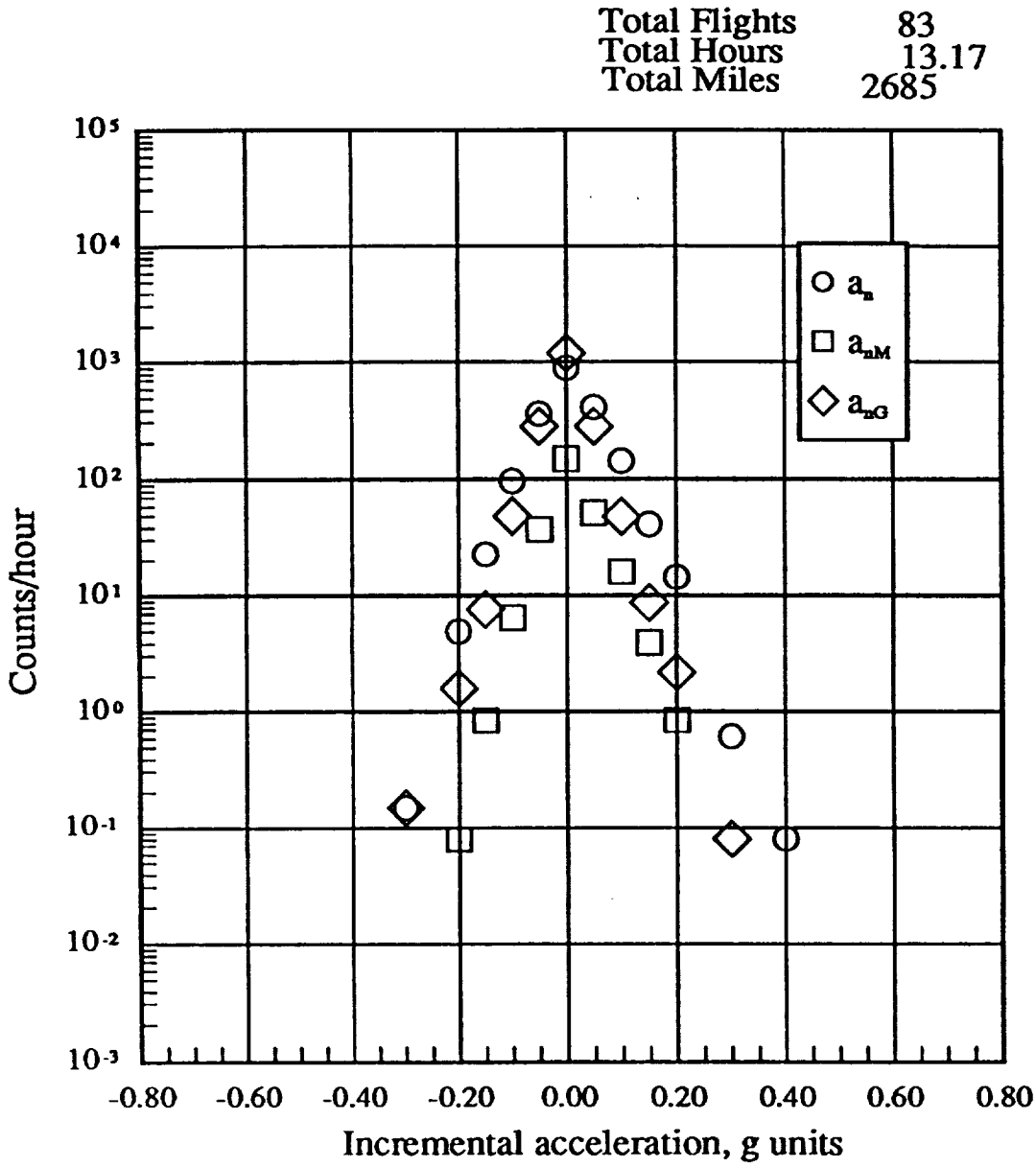

(d) a_n, a_{nM}, a_{nG}, -500 to 4500 ft

Figure 20.- Continued.

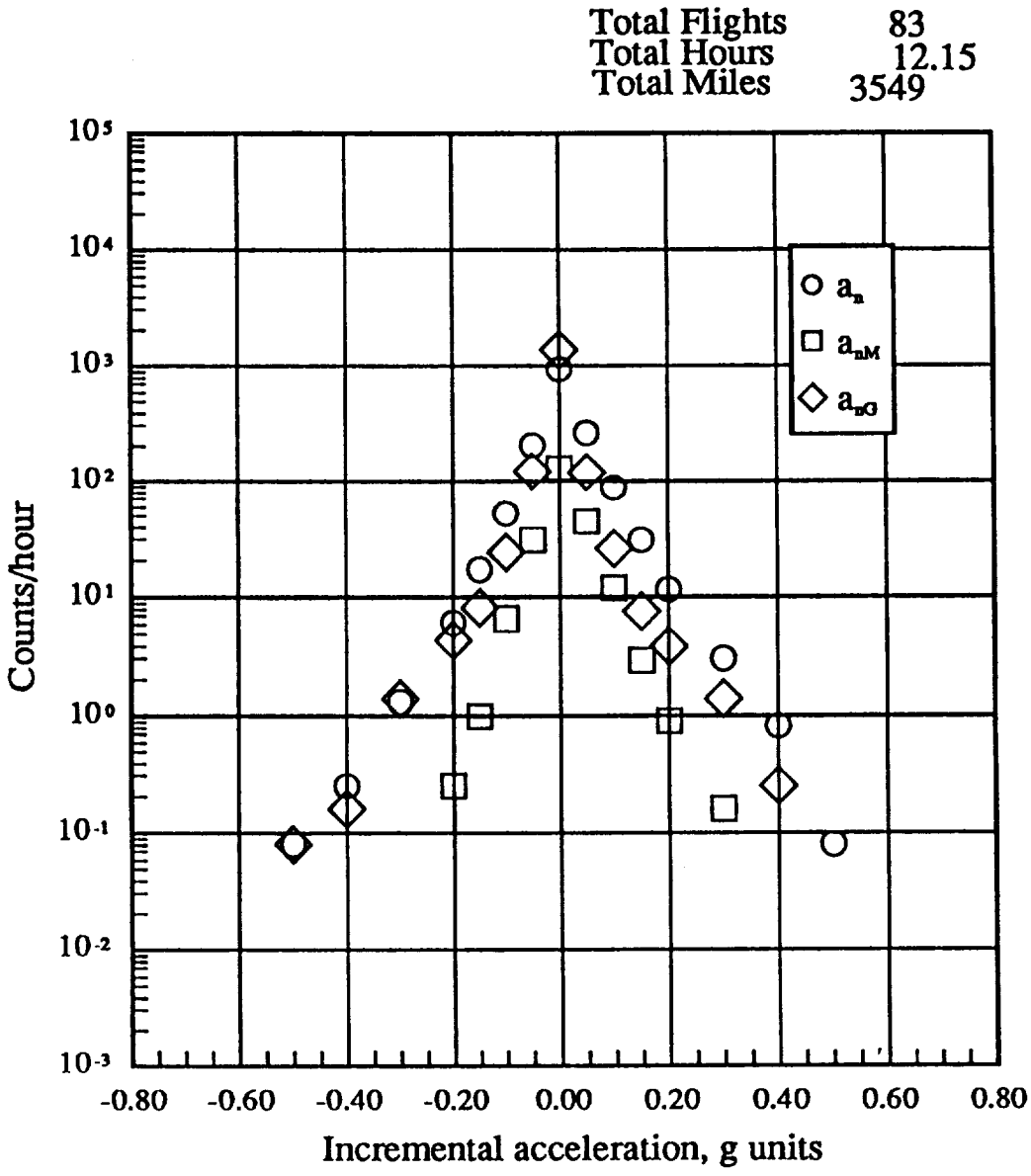

(e) a_n, a_{nM}, a_{nG}, 4500 to 9500 ft

Figure 20.- Continued.

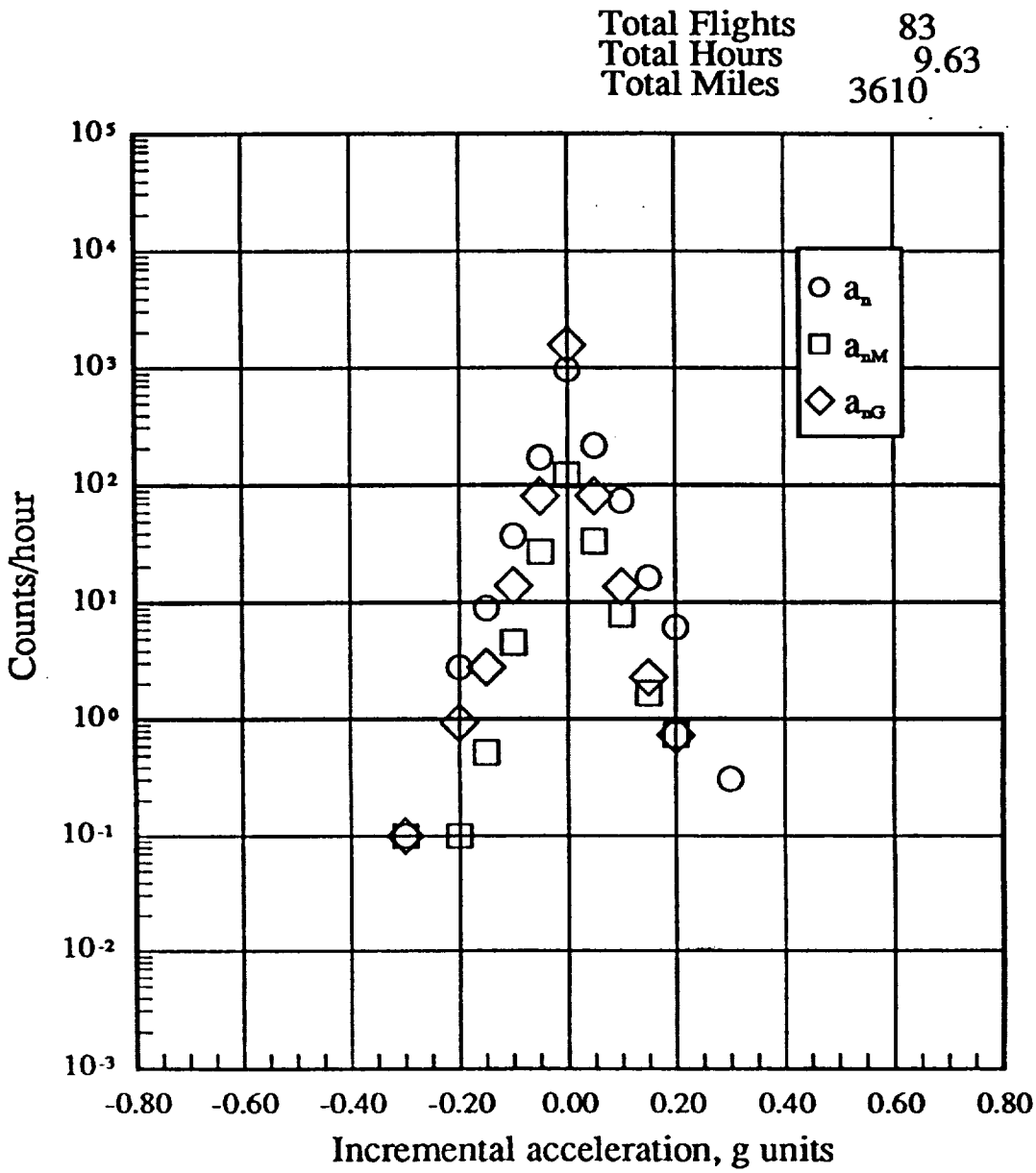

(f) a_n, a_{nM}, a_{nG}, 9500 to 14500 ft

Figure 20.- Continued.

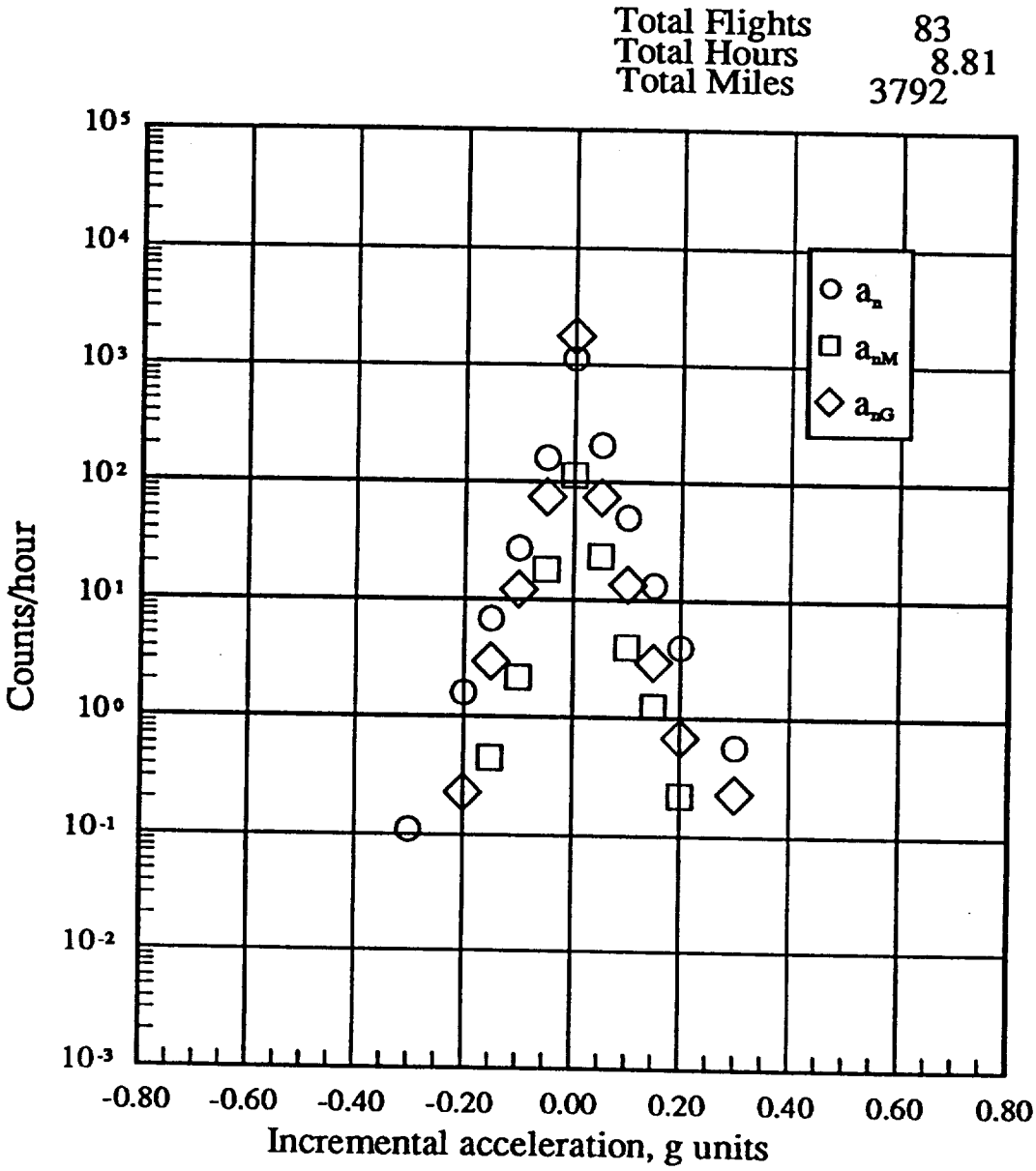

(g) a_n, a_{nM}, a_{nG}, 14500 to 19500 ft

Figure 20.- Continued.

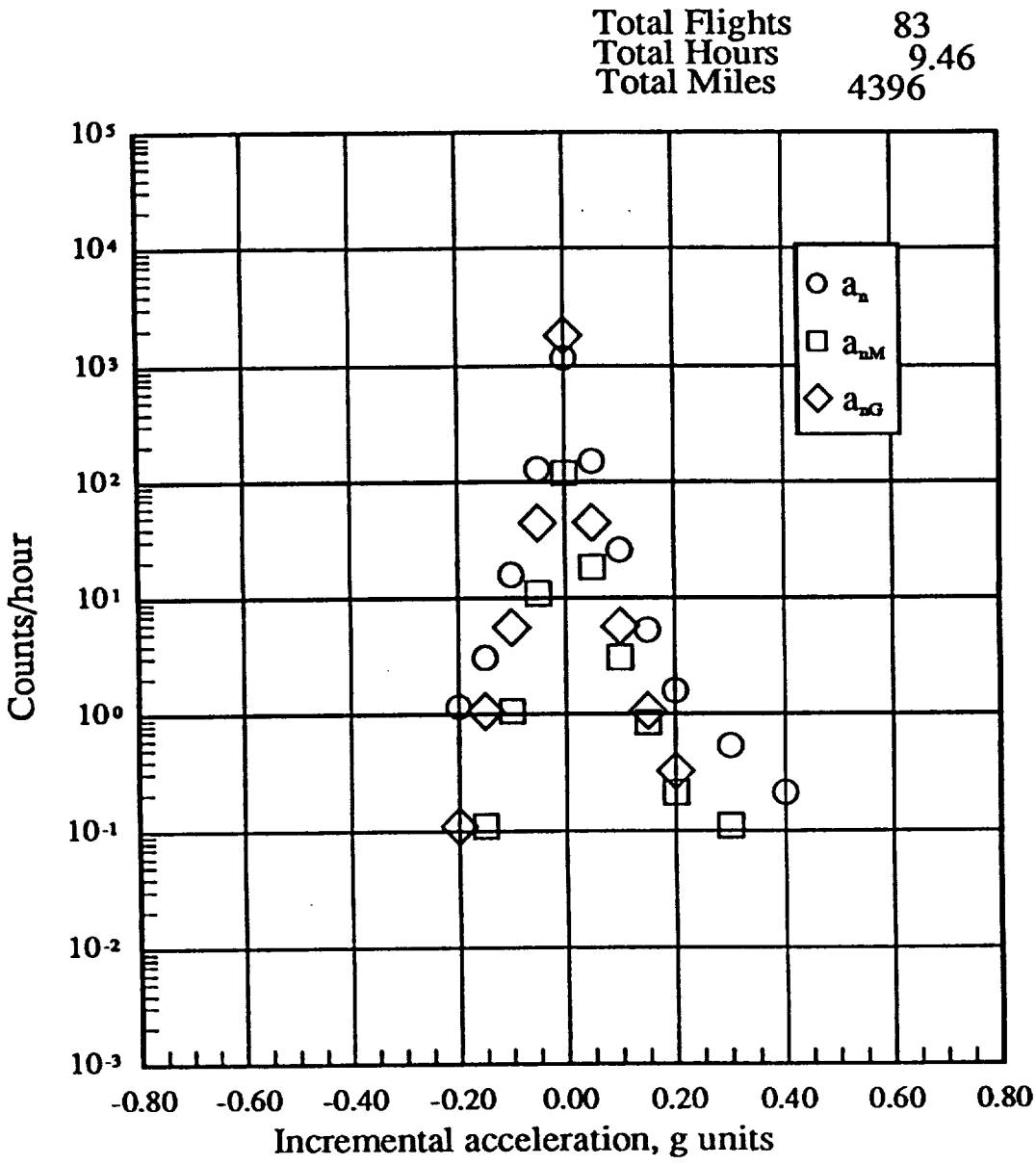

(h) a_n, a_{nM}, a_{nG}, 19500 to 24500 ft

Figure 20.- Continued.

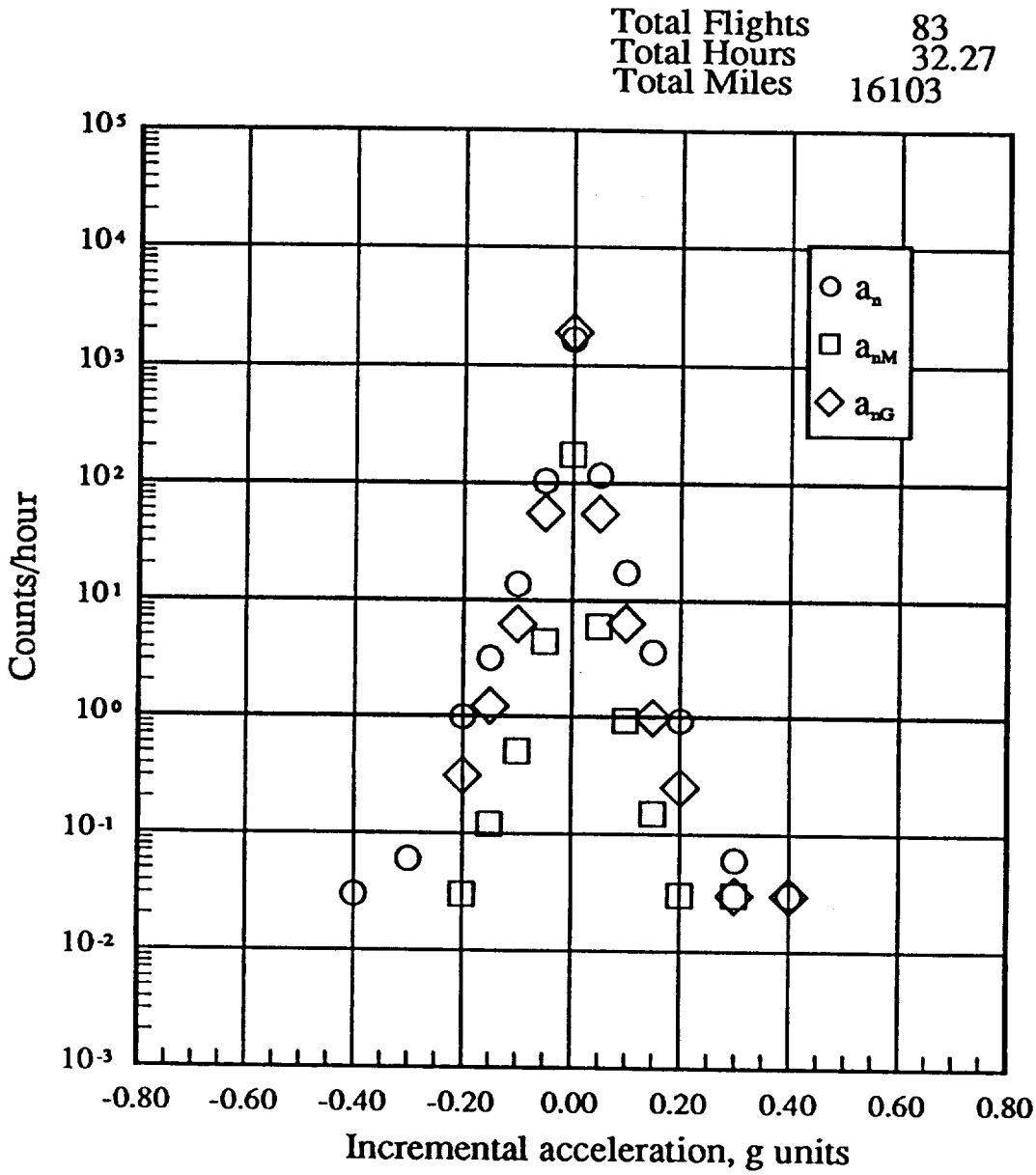

(i) a_n, a_{nM}, a_{nG}, 24500 to 29500 ft

Figure 20.- Continued.

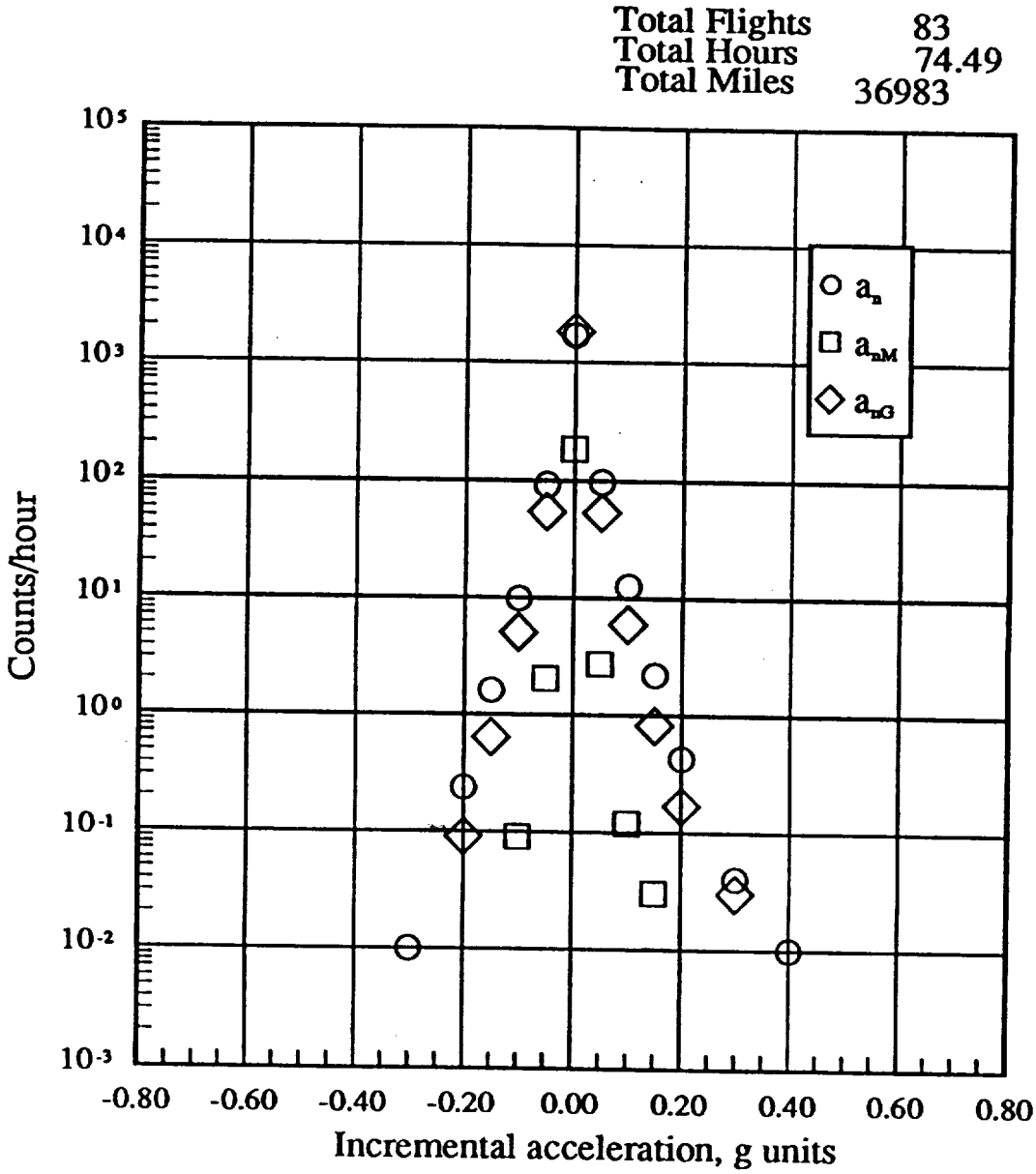

(j) a_n, a_{nM}, a_{nG}, 29500 to 34500 ft

Figure 20.- Continued.

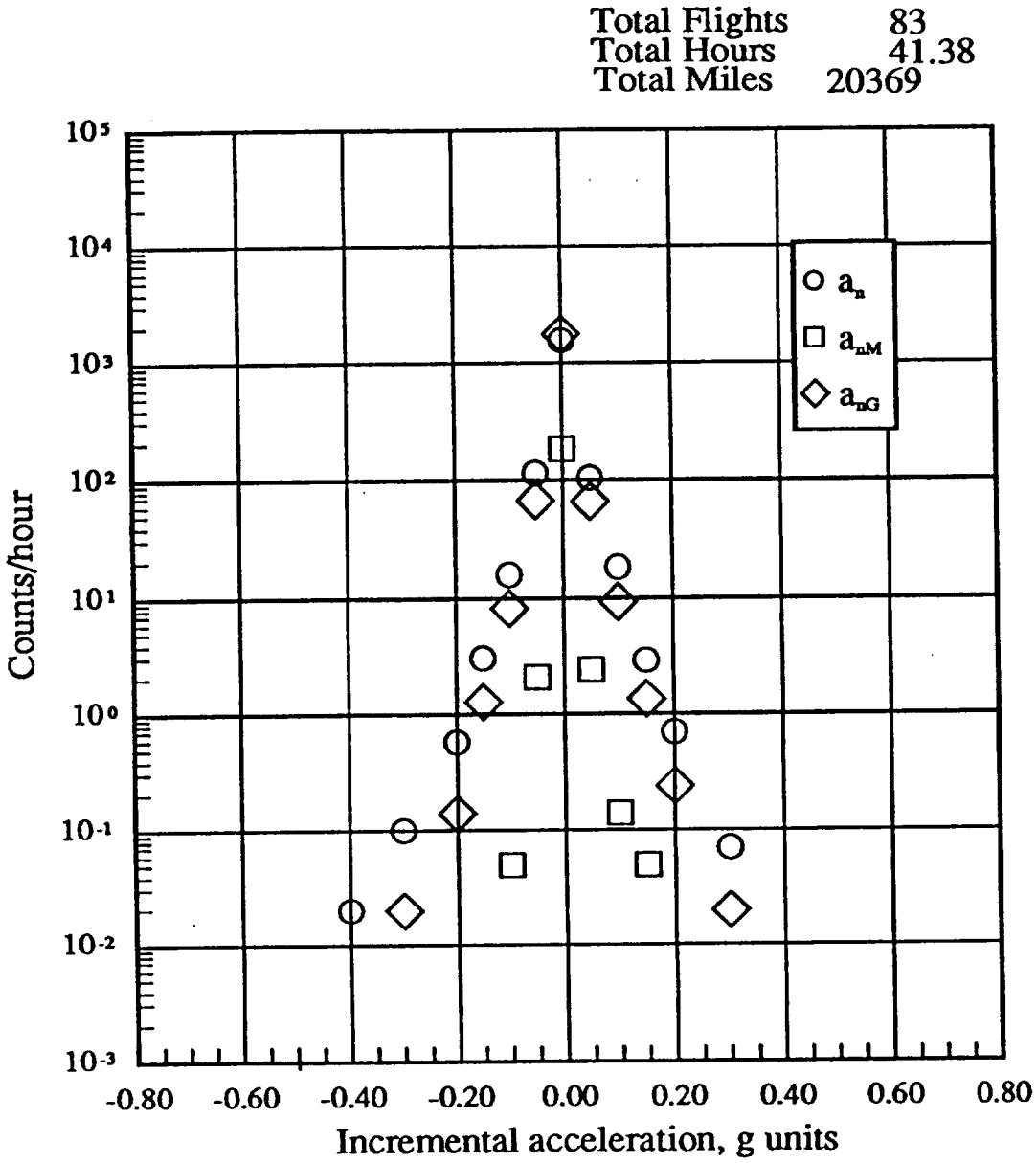

(k) a_n, a_{nM}, a_{nG}, 34500 to 39500 ft

Figure 20.- Continued.

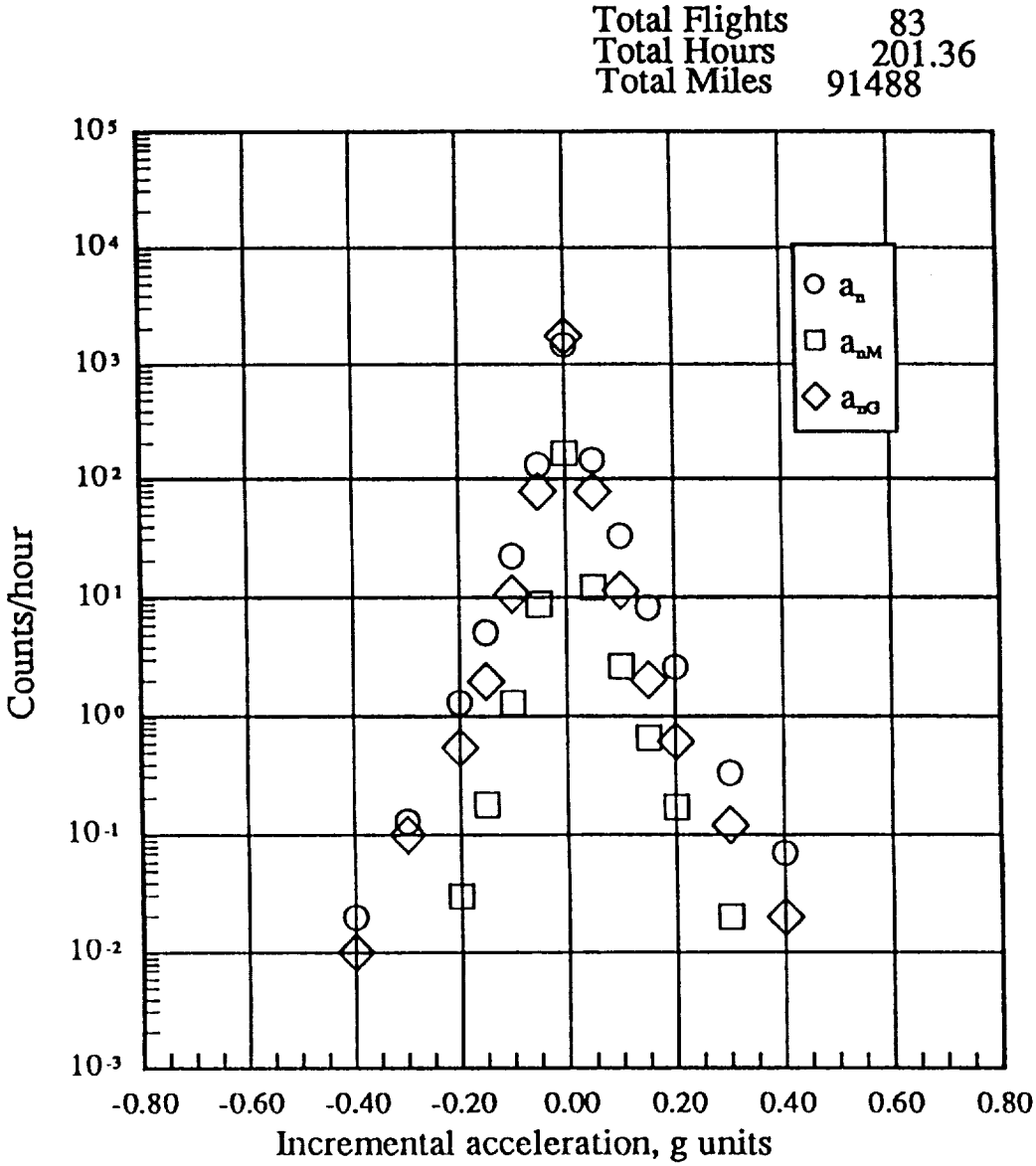

(l) a_n, a_{nM}, a_{nG}, -500 to 44500 ft

Figure 20.- Continued.

PRESSURE ALTITUDE BANDS

a_y g's	-500 TO 4500 FT	4500 TO 9500 FT	9500 TO 14500 FT	14500 TO 19500 FT	19500 TO 24500 FT	24500 TO 29500 FT	29500 TO 34500 FT	34500 TO 39500 FT	39500 TO 44500 FT	-500 TO 44500 FT
.48	0	0	0	0	0	0	0	0	0	0
.44	0	0	0	0	0	0	0	0	0	0
.40	0	0	0	0	0	0	0	0	0	0
.36	0	0	0	0	0	0	0	0	0	0
.32	0	0	0	0	0	0	0	0	0	0
.28	0	0	0	0	0	0	0	0	0	0
.24	0	0	0	0	0	0	0	0	0	0
.20	0	0	0	0	0	0	0	0	0	0
.16	0	0	0	0	0	0	0	0	0	0
.12	0	0.41	0	0	0	0	0	0	0	0.02
.08	0.61	1.48	0	1.25	0.11	0.15	0.01	0.02	0	0.22
.06	2.89	4.12	0.52	2.84	0.32	0.53	0.28	0.29	0	0.85
.04	41.61	15.23	7.37	11.46	2.64	3.94	2.30	3.26	0	6.77
.02	311.69	151.28	124.30	93.08	60.25	43.57	30.84	43.55	0	69.70
0	1023.39	983.13	882.14	964.59	1094.29	1613.98	1808.51	1762.66	0	1551.98
-.02	321.87	153.33	131.78	98.87	83.72	51.16	28.65	32.53	0	70.35
-.04	35.54	14.57	14.33	15.78	3.38	4.18	1.85	2.54	0	6.62
-.06	2.05	3.54	2.08	3.06	0.42	0.65	0.27	0.17	0	0.84
-.08	0.38	1.15	0.10	0.79	0	0.03	0.04	0.05	0	0.16
-.12	0	0.34	0	0	0	0	0	0	0	0.02
-.16	0	0	0	0	0	0	0	0	0	0
-.20	0	0	0	0	0	0	0	0	0	0
-.24	0	0	0	0	0	0	0	0	0	0
-.28	0	0	0	0	0	0	0	0	0	0
-.32	0	0	0	0	0	0	0	0	0	0
-.36	0	0	0	0	0	0	0	0	0	0
-.40	0	0	0	0	0	0	0	0	0	0
-.44	0	0	0	0	0	0	0	0	0	0
-.48	0	0	0	0	0	0	0	0	0	0
FLIGHT HOURS @ ALT	13.2	12.1	9.6	8.8	9.5	32.3	74.5	41.4	0	201.4
FLIGHT HOURS @ ALT	2684.9	3549.1	3609.7	3791.9	4396.4	16102.9	36983.4	20369.4	0	91487.0

TOTAL FLIGHTS	83
TOTAL FLIGHT HOURS FLAPS UP AND DOWN	201.4
TOTAL FLIGHT MILES FLAPS UP AND DOWN	91487

(a) a_y Level crossing counts per hour within pressure altitude bands

Figure 21. - Lateral acceleration exceedances.

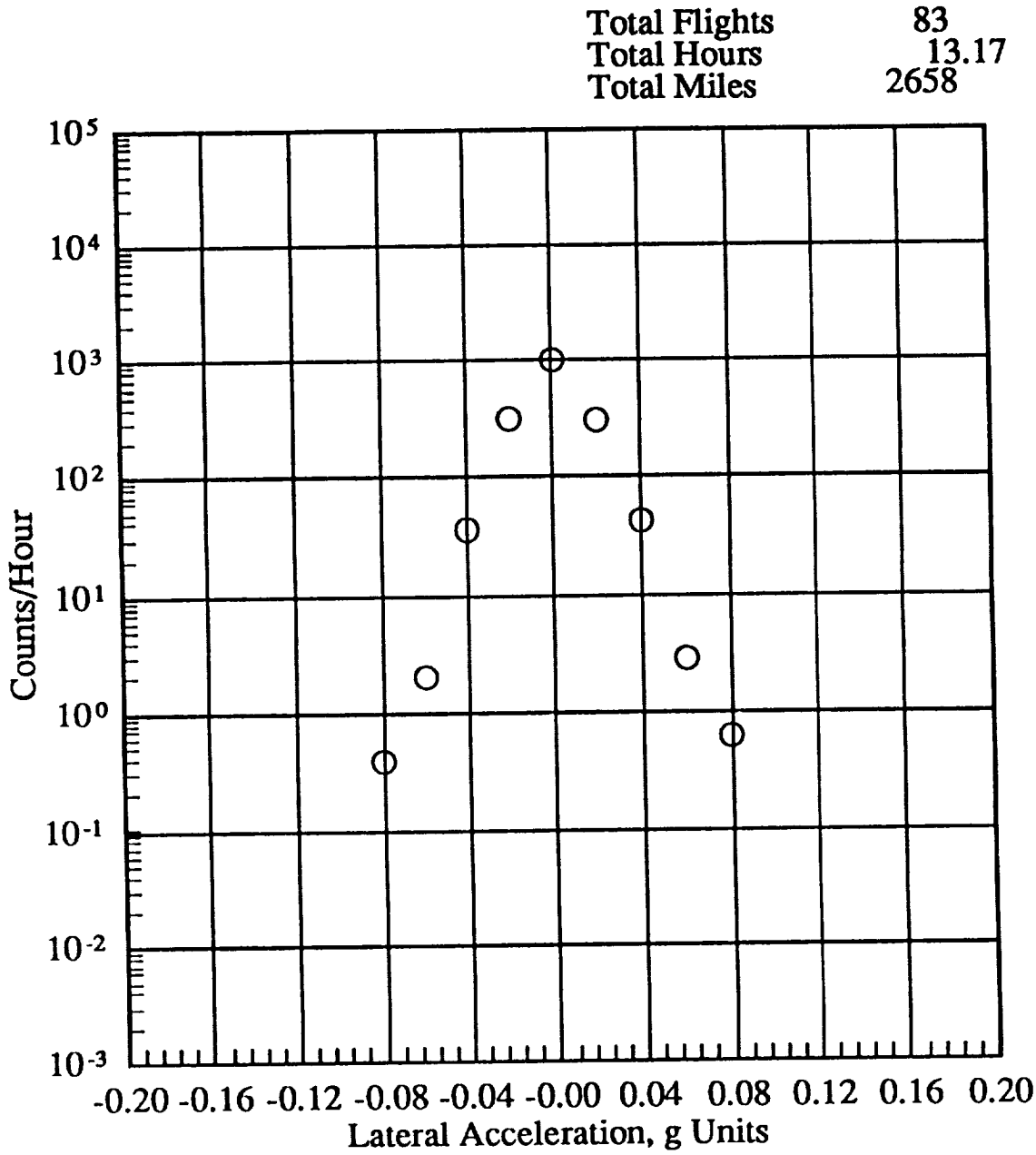

(b) a_y -500 to 4500 ft

Figure 21.- Continued.

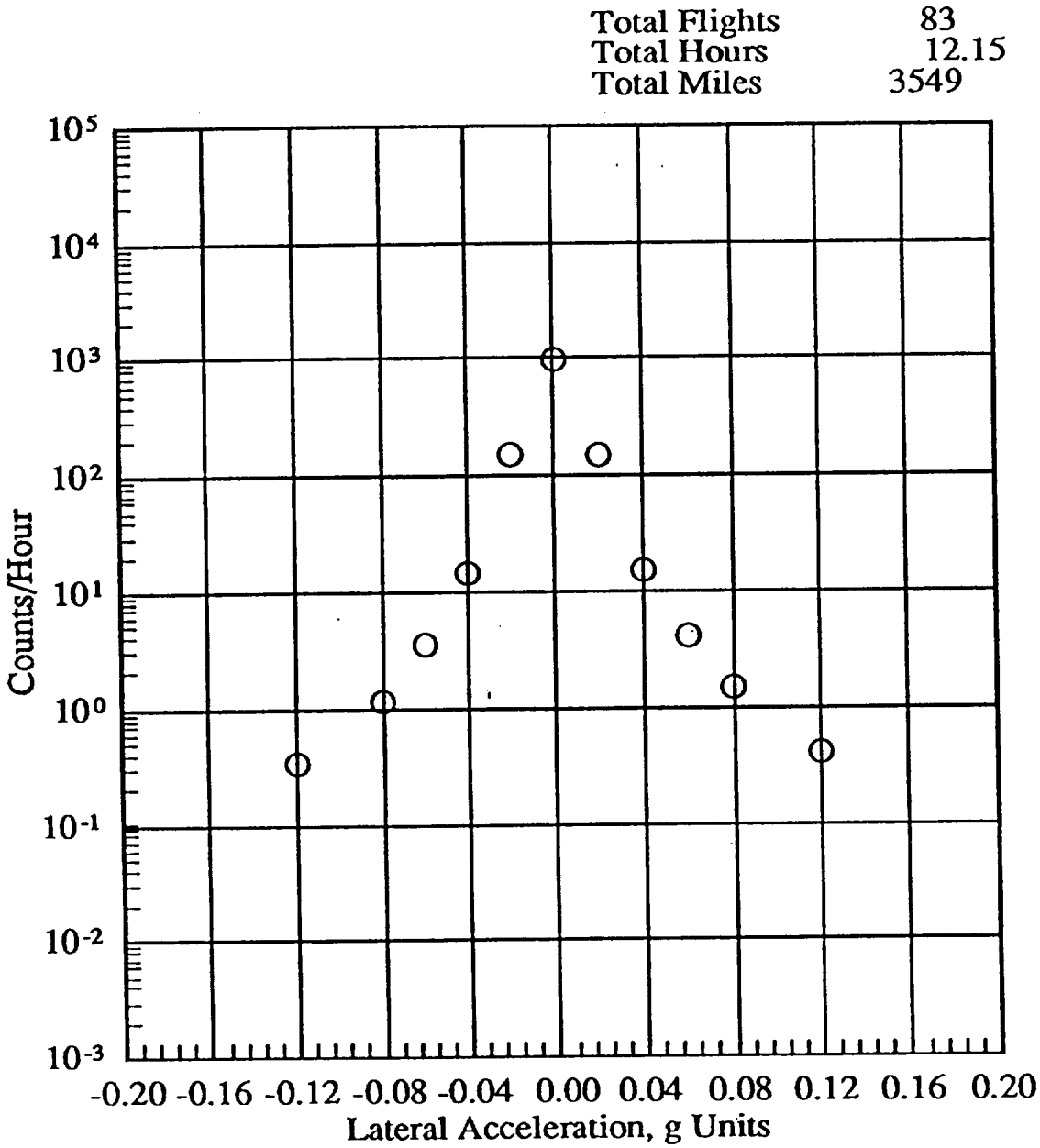

(c) a_y 4500 to 9500 ft

Figure 21.- Continued.

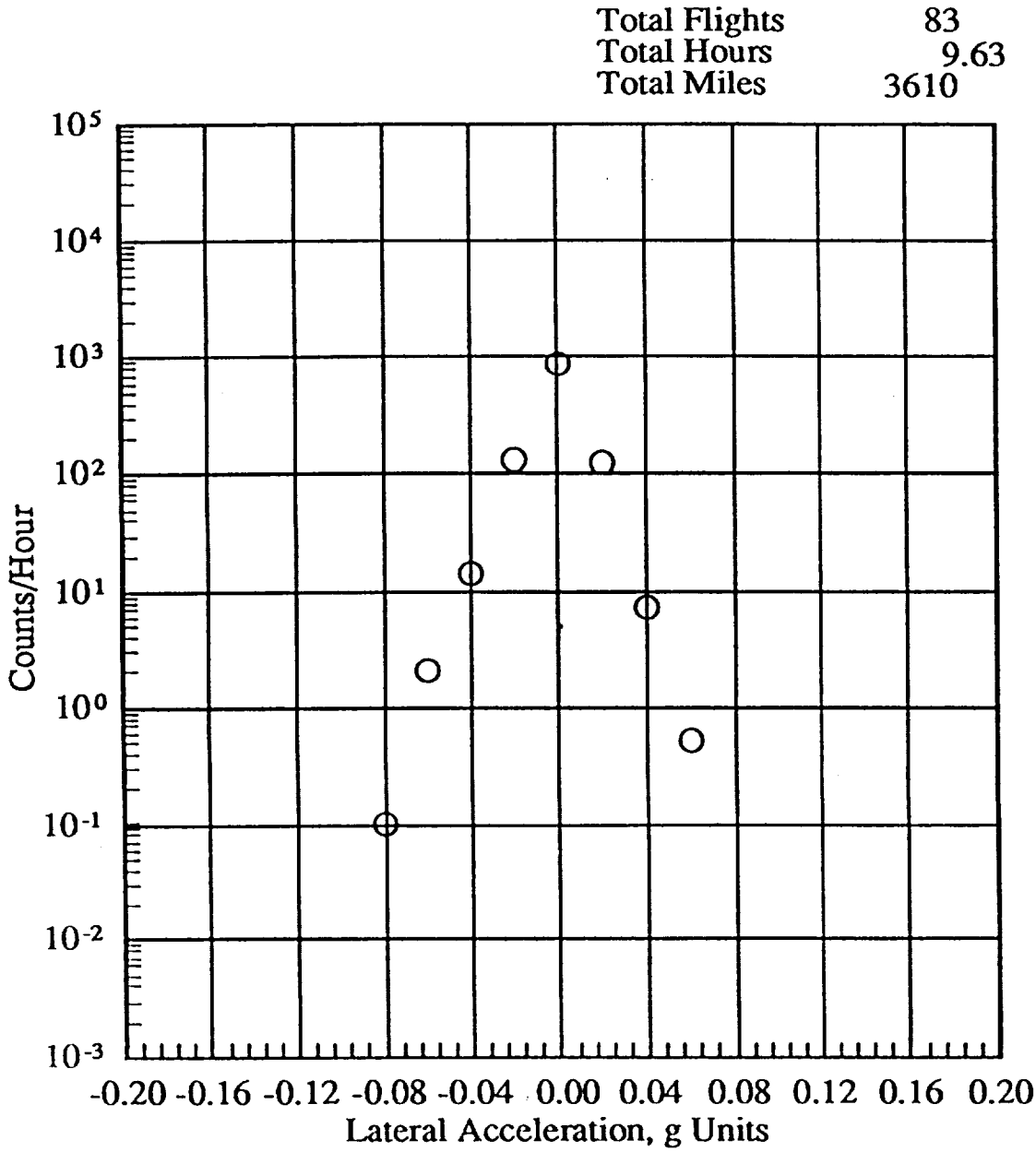

(d) a_y 9500 to 14500 ft

Figure 21.- Continued.

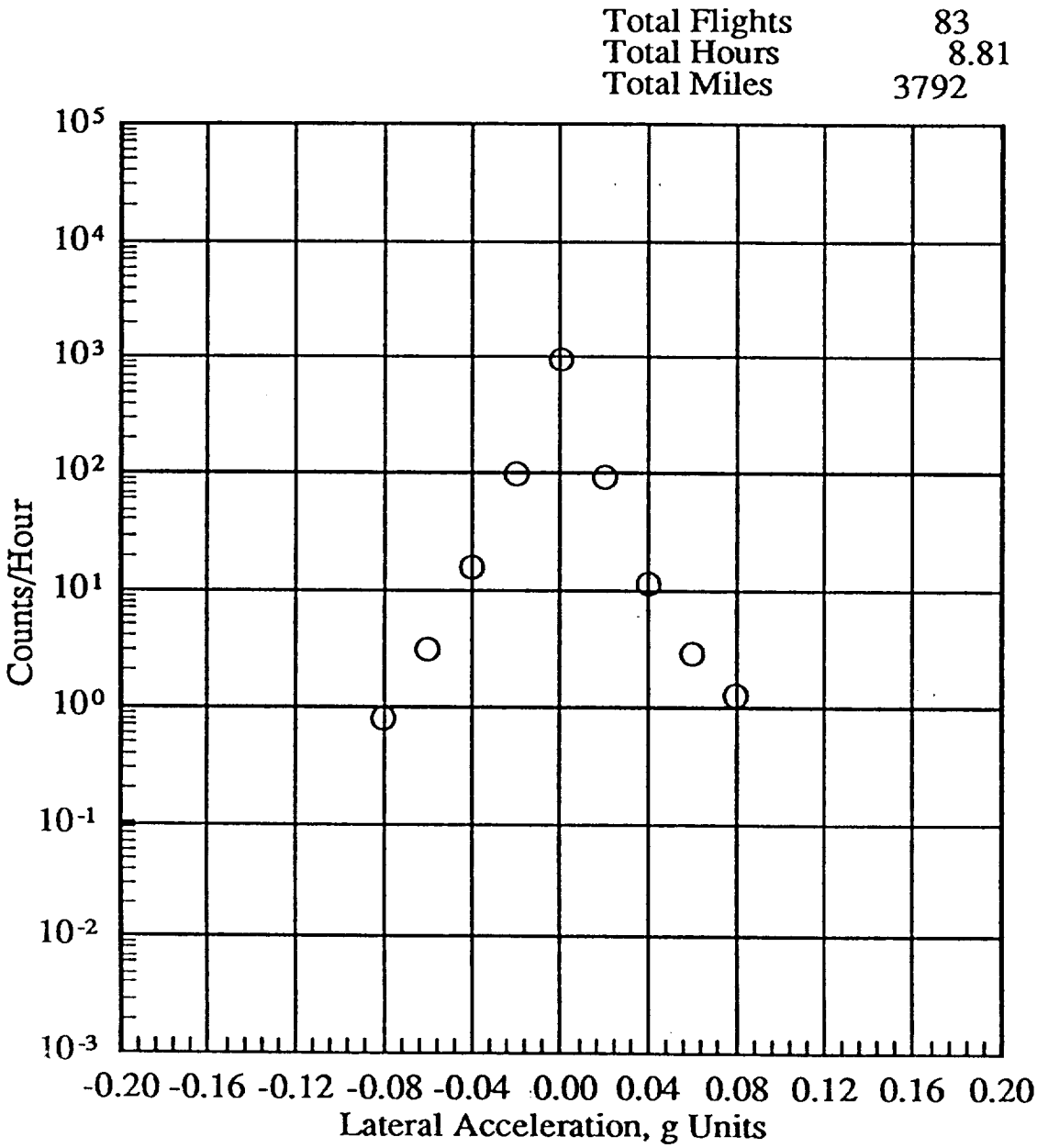

(e) a_y 14500 to 19500 ft

Figure 21.- Continued.

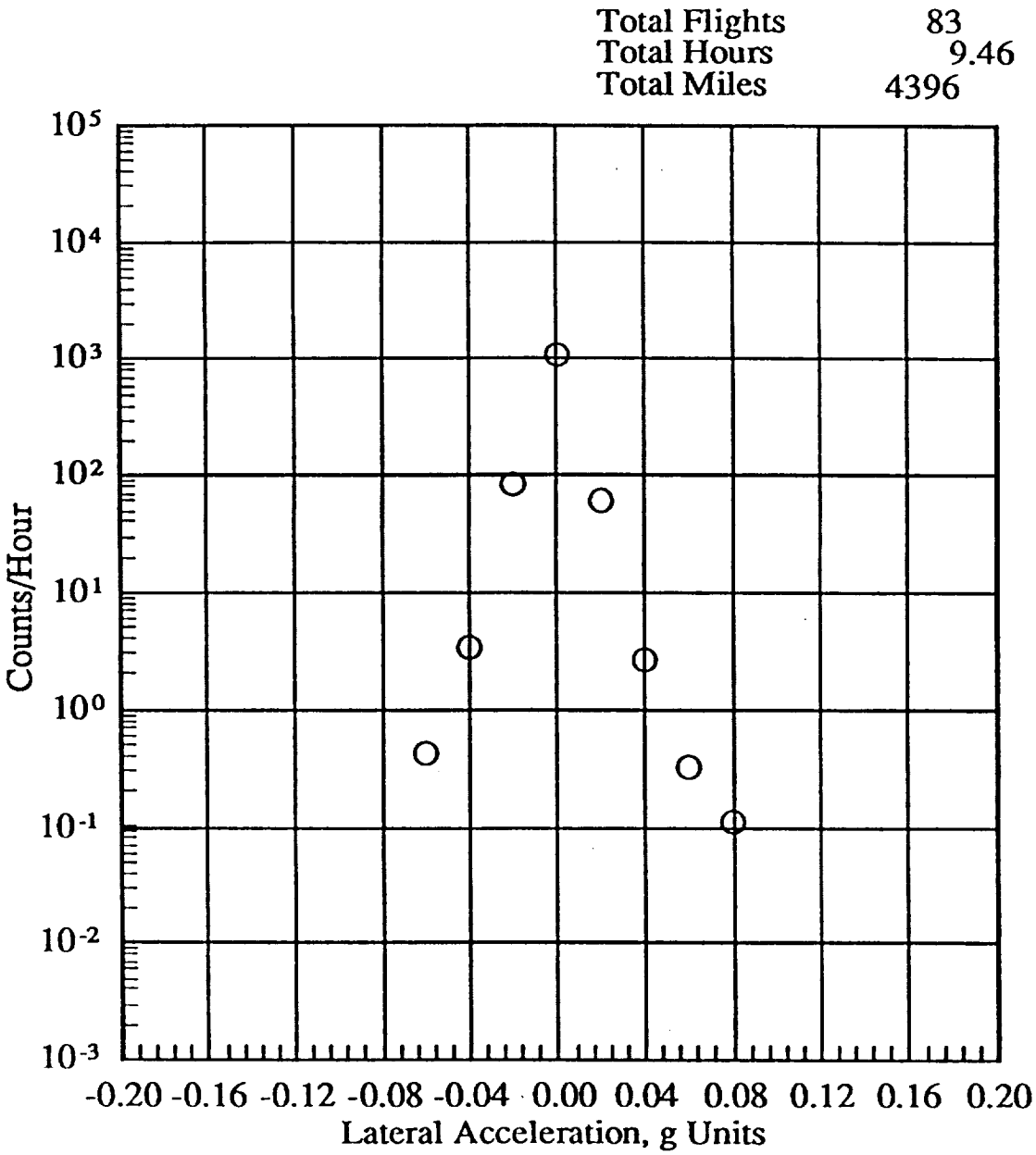

(f) a, 19500 to 24500 ft

Figure 21.- Continued.

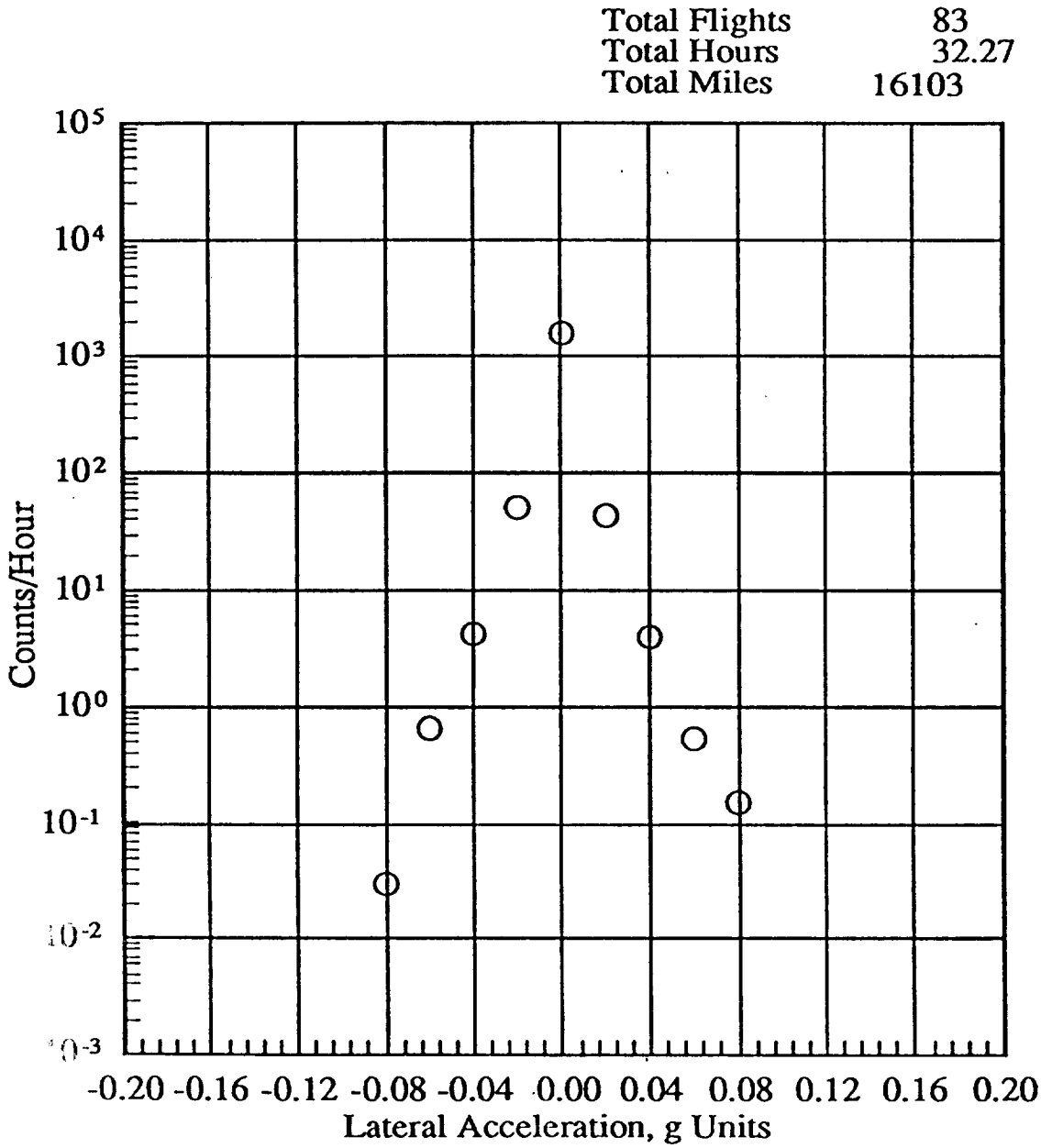

(g) a_y 24500 to 29500 ft

Figure 21.- Continued.

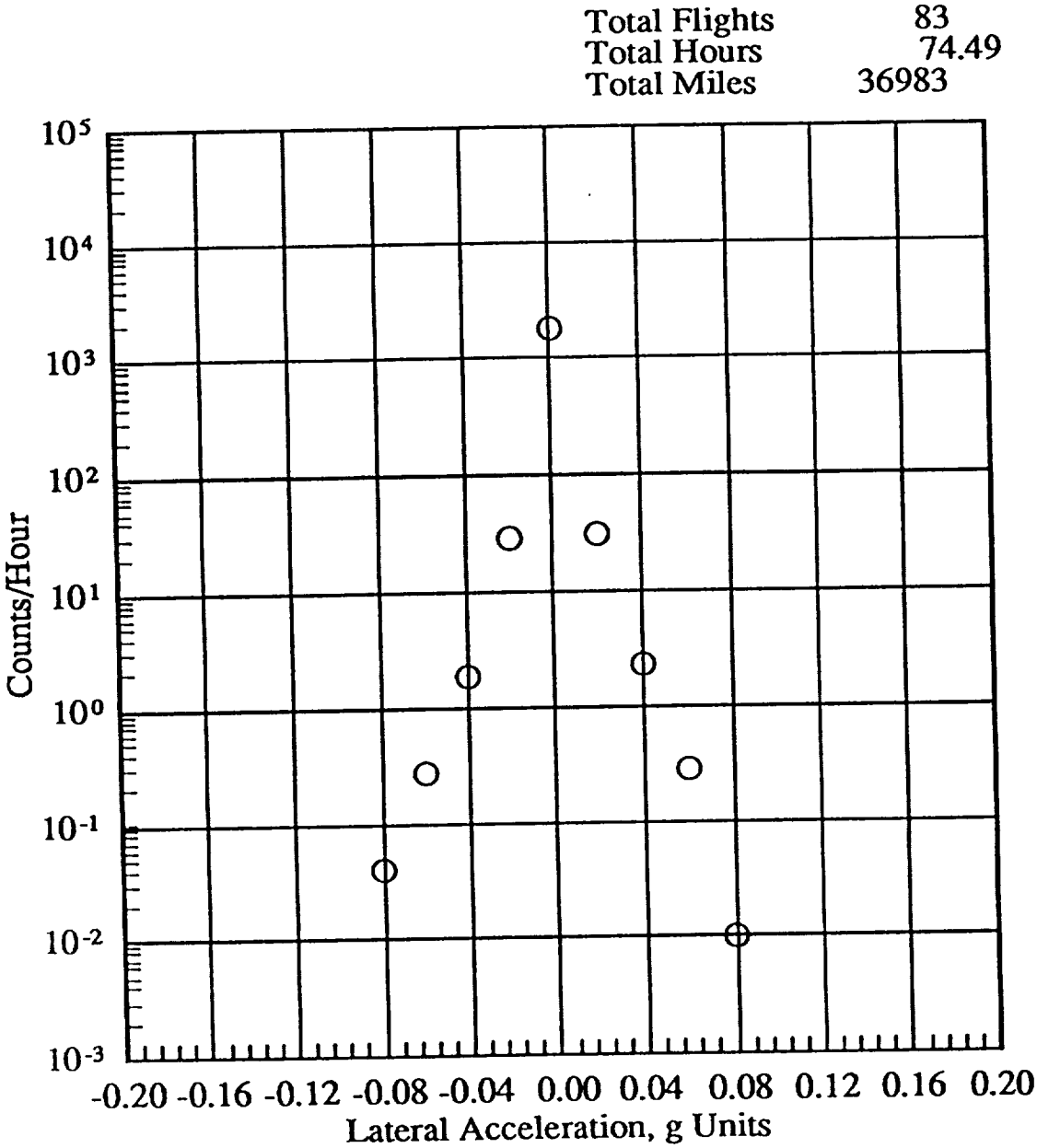

(h) a_y 29500 to 34500 ft

Figure 21.- Continued.

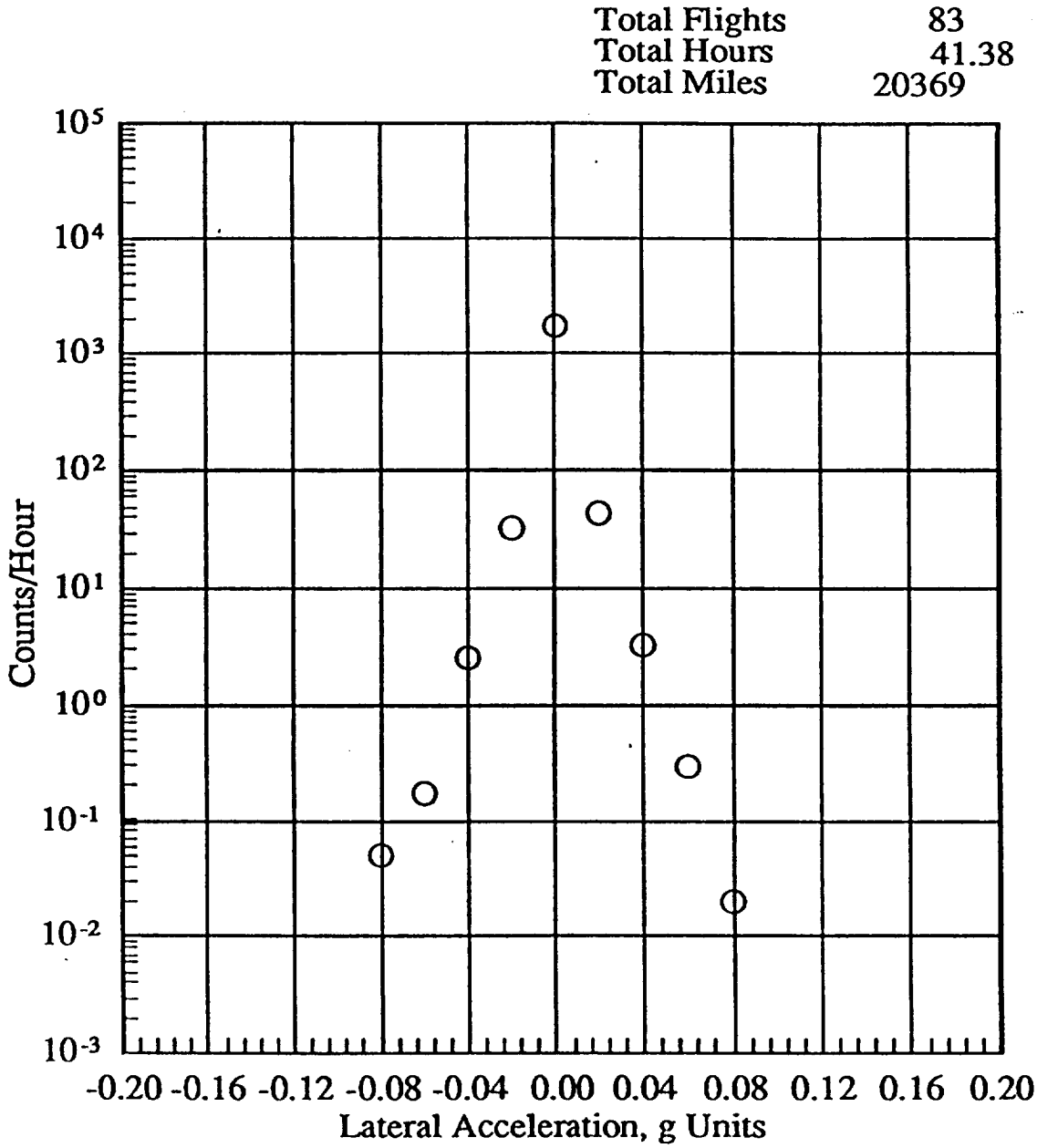

(i) a, 34500 to 39500 ft

Figure 21.- Continued.

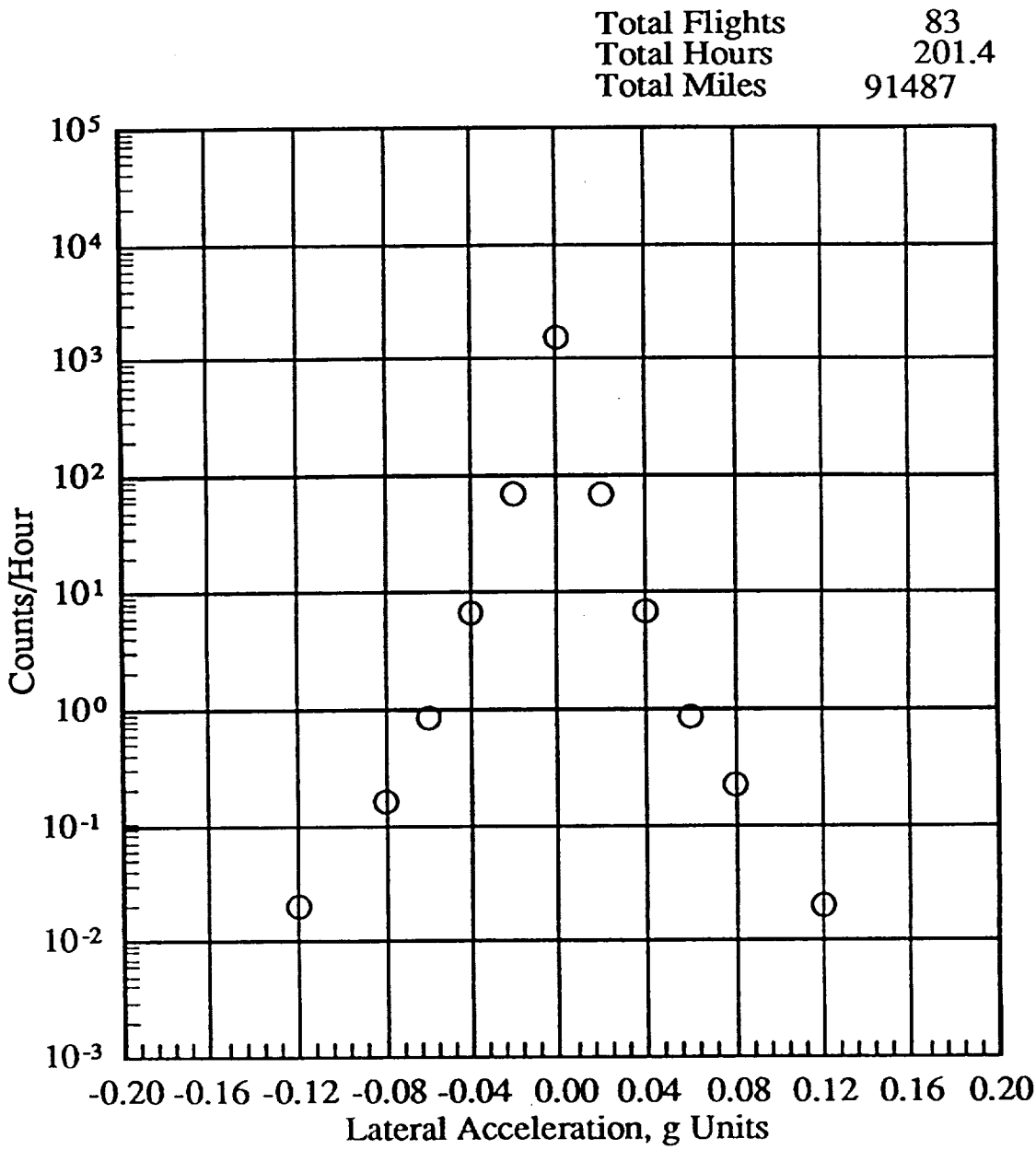

(j) a_y -500 to 44500 ft

Figure 21.- Concluded.

PRESSURE ALTITUDE BANDS

U_{de} FT/SEC	-500 TO 4500 FT	4500 TO 9500 FT	9500 TO 14500 FT	14500 TO 19500 FT	19500 TO 24500 FT	24500 TO 29500 FT	29500 TO 34500 FT	34500 TO 39500 FT	39500 TO 44500 FT	-500 TO 44500 FT
100.00	0	0	0	0	0	0	0	0	0	0
90.00	0	0	0	0	0	0	0	0	0	0
80.00	0	0	0	0	0	0	0	0	0	0
70.00	0	0	0	0	0	0	0	0	0	0
60.00	0	0	0	0	0	0	0	0	0	0
50.00	0	0	0	0	0	0	0	0	0	0
40.00	0	0	0	0	0	0	0	0	0	0
30.00	0	0	0	0	0	0	0	0	0	0
20.00	0.23	0.08	0	0	0	0	0	0	0	0.02
15.00	1.67	0.58	0	0	0	0	0	0	0	0.14
12.00	5.24	1.66	0.21	0.11	0	0.03	0.01	0	0	0.46
9.00	21.26	3.62	0.52	0.11	0	0.03	0.03	0.05	0	1.56
6.00	85.80	12.84	3.63	2.27	0.42	0.28	0.28	0.27	0	6.88
3.00	340.17	77.28	35.51	24.63	9.41	6.97	7.64	12.06	0	36.54
0	1187.02	1373.91	1570.51	1780.70	1814.16	1899.88	1833.43	1784.85	0	1748.30
-3.00	337.51	78.93	32.30	22.93	8.56	6.97	6.51	11.29	0	35.63
-6.00	87.40	13.00	4.15	1.70	0.21	0.40	0.13	0.31	0	6.96
-9.00	21.49	4.03	1.14	0.23	0	0.09	0.01	0.02	0	1.74
-12.00	4.40	1.15	0.21	0	0	0	0	0	0	0.37
-15.00	0.91	0.58	0.21	0	0	0	0	0	0	0.10
-20.00	0.15	0.08	0	0	0	0	0	0	0	0.01
-30.00	0.08	0.08	0	0	0	0	0	0	0	0.01
-40.00	0	0	0	0	0	0	0	0	0	0
-50.00	0	0	0	0	0	0	0	0	0	0
-60.00	0	0	0	0	0	0	0	0	0	0
-70.00	0	0	0	0	0	0	0	0	0	0
-80.00	0	0	0	0	0	0	0	0	0	0
-90.00	0	0	0	0	0	0	0	0	0	0
-100.00	0	0	0	0	0	0	0	0	0	0
FLIGHT HOURS @ ALT	13.2	12.1	9.6	8.8	9.5	32.3	74.5	41.4	0	201.4
FLIGHT MILES @ ALT	2684.9	3549.1	3609.1	3791.7	4369.4	16102.9	36983.4	20369.4	0	91487.0

TOTAL FLIGHTS	83
TOTAL FLIGHT HOURS FLAPS UP AND DOWN	201.4
TOTAL FLIGHT MILES FLAPS UP AND DOWN	91487

(a) U_{de} Level crossing counts per hour within pressure altitude bands

Figure 22.- U_{de} Exceedances.

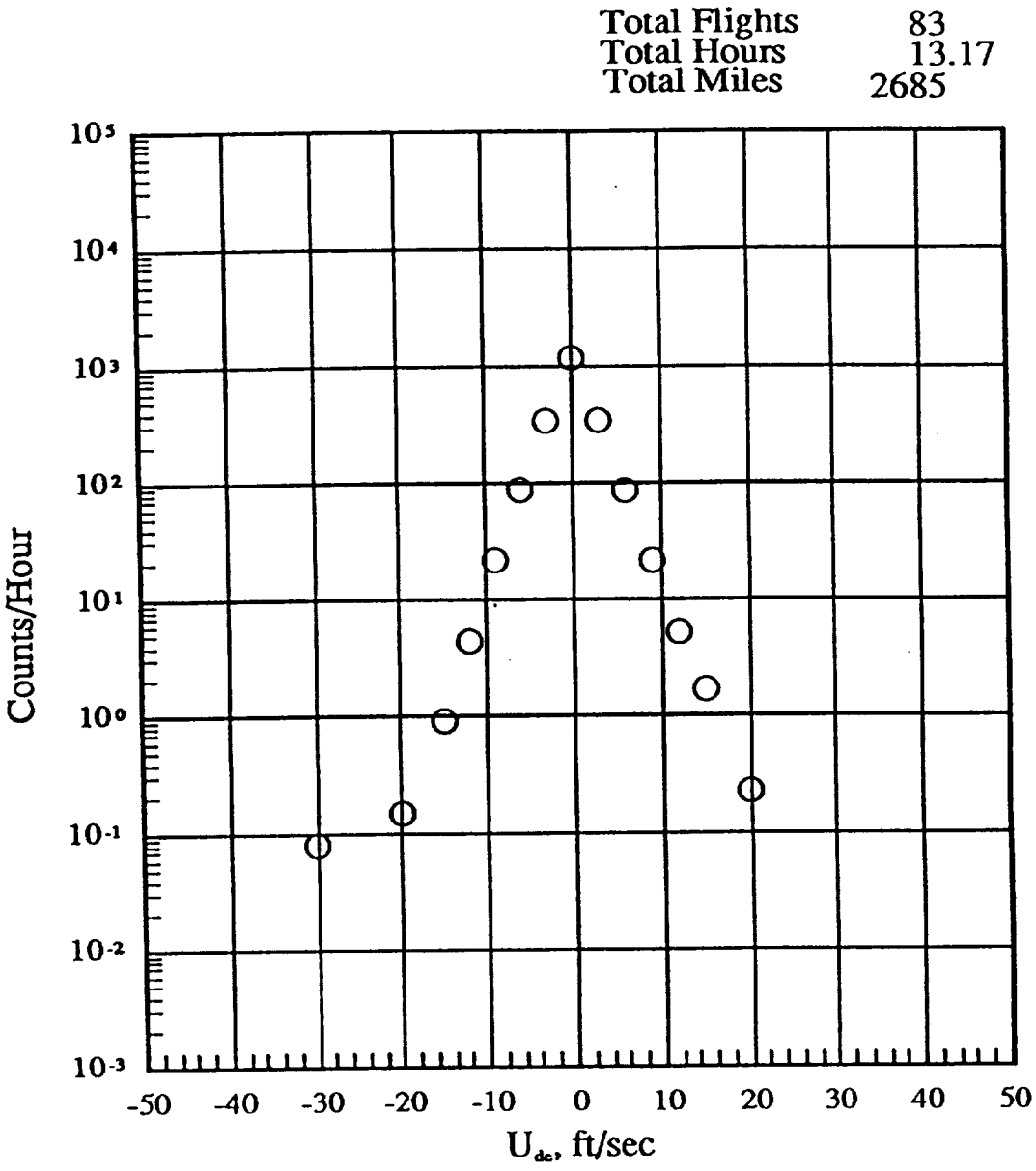

(b) -500 to 4500 ft

Figure 22.- Continued.

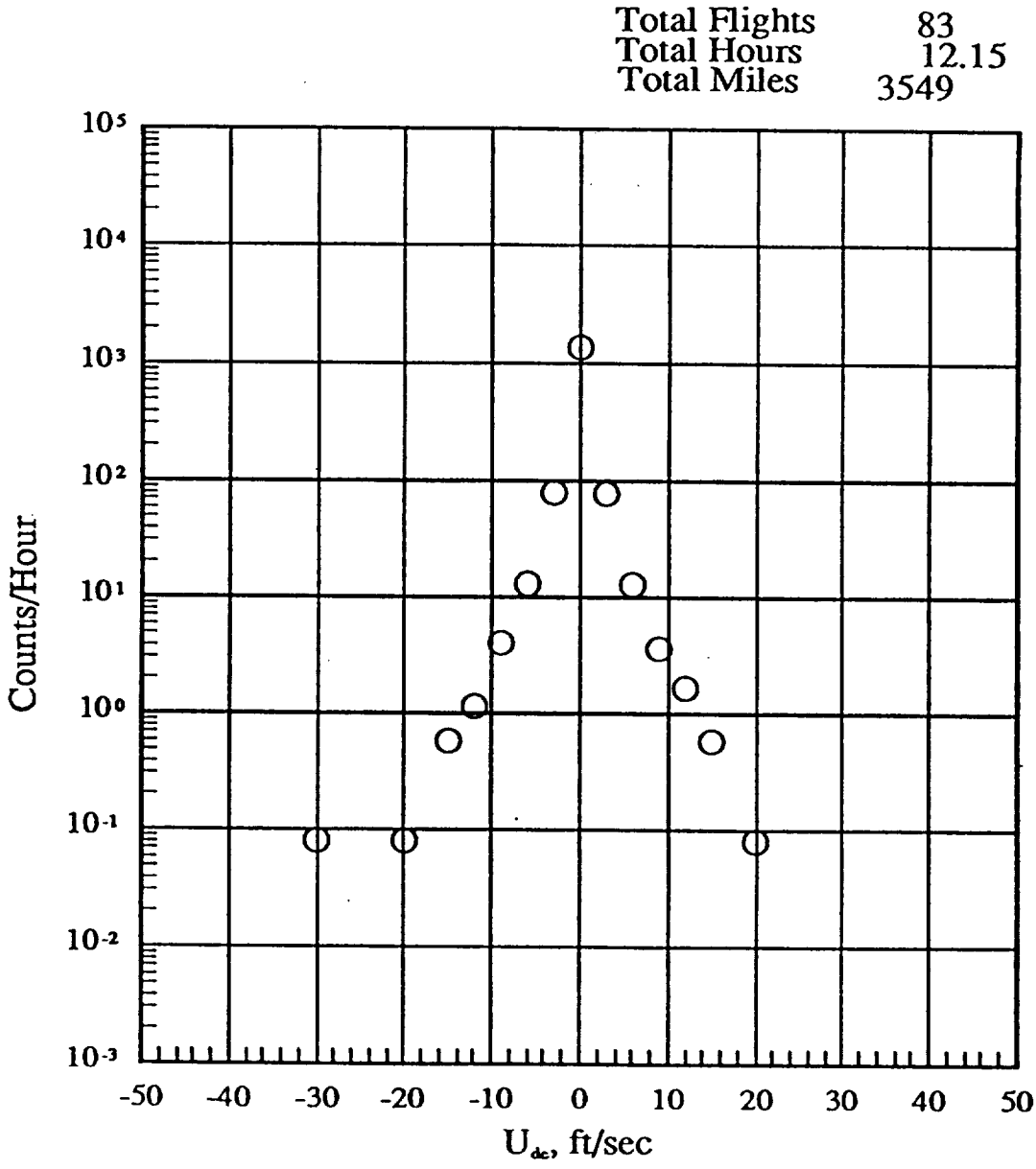

(c) 4500 to 9500 ft

Figure 22.- Continued.

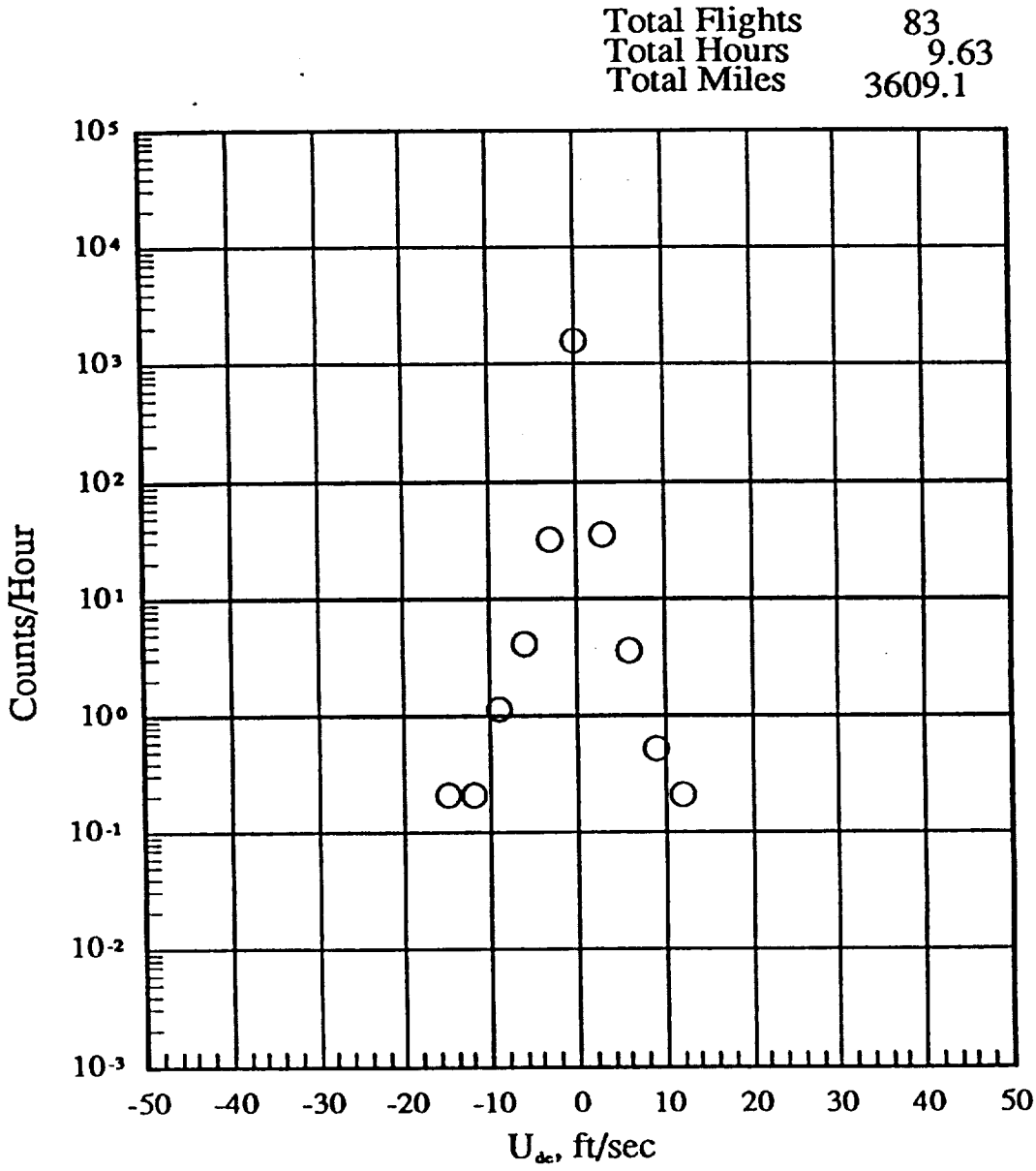

(d) 9500 to 14500 ft

Figure 22.- Continued.

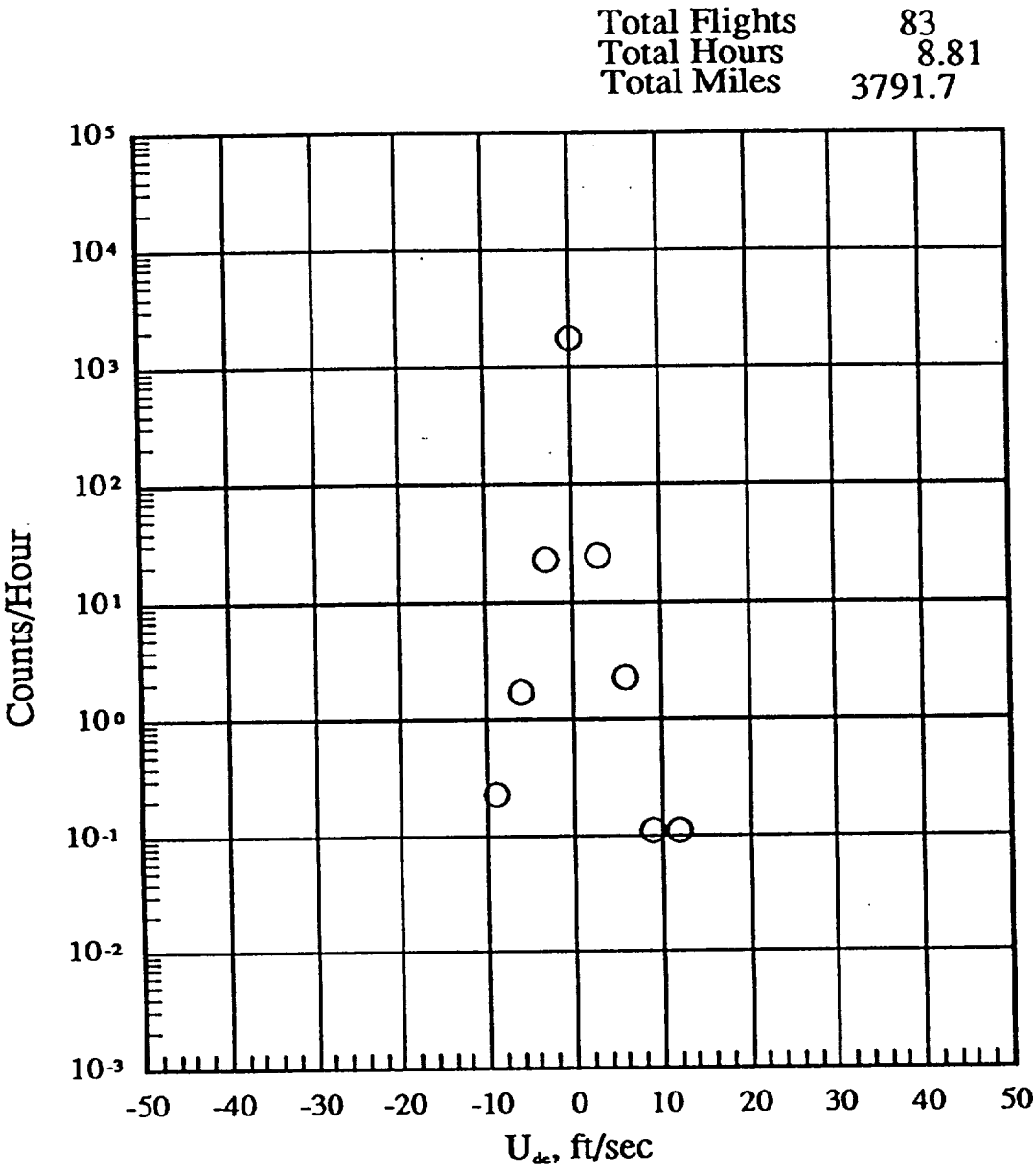

(e) 14500 to 19500 ft

Figure 22.- Continued.

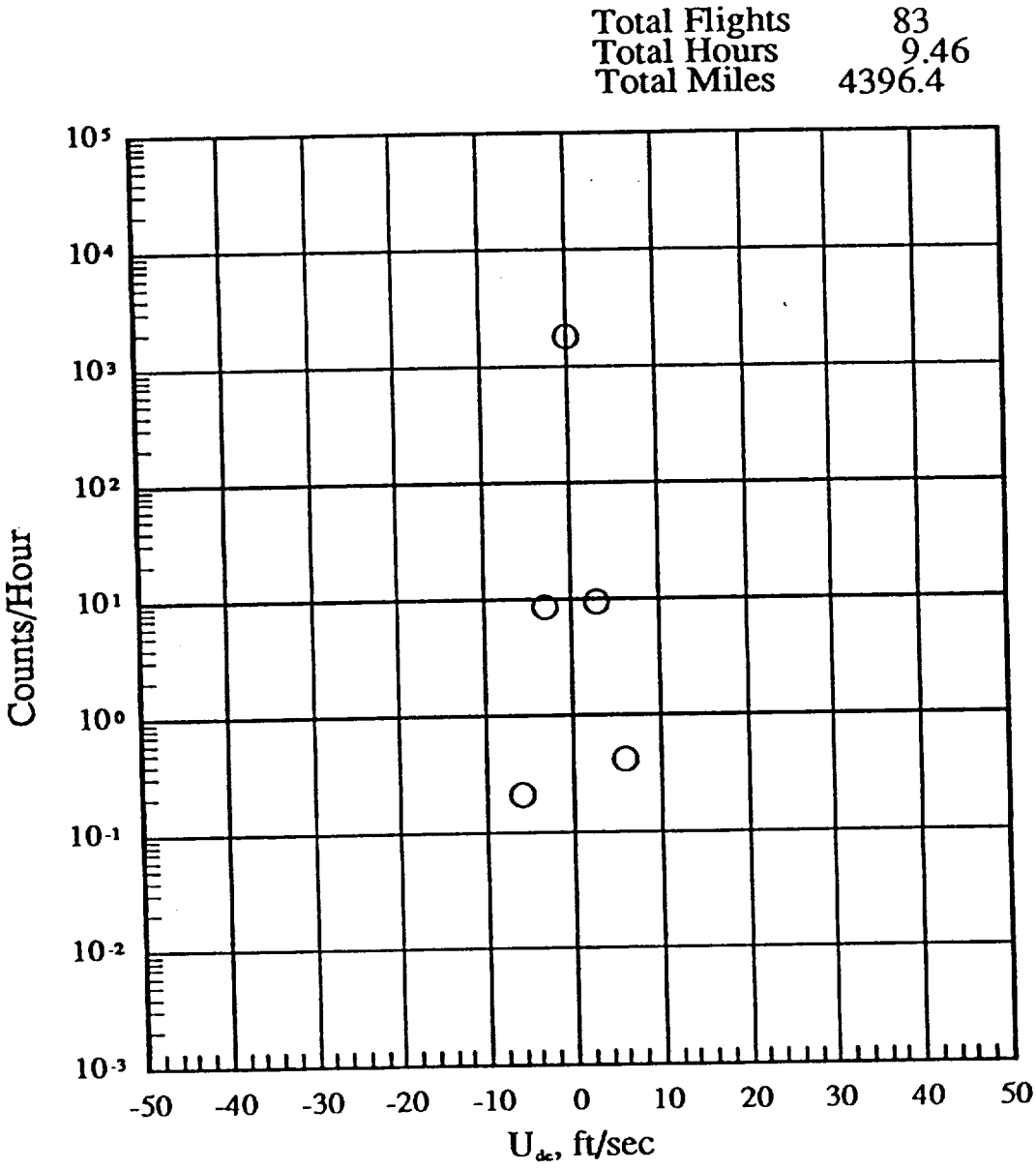

(f) 19500 to 24500 ft

Figure 22.- Continued.

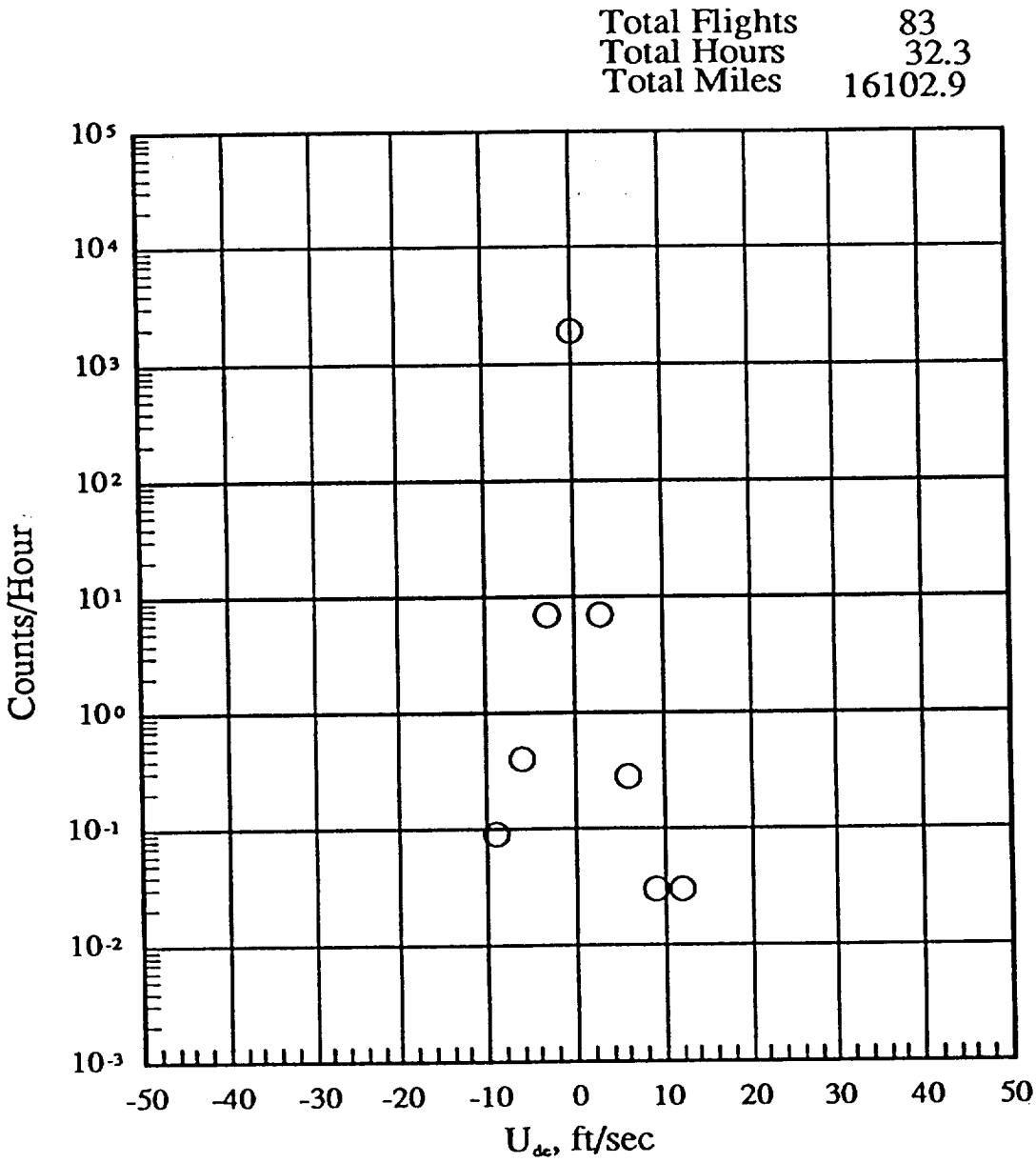

(g) 24500 to 29500 ft

Figure 22.- Continued.

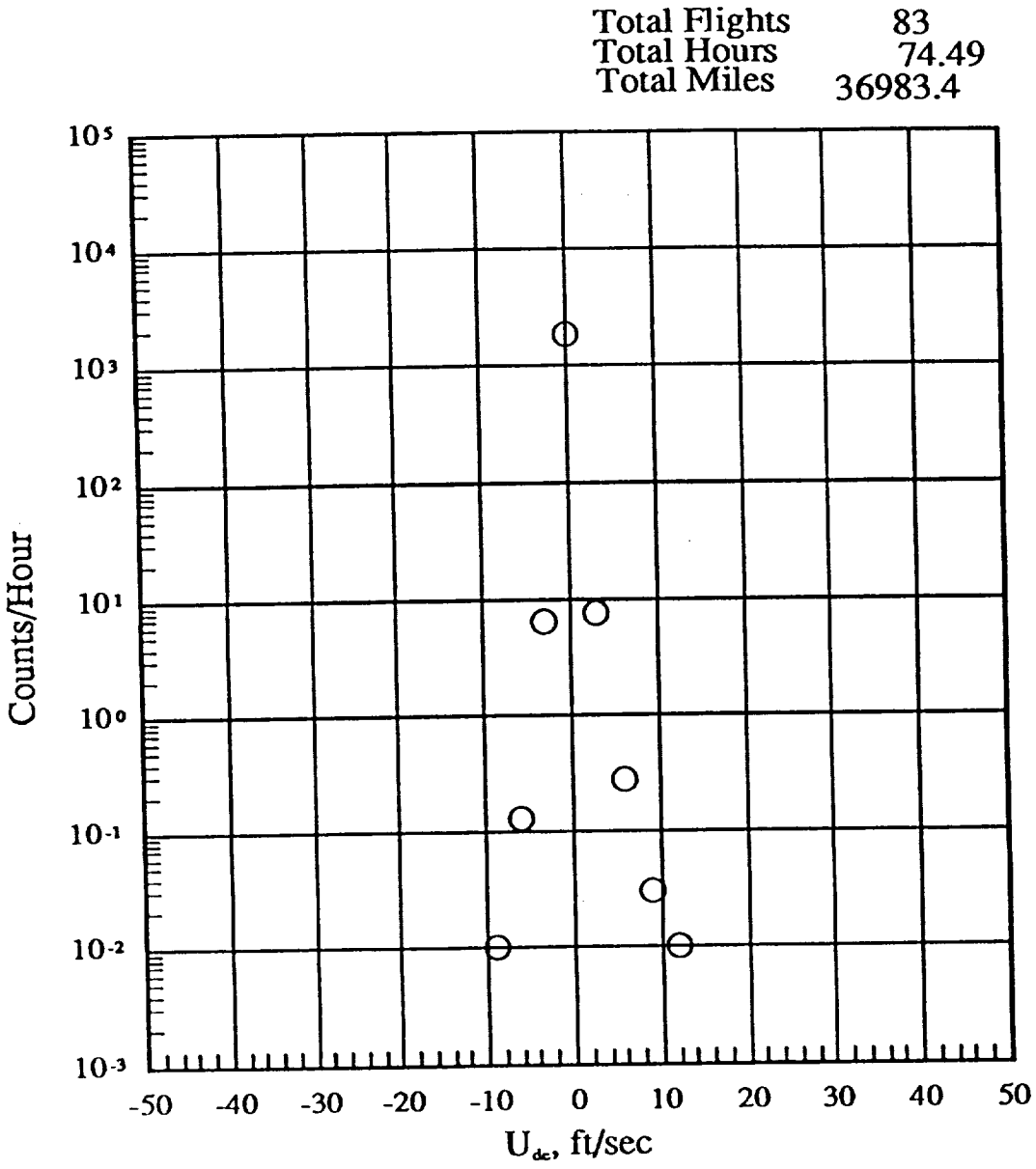

(h) 29500 to 34500 ft

Figure 22.- Continued.

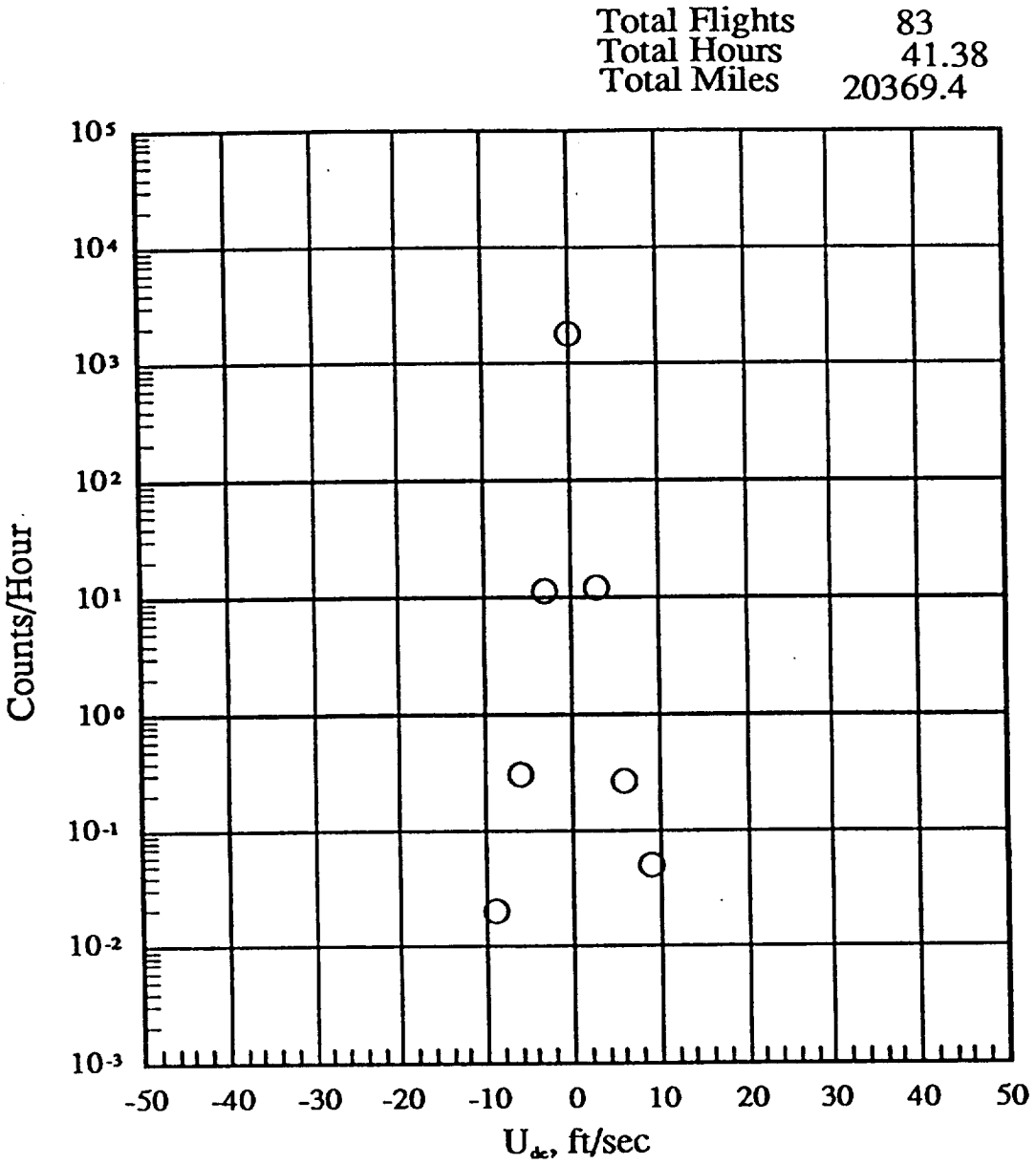

(i) 34500 to 39500 ft

Figure 22.- Continued.

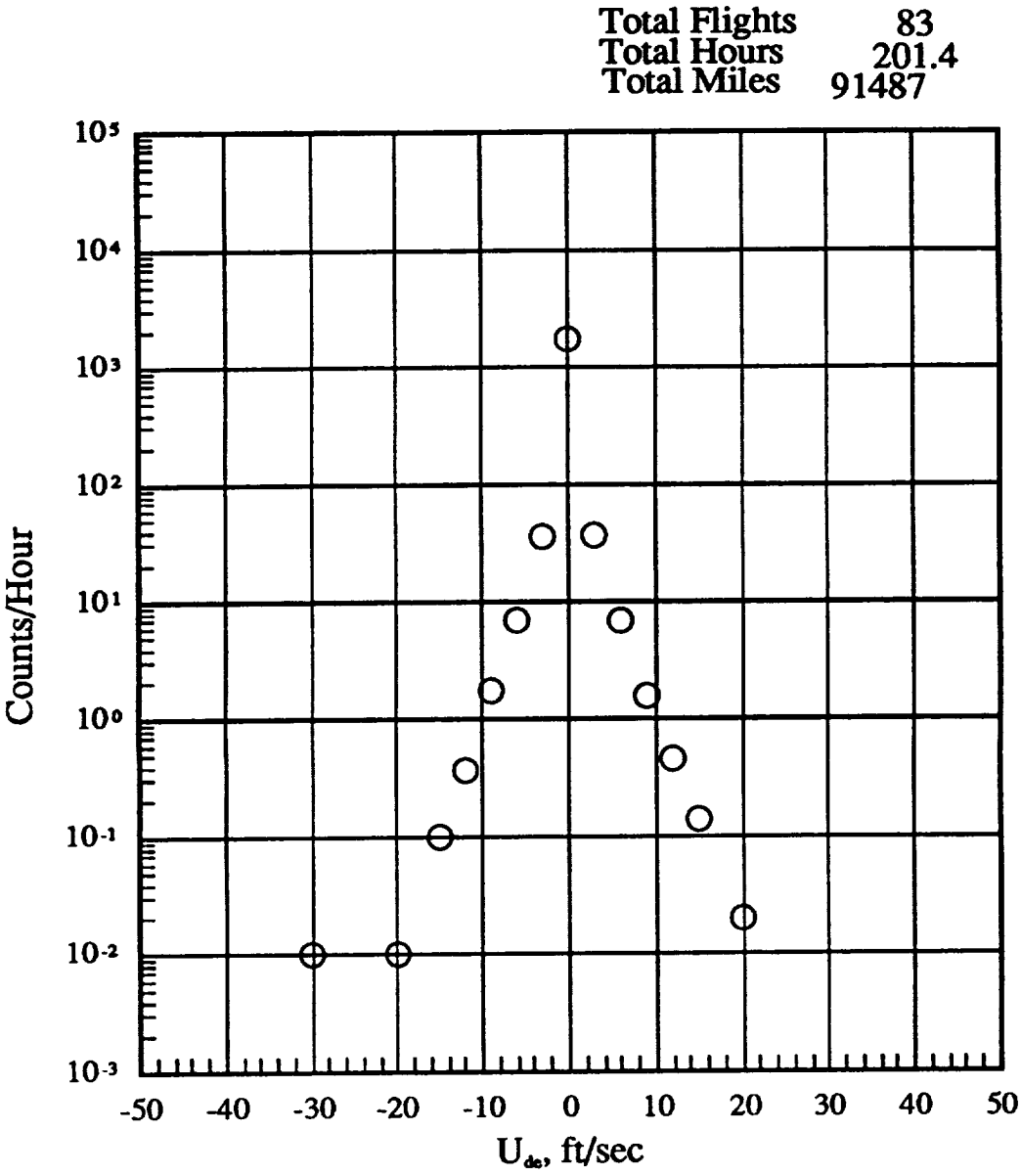

(j) -500 to 44500 ft

Figure 22.- Concluded.

ANY FLAP, ALL ALTITUDES

Maximum g Level for Each Flight		a_n	a_{nM}	a_{nG}
From	To			
.70	.75	0	0	0
.65	.70	0	0	0
.60	.65	0	0	0
.55	.60	1.20	0	0
.50	.55	0	0	0
.45	.50	3.61	0	1.20
.40	.45	3.61	0	1.20
.35	.40	13.25	1.20	7.23
.30	.35	8.43	3.61	3.61
.25	.30	31.33	2.41	9.64
.20	.25	25.30	20.48	28.92
.15	.20	12.05	38.55	32.53
.10	.15	1.20	28.92	15.66
.05	.10	0	4.82	0
-.05	-.10	0	12.05	0
-.10	-.15	1.20	57.83	25.30
-.15	-.20	20.48	21.69	37.35
-.20	-.25	37.35	7.23	15.66
-.25	-.30	24.10	0	10.84
-.30	-.35	7.23	1.20	4.82
-.35	-.40	3.61	0	3.61
-.40	-.45	4.82	0	1.20
-.45	-.50	0	0	0
-.50	-.55	0	0	1.20
-.55	-.60	1.20	0	0
-.60	-.65	0	0	0
-.65	-.70	0	0	0
-.70	-.75	0	0	0

Maximum g Level For Each Flight		a_y
From	To	
.28	.30	0
.26	.28	0
.24	.26	0
.22	.24	0
.20	.22	0
.18	.20	0
.16	.18	0
.14	.16	0
.12	.14	4.82
.10	.12	2.41
.08	.10	15.66
.06	.08	28.92
.04	.06	45.78
.02	.04	2.41
-.02	-.04	7.23
-.04	-.06	39.76
-.06	-.08	36.14
-.08	-.10	8.43
-.10	-.12	4.82
-.12	-.14	2.41
-.14	-.16	1.20
-.16	-.18	0
-.18	-.20	0
-.20	-.22	0
-.22	-.24	0
-.24	-.26	0
-.26	-.28	0
-.28	-.30	0

TOTAL FLIGHTS	83
TOTAL FLIGHT HOURS	201.4
TOTAL FLIGHT MILES	91487

(a) Percent of flights for peak positive and negative g

Figure 23. - Maximum acceleration per flight statistics.

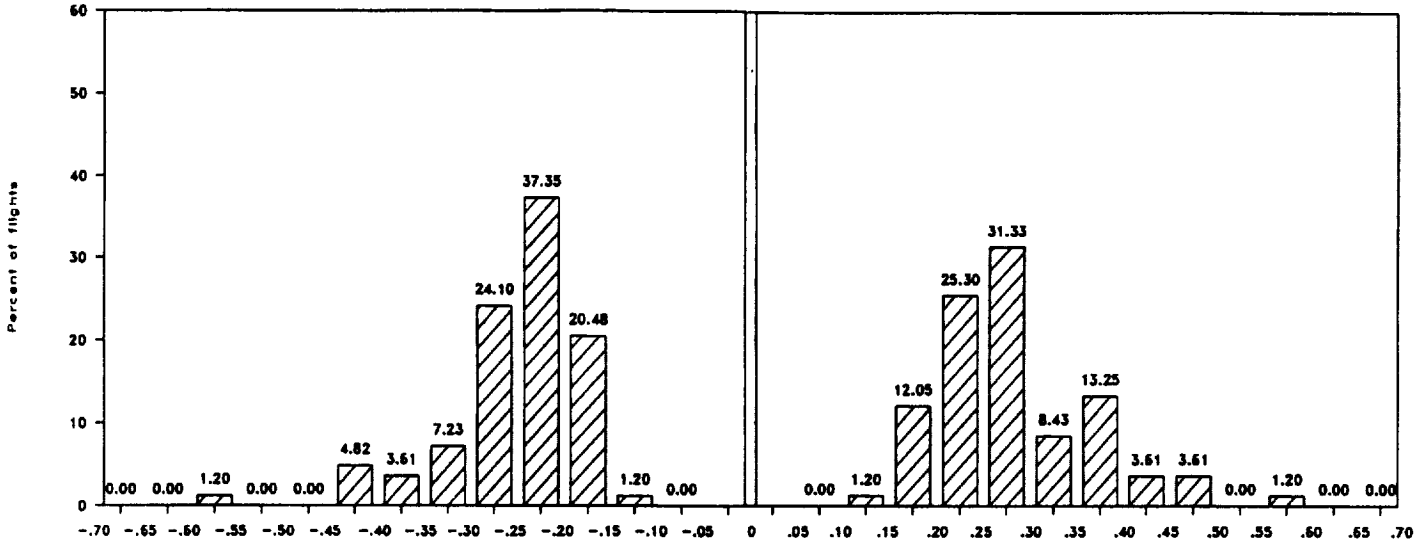

(b) a_n

Total Flights 83
Total Hours 201.4
Total Miles 91487

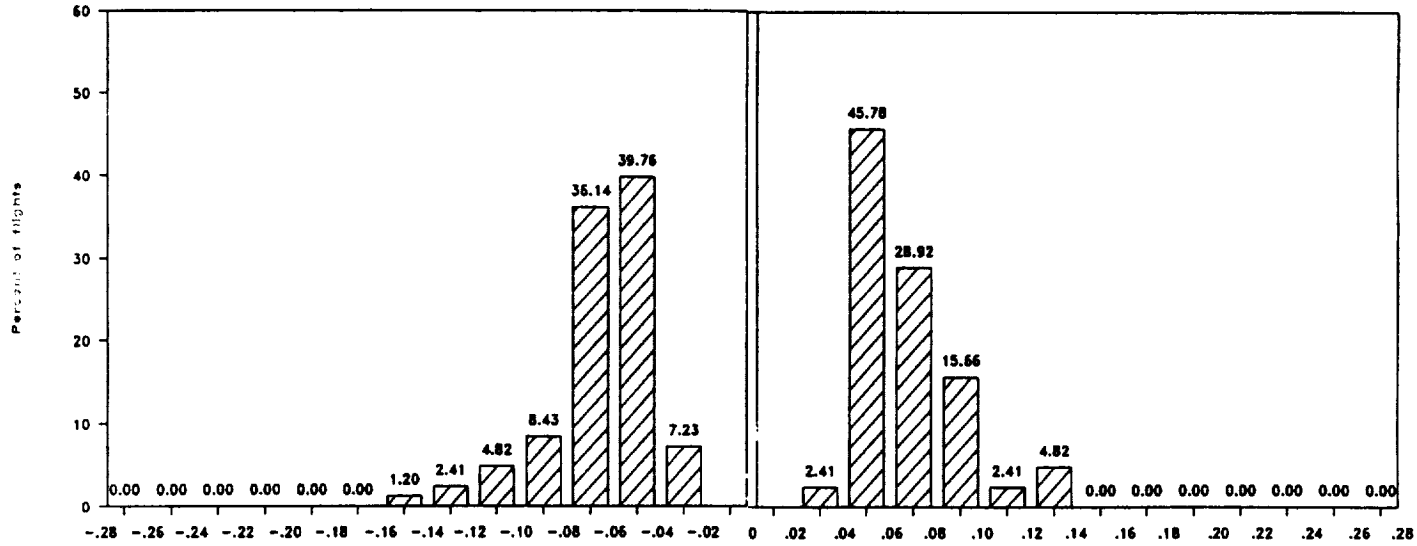

(c) a_y

Figure 23.- Continued.

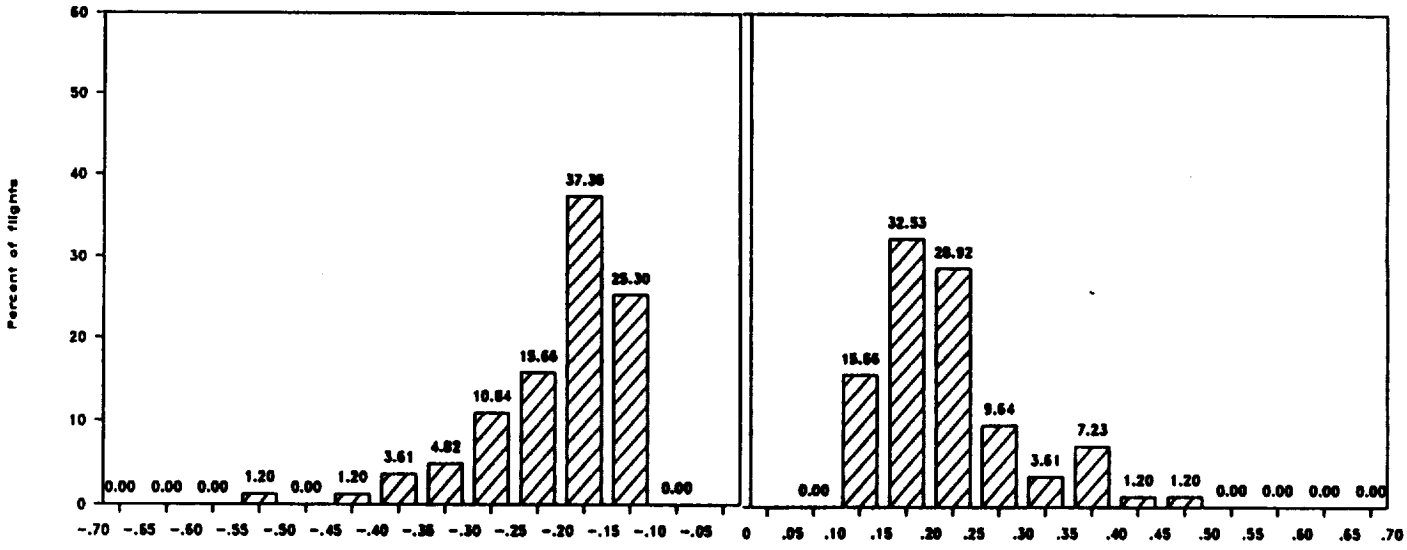

(d) a_{nG}

Total Flights 83
Total Hours 201.4
Total Miles 91487

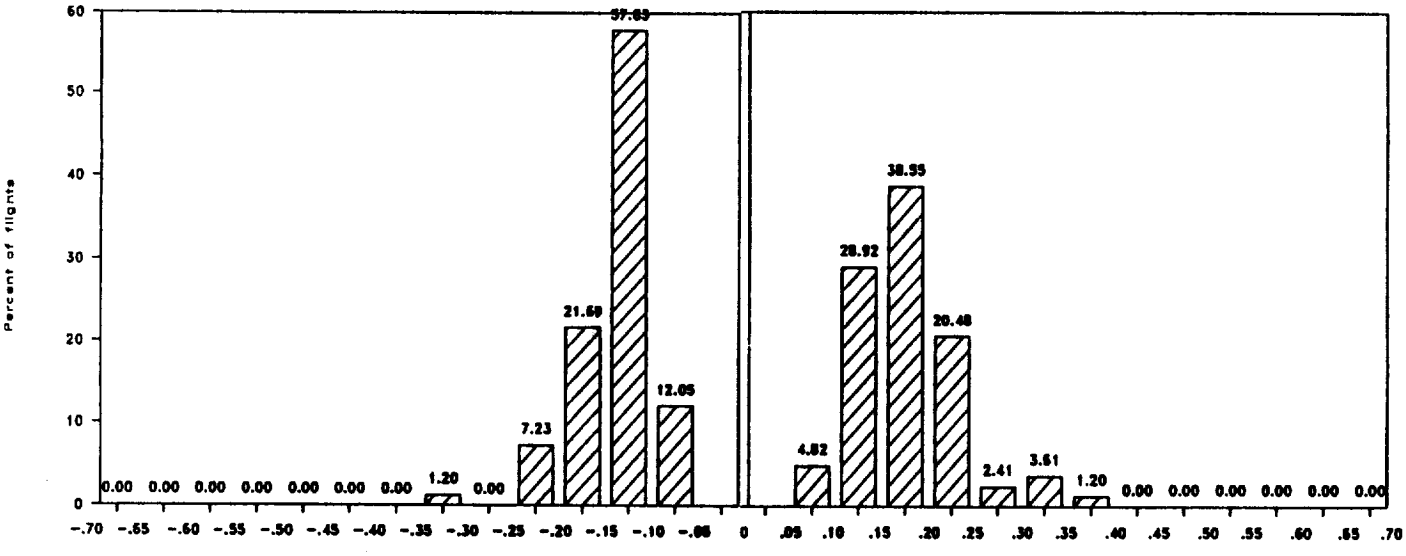

(e) a_{nM}

Figure 23.- Continued.

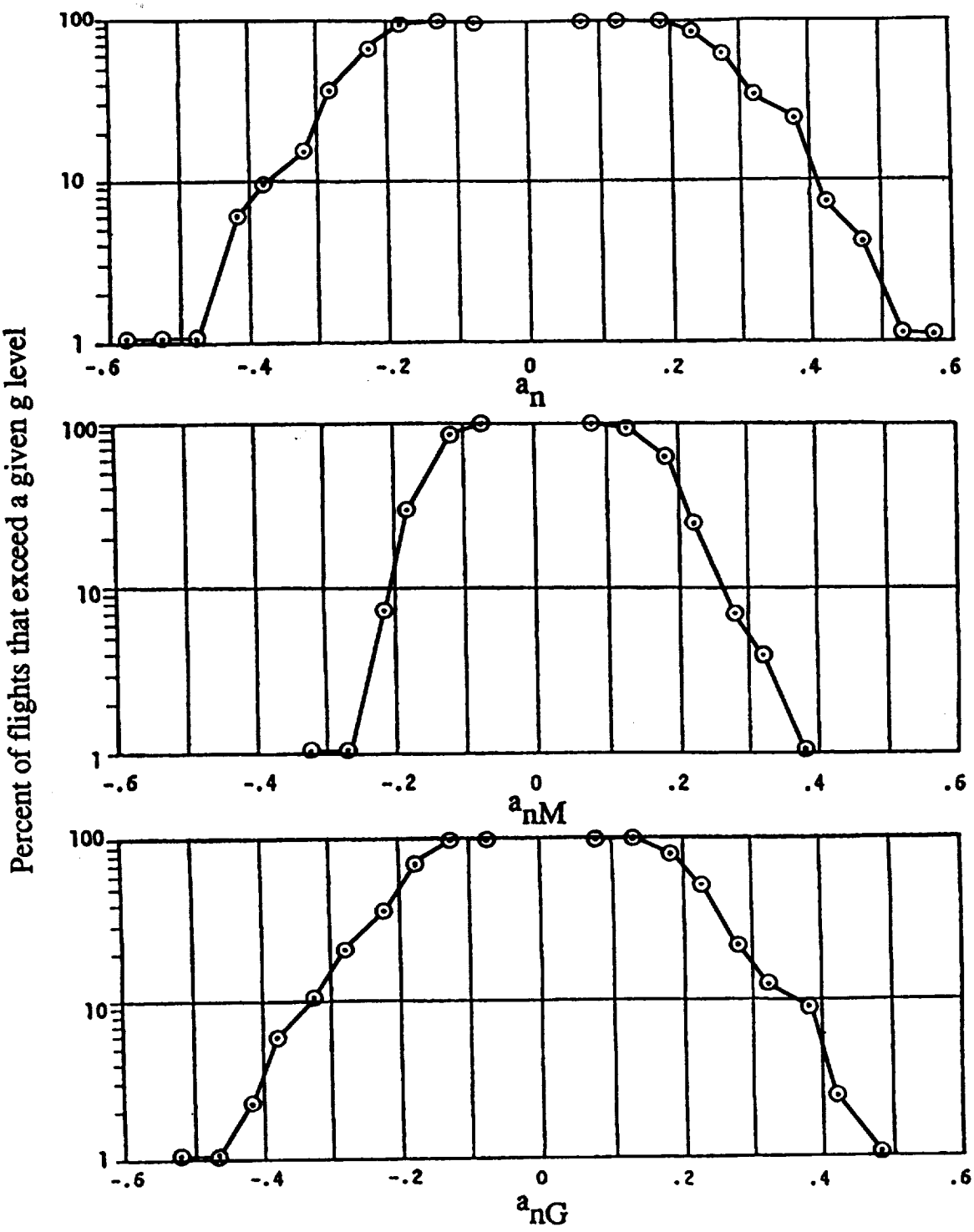

(f) Percent of flights to exceed a given level of a_n a_{nM} a_{nG}.

Figure 23.- Concluded.

a_n g's	FLAP DETENT 4 DEG	10 DEG	18 DEG	22 DEG	27 DEG	33 DEG	42 DEG
1.60	0	0	0	0	0	0	0
1.40	0	0	0	0	0	0	0
1.20	0	0	0	0	0	0	0
1.00	0	0	0	0	0	0	0
.80	0	0	0	0	0	0	0
.70	0	0	0	0	0	0	0
.60	0	0	0	0	0	0	0
.50	0	0	0	0	0	0	0
.40	0	0	0	0	0	0	0
.30	0.71	0	0	0	0	0	0
.20	13.57	7.69	0	0	0	0	0
.15	30.71	26.92	0	0	0	0	0
.10	102.85	80.77	0	0	0	0	0
.05	301.43	342.31	Insufficient	Insufficient	0	0	0
0	593.57	792.31	Data	Data	0	0	0
-.05	669.28	876.92	Sample	Sample	0	0	0
-.10	267.85	338.46	0	0	0	0	0
-.15	71.43	76.92	0	0	0	0	0
-.20	12.14	26.92	0	0	0	0	0
-.30	0	0	0	0	0	0	0
-.40	0	0	0	0	0	0	0
-.50	0	0	0	0	0	0	0
-.60	0	0	0	0	0	0	0
-.70	0	0	0	0	0	0	0
-.80	0	0	0	0	0	0	0
-1.00	0	0	0	0	0	0	0
-1.20	0	0	0	0	0	0	0
-1.40	0	0	0	0	0	0	0
-1.60	0	0	0	0	0	0	0
FLIGHT HOURS IN DETENT	1.40	0.26	0	0.01	0	0	0

TOTAL FLIGHTS	83
TOTAL FLIGHT HOURS FLAPS UP AND DOWN	201.1
TOTAL FLIGHT MILES FLAPS UP AND DOWN	91413
TOTAL HOURS IN DETENT	1.7

(a) Flap detents - Takeoff

Figure 24. - Normal acceleration exceedances for flap detents

a_n g's	FLAP DETENT 4 DEG	10 DEG	18 DEG	22 DEG	27 DEG	33 DEG	42 DEG
1.60	0	0	0	0	0	0	0
1.40	0	0	0	0	0	0	0
1.20	0	0	0	0	0	0	0
1.00	0	0	0	0	0	0	0
.80	0	0	0	0	0	0	0
.70	0	0	0	0	0	0	0
.60	0	0	0	0	0	0	0
.50	0	0	0	0	0	0	0
.40	0	0	0	0	0	0	0
.30	0.67	0.38	0	1.13	0	0	0
.20	8.05	6.77	20.59	15.85	7.14	8	5.36
.15	37.58	39.85	41.18	43.40	35.71	52.00	26.82
.10	179.19	136.84	161.76	140.00	92.86	180.00	130.65
.05	308.05	333.08	467.65	401.51	607.14	586.00	538.31
0	1067.79	861.28	864.71	860.00	1035.71	976.00	1198.85
-.05	218.79	211.28	194.12	261.89	628.57	500.00	509.58
-.10	54.36	43.23	26.47	55.47	185.71	132.00	103.07
-.15	14.77	7.14	17.65	10.94	100.00	36.00	19.16
-.20	10.07	1.87	0	2.26	28.57	0	1.53
-.30	2.01	0	0	0.78	0	0	0.38
-.40	0.67	0	0	0	0	0	0
-.50	0.67	0	0	0	0	0	0
-.60	0	0	0	0	0	0	0
-.70	0	0	0	0	0	0	0
-.80	0	0	0	0	0	0	0
-1.00	0	0	0	0	0	0	0
-1.20	0	0	0	0	0	0	0
-1.40	0	0	0	0	0	0	0
-1.60	0	0	0	0	0	0	0
FLIGHT HOURS IN DETENT	1.49	2.66	0.34	2.65	0.14	0.25	2.61

TOTAL FLIGHTS	83
TOTAL FLIGHT HOURS FLAPS UP AND DOWN	201.1
TOTAL FLIGHT MILES FLAPS UP AND DOWN	91413
TOTAL HOURS IN DETENT	10.1

(b) Flap detents - Landing

Figure 24. - Continued

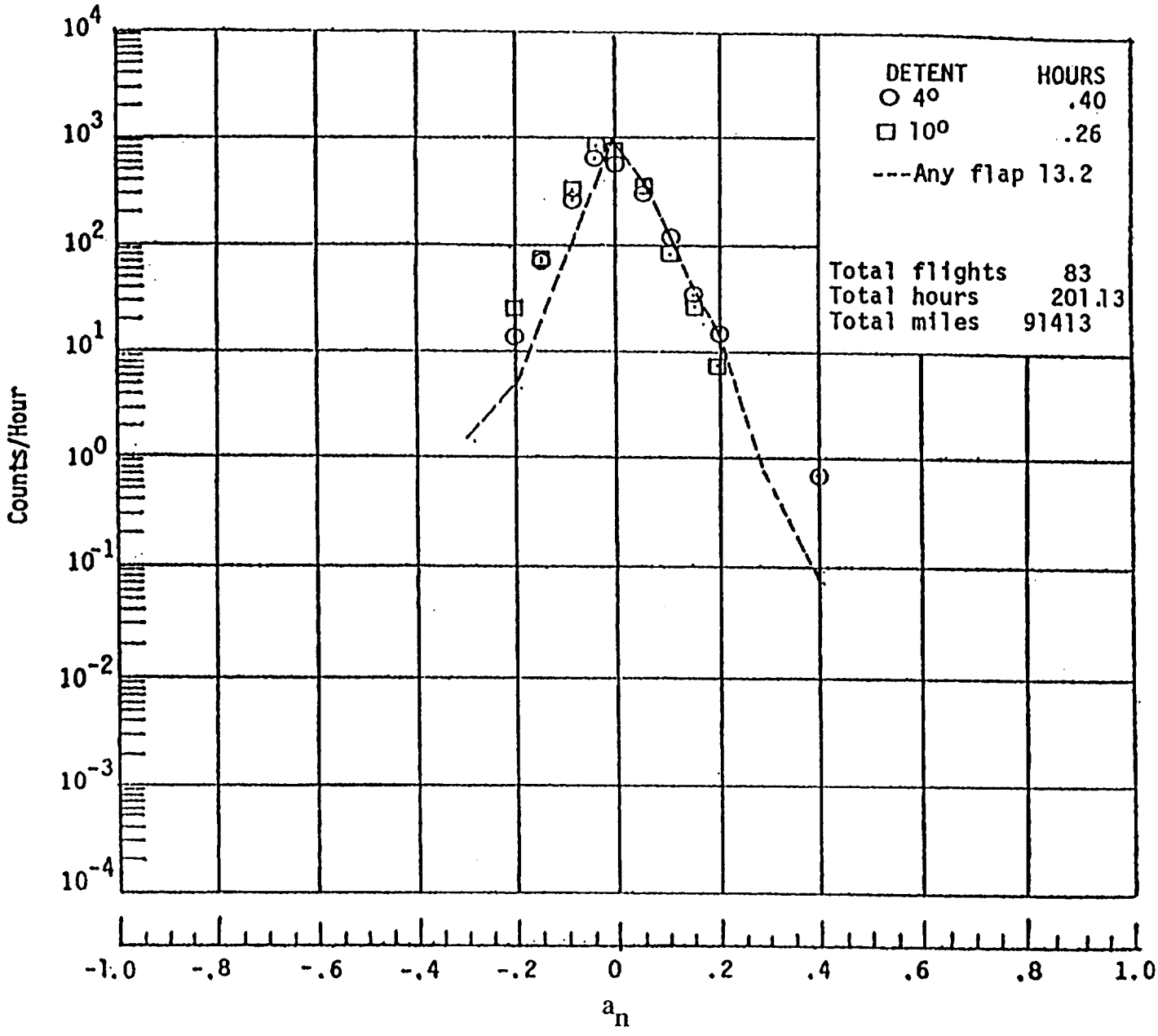

(c) Take off

Figure 24.- Continued.

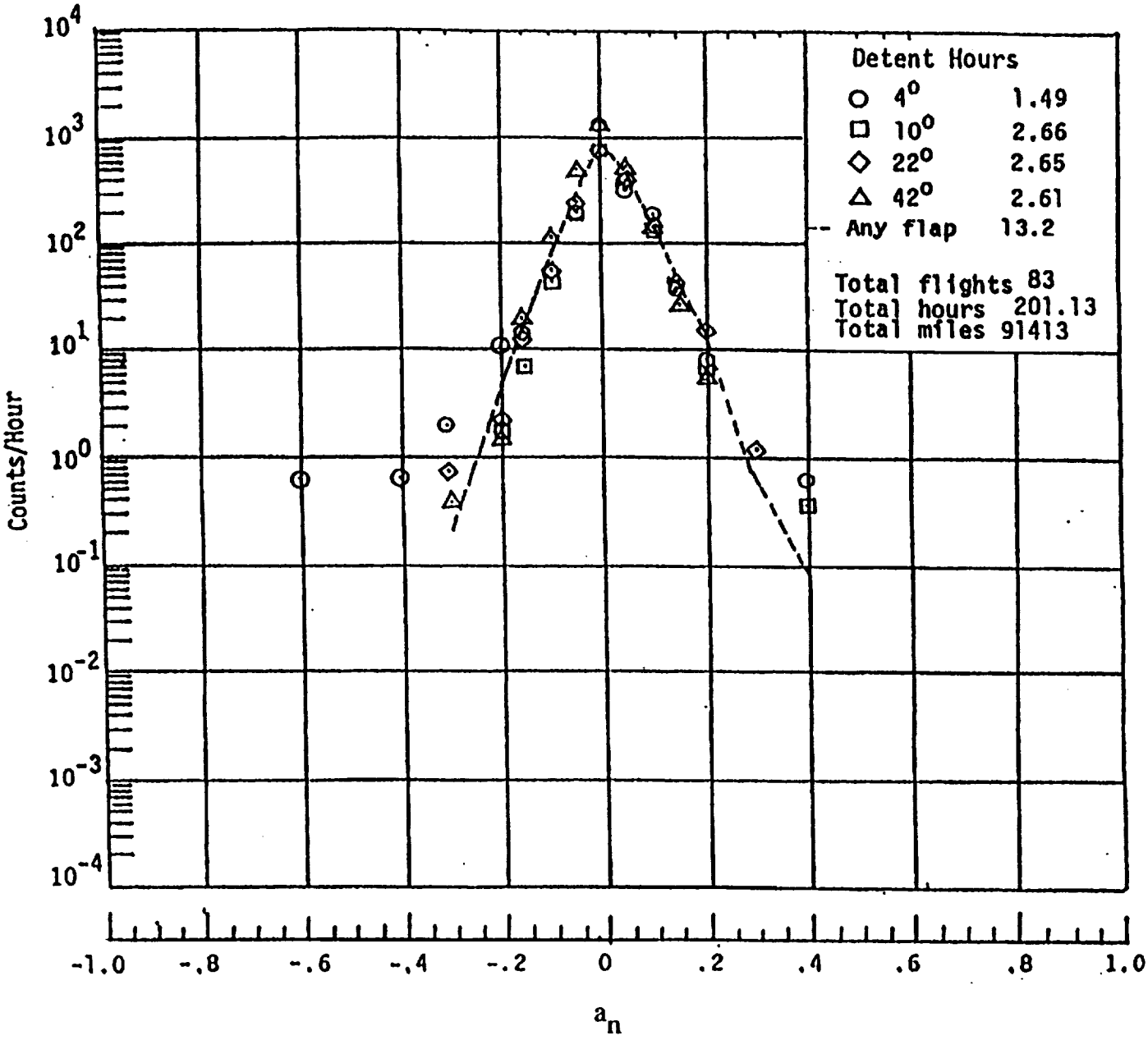

(d) Landing

Figure 24.- Concluded.

Element	Analog	Digital
o Measurement & Recording System	o Continuous with 5 Hz accelerometer cut-off	o 4 samples per second with 4 Hz accelerometer cut-off
o Filtering	o None	o Filter cut-off at 1.2 Hz (to eliminate elastic response)
o Maneuver & Gust Separation	o By eye	o By computer, defined by frequency
o Gust Counting	o Peaks by eye	o Level crossings by computer
o Weights	o Maximum weights or rough estimate	o Calculated (believed to be within 2%)
o Lift-Curve Slope	o Compressible rigid wing-only theory	o Compressible elastic total airplane provided by manufacturer
o Autopilot Effects	o Not monitored	o Monitored but not accounted for
o Total Hours	o 25,000 (ref. 4)	o 5,000

Figure 25.- Comparison of analog VGH and digital VGH systems.

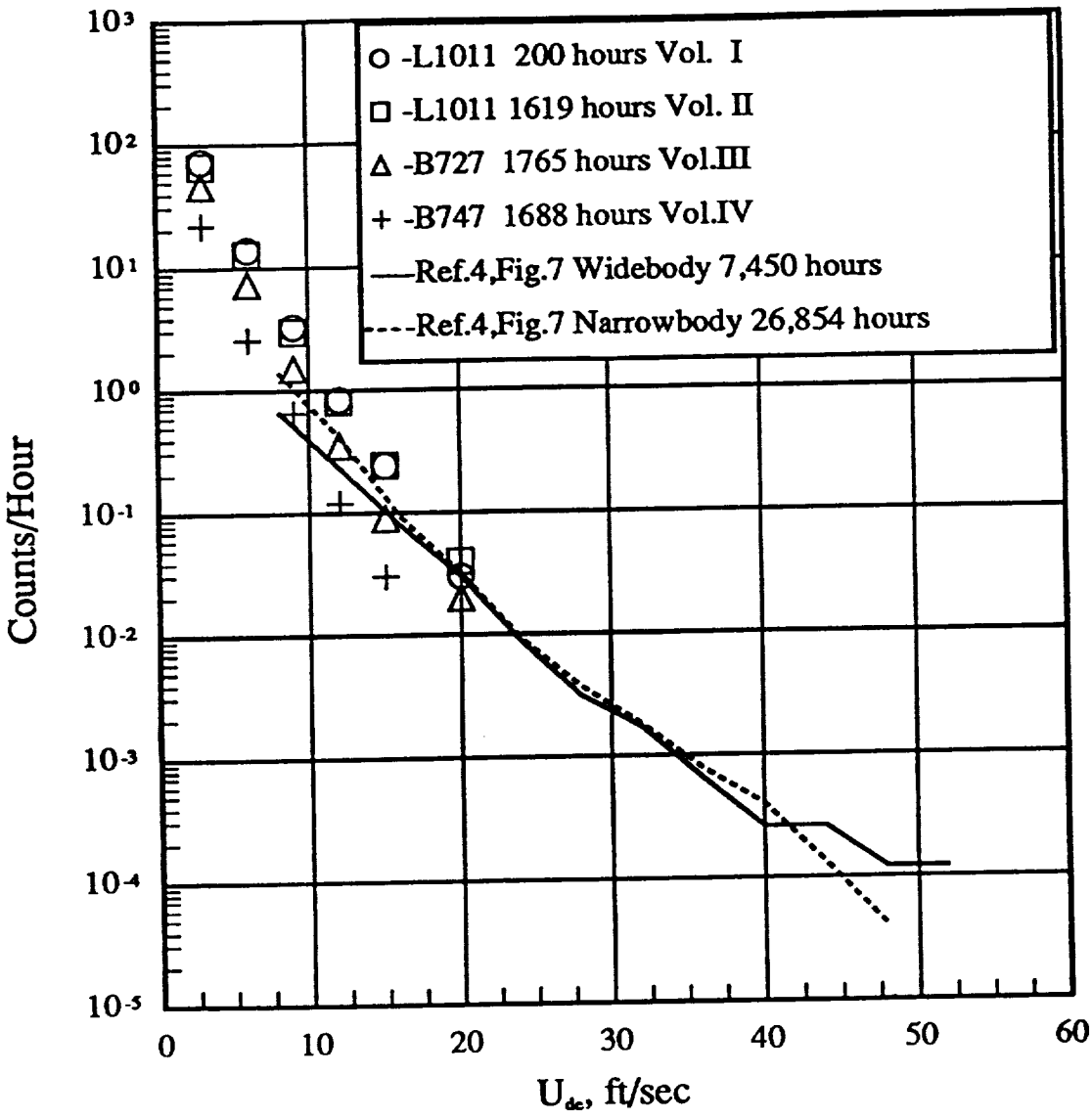

Figure 26-. Comparison of U_{de} results

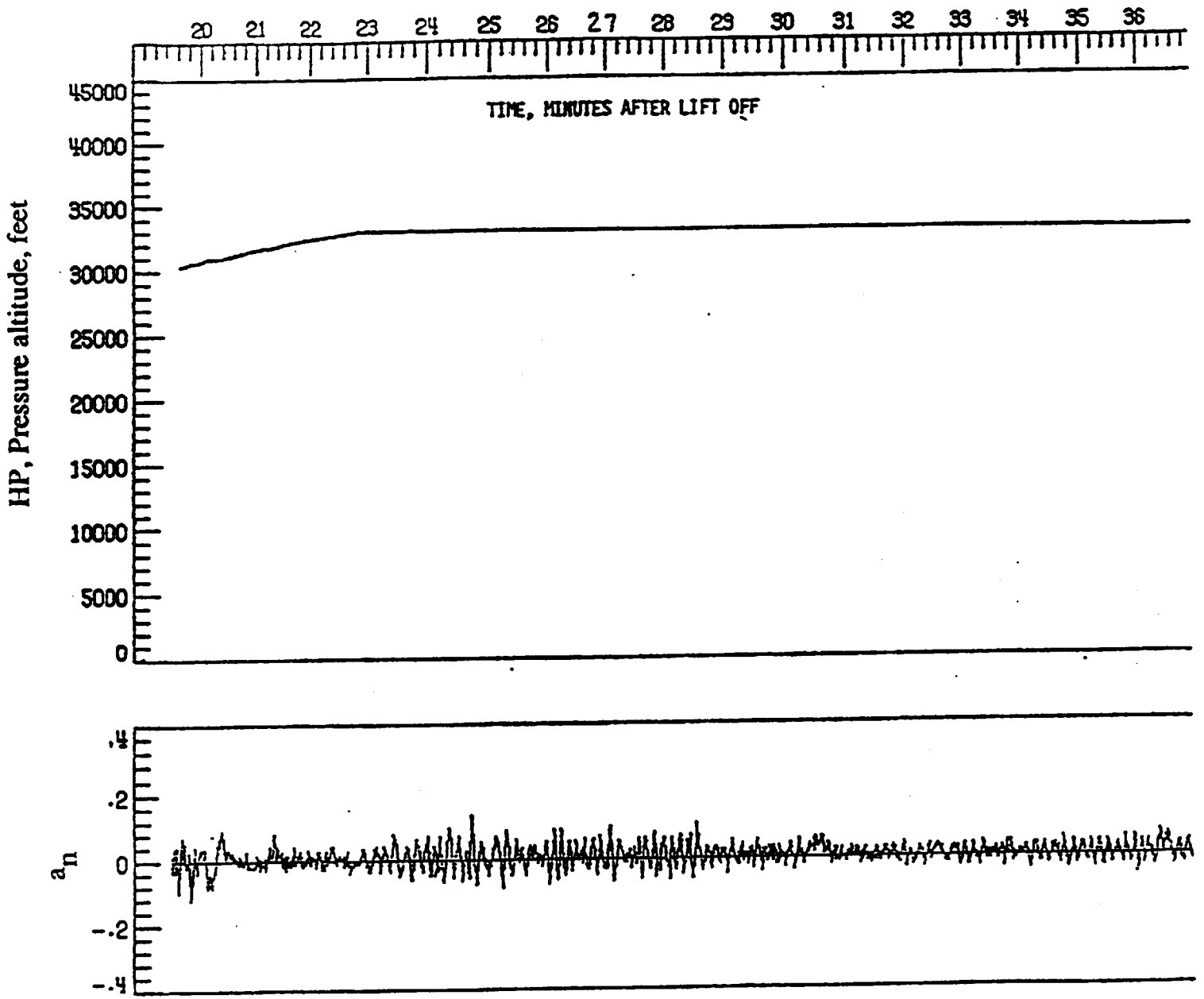

Figure 27. - Low frequency oscillation on normal acceleration.

NASA
National Aeronautics and Space Administration

Report Documentation Page

1. Report No.	2. Government Accession No.	3. Recipient's Catalog No.
NASA CR-181909, Vol. I DOT/FAA-CT-89/36-I		

4. Title and Subtitle	5. Report Date
The NASA Digital VGH Program - Exploration of Methods and Final Results Volume I - Development of Methods	December 1989
	6. Performing Organization Code

7. Author(s)	8. Performing Organization Report No.
Norman L. Crabill	
	10. Work Unit No. 505-63-01-05

9. Performing Organization Name and Address	11. Contract or Grant No.
Eagle Engineering, Inc. Tower Box 77, 2101 Executive Drive Hampton, VA 23666	NASW-4430
	13. Type of Report and Period Covered: Contractor Report

12. Sponsoring Agency Name and Address	14. Sponsoring Agency Code
National Aeronautics and Space Administration Washington, DC 20546-0001 and U.S. Department of Transportation FAA Technical Center Atlantic City International Airport, NJ 08405	

15. Supplementary Notes

Langley Technical Monitor: Joseph W. Stickle

FAA Technical Center COTR: Thomas DeFiore

16. Abstract

Two hundred hours of Lockheed L 1011 Digital Flight Data Recorder data taken in 1973 were used to develop methods and procedures for obtaining statistical data useful for updating airliner airworthiness design criteria. Five thousand hours of additional data taken in 1978-1982 are reported in Volumes II, III, IV and V.

17. Key Words (Suggested by Author(s))	18. Distribution Statement
Flight Recorders; Digital Flight Data Recorders, VGH,DVGH, Airworthiness, Airliner, L-1011	Unclassified - Unlimited Subject Category 06

19. Security Classif. (of this report)	20. Security Classif. (of this page)	21. No. of pages	22. Price
Unclassified	Unclassified	132	A07

NASA FORM 1626 OCT 86